The Abdus Salam International Centre for Theoretical Physics

2167-27

**Advanced School on Direct and Inverse Problems of Seismology**

*27 September - 8 October, 2010*

**The study of fluid induced and triggered seismicity**
**Theory - 2**

Torsten Dahm

*Institut fuer Geophysik*
*Universitaat Hamburg*
*Germany*

# The study of fluid-induced and triggered seismicity: case studies

*ICTP Course 2010*

Torsten Dahm

torsten.dahm@zmaw.de

Institut für Geophysik, Universität Hamburg, Germany

# Lecture B: case studies

I. Fluid injection and pore pressure diffusion

II. Hydro-fracturing & magma intrusions

- Gas field stimulation
- Long lasting intrusions

III. Gas field depletion and induced earthquakes

# I) fluid & pore pressure diffusion

Examples:

– Denver 1962-1968: three M>5 events, 21 month after end of injection

– Chalia chemical waste disposal 1972-1985, M5 event 12 km south of well 14 years after injection

– Ashtabula, Ohio, sequence 1987-2003, M< 4.3, 9 years after end of injection

# Example: Temperature-diffusion in salt mine

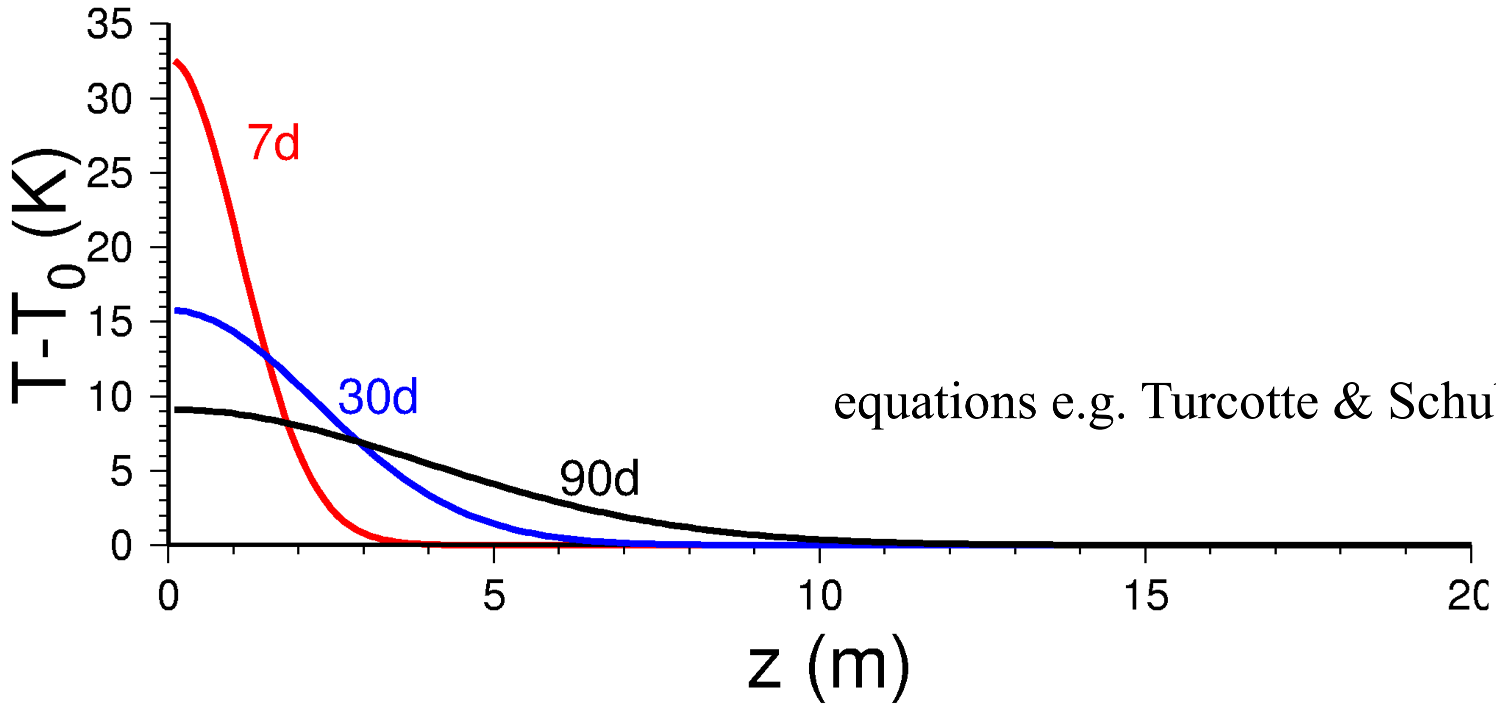


equations e.g. Turcotte & Schubert(2002)

1-D Temperature diffusion after "heat injection" at plane z=0.

Temperature (and stress) slowly spreads out and "relaxes" at "injection point"

The same laws apply for fluid diffusion or for dissolution problems

# The Ashtabula, Ohio, sequence related to waste fluid injection

into 1.8 km deep sandstone

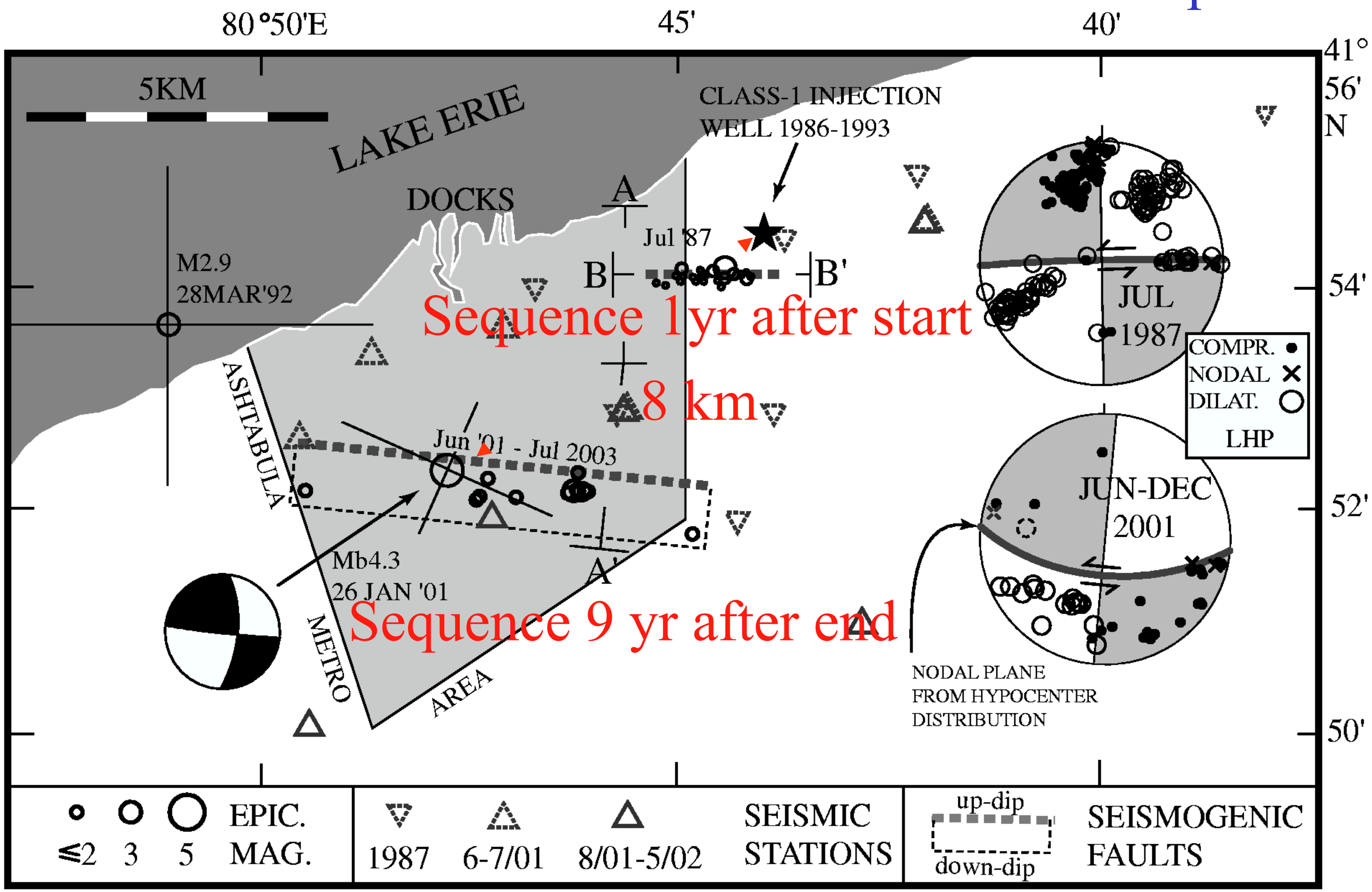


Hypo depth in basement 2 km below the injection layer

Seeber at al., 2004, BSSA 94, 76-87

# Temporal evolution

largest earthquake

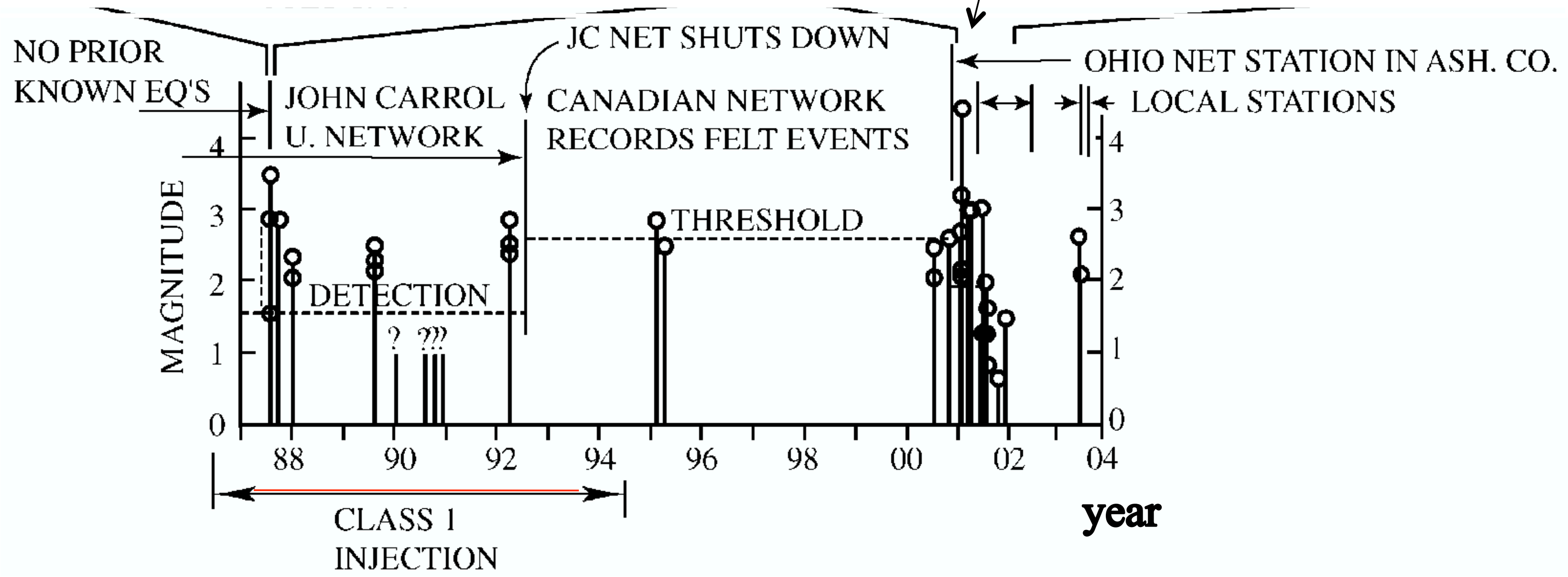


164 m^3/day at 10 MPa (59.860 t/yr)

Seeber at al., 2004, BSSA 94, 76-87

# Diffusivity: comparison of RIS and injection

Talwani & Acree (1985): PAGEOPH 122, 947-965

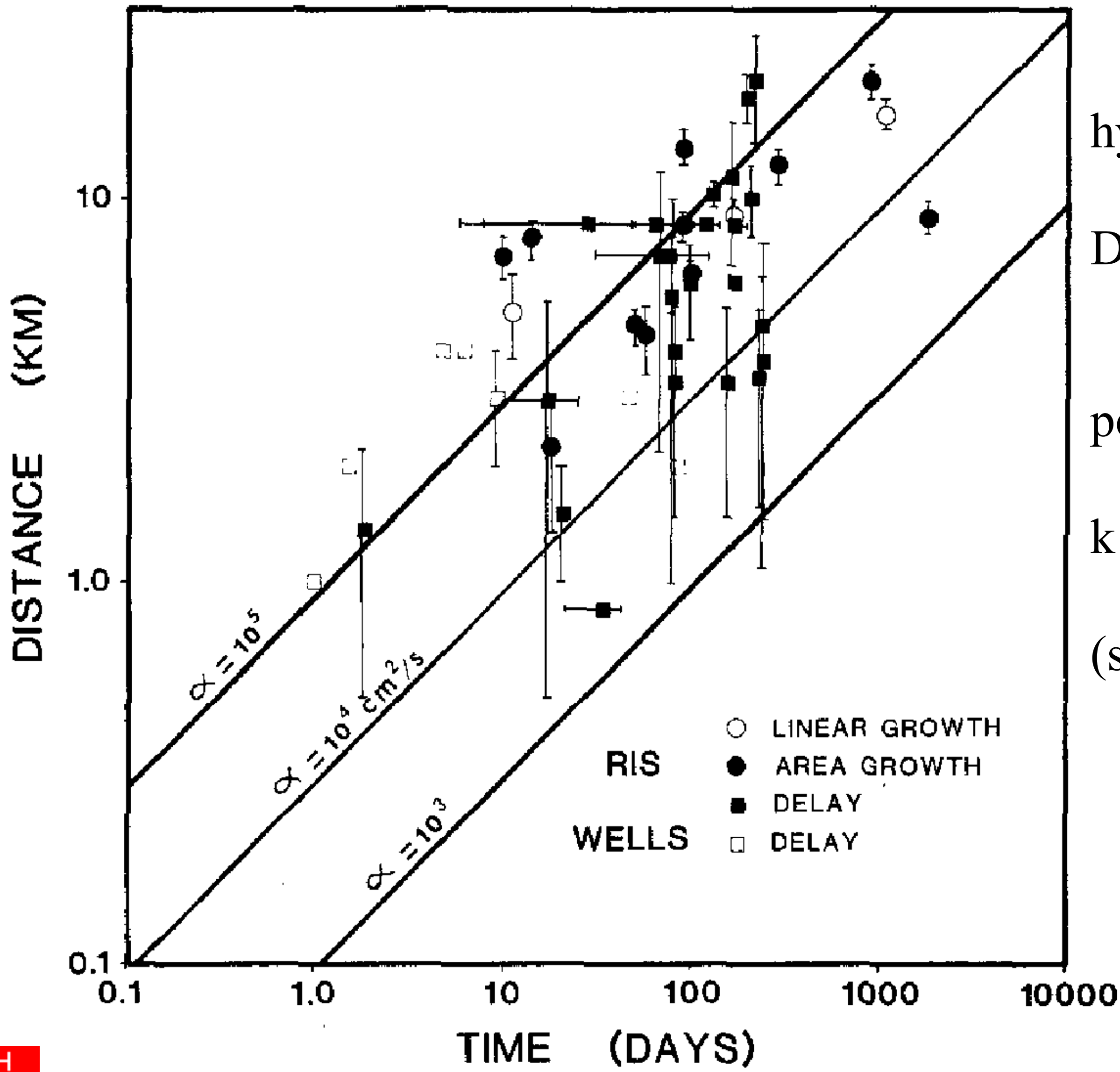


hydraulic diffusivity:

$D \approx 1 - 10\ m^2 / s$

permeability range:

$k \approx 10^{-16} - 10^{-14}\ m^2$

(see Kümpel 1991 for formula)

# Fluid-injection triggered events

1. Injection related pore pressure rise may trigger earthquakes (Coulomb failure)
2. Pore pressure decreases at the well after injection stops, but pressure front continuous to spread away from injection well for tens of years up to 8 - 14 km distance or more
3. Pore pressure transients can be simulated as diffusion process

# Case II

## Hydrofracture induced seismicity

# Hydrofrac stimulations in Canyonsand gas field, W. Texas

injection borehole

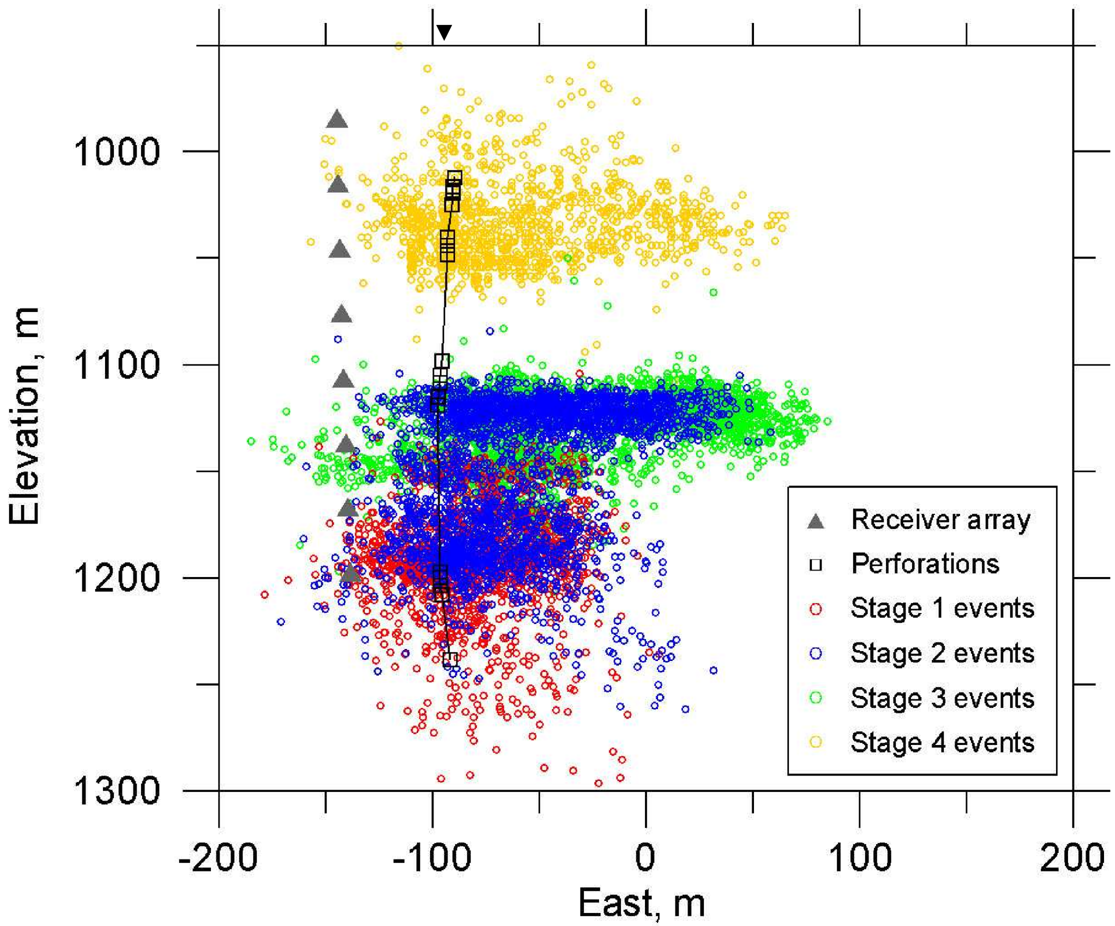


fracture-induced seismicity
(color = different experiments)

growth direction (2D)

Fischer et al. (JGR, 2008)

# distance time plot, stage 3

growth direction

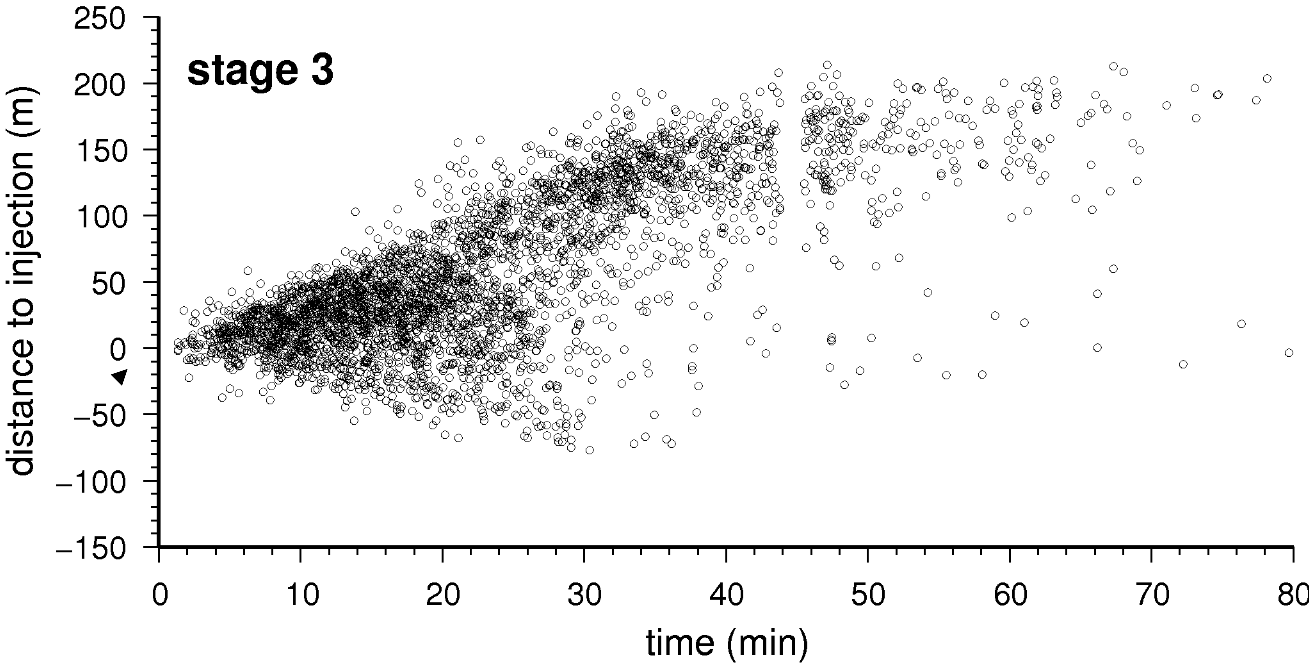


injection point

# distance time plot, stage 3

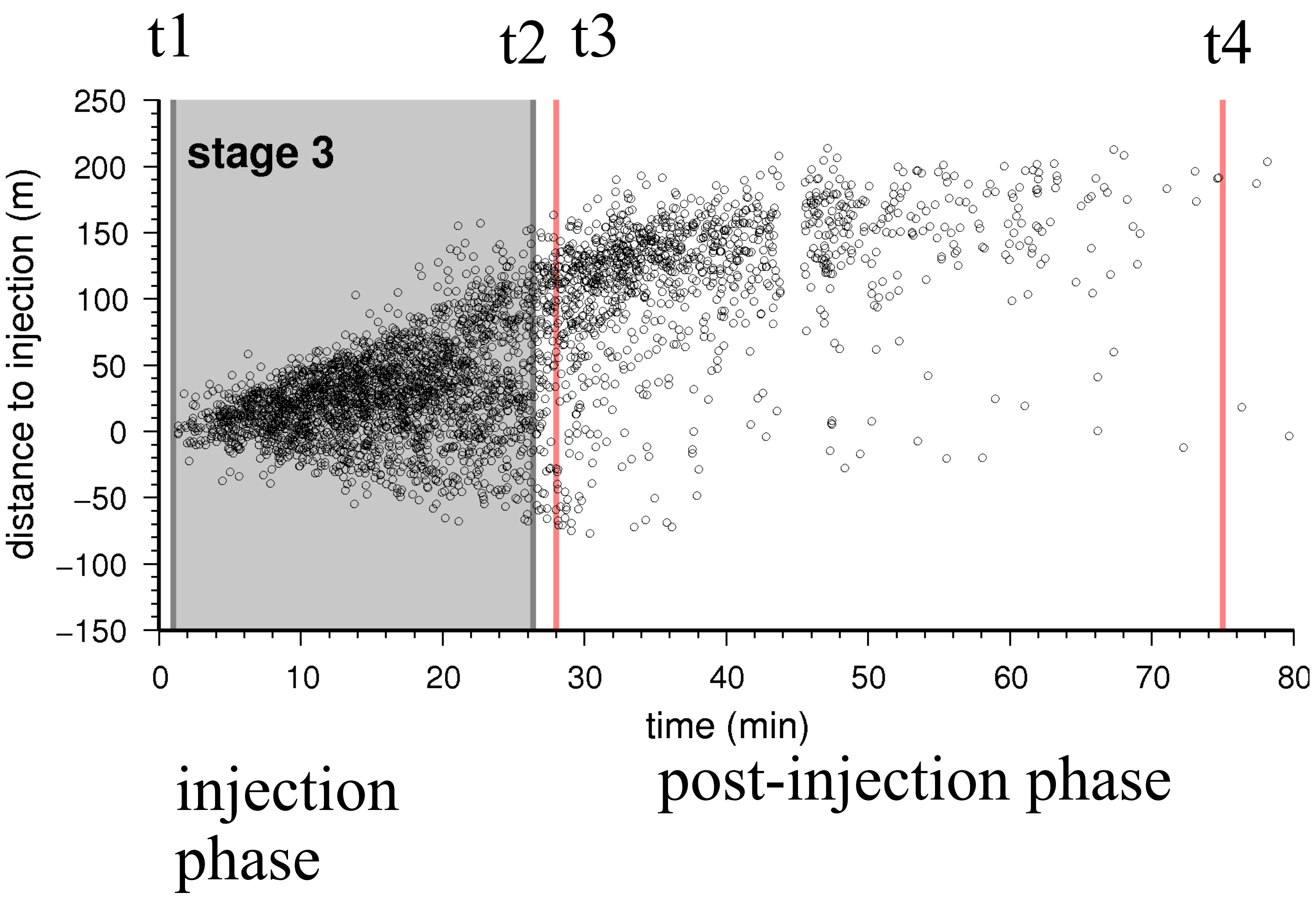

# distance time plot, stage 3

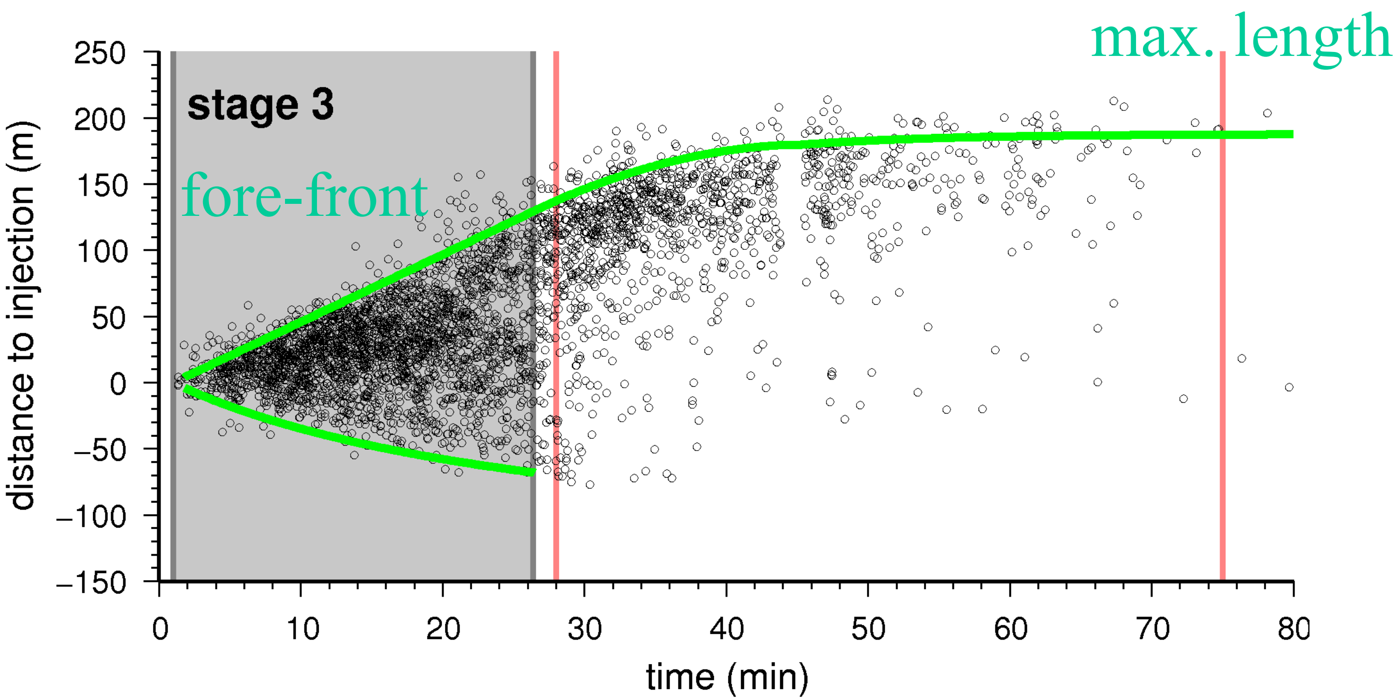

# distance time plot, stage 3

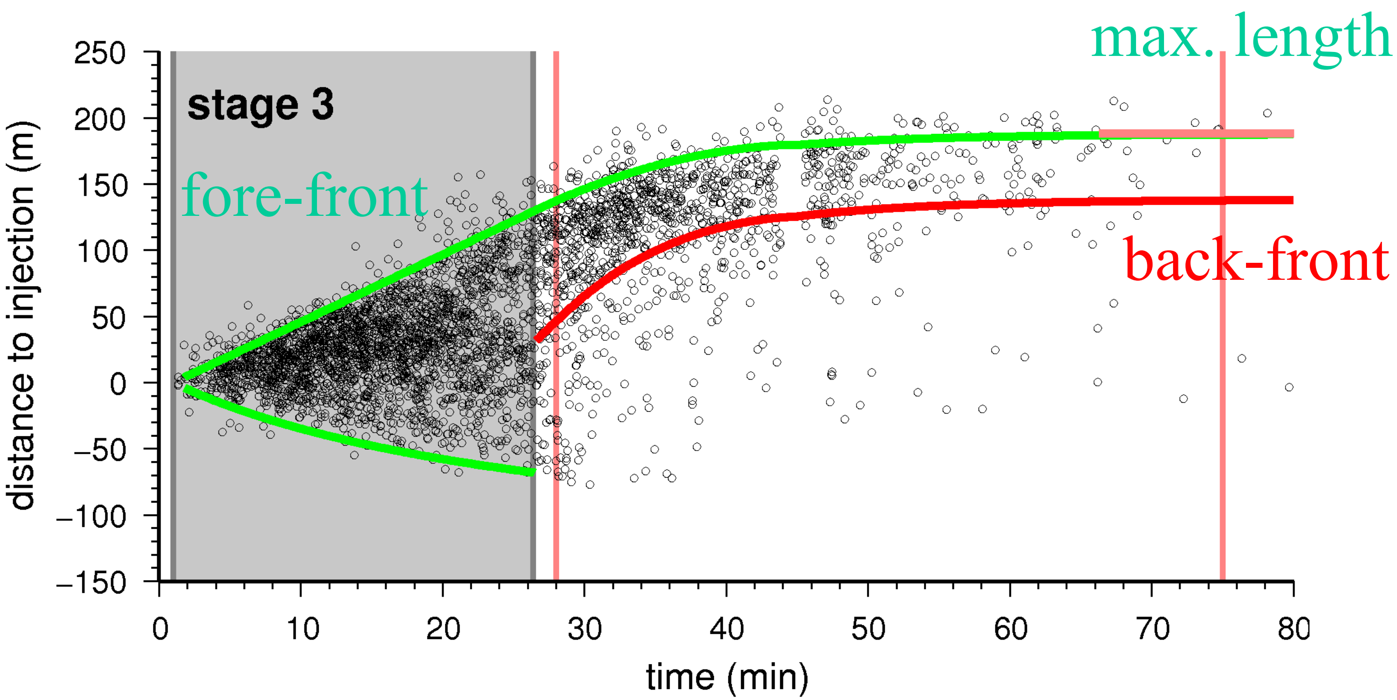

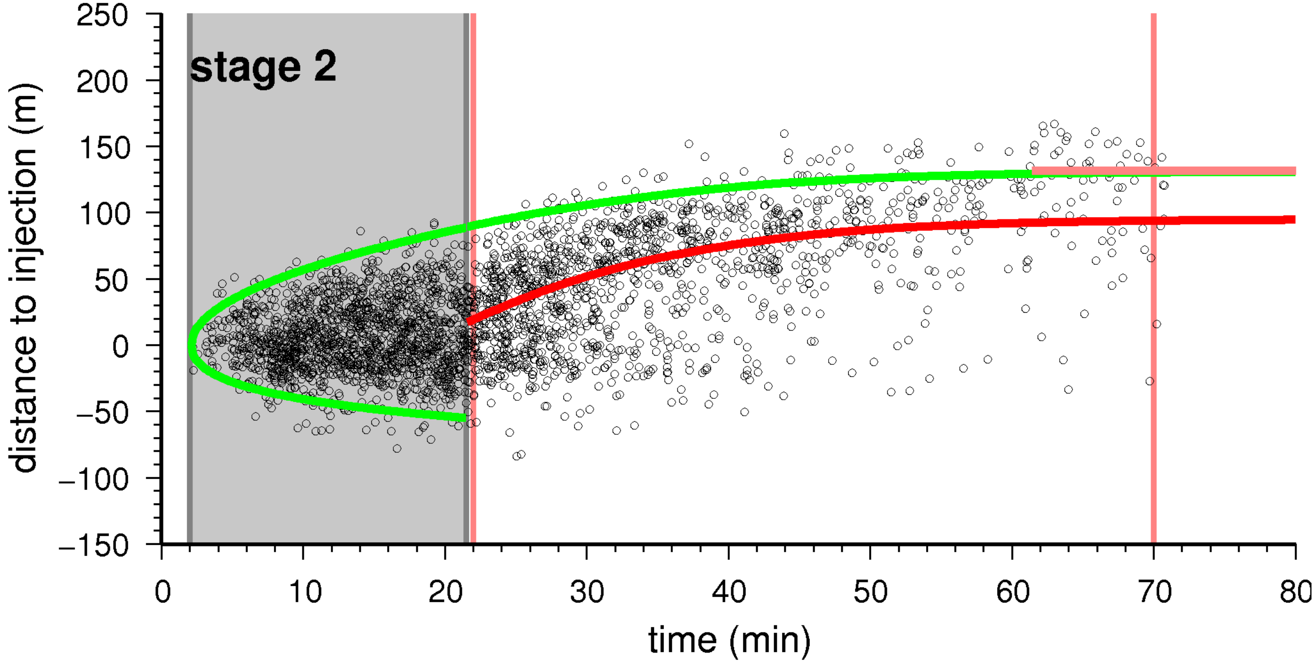


Hypotheses:

a) Front and backfront are controlled by pressure diffusion (see RIS and waste fluid injection)

b) Front- and backfront, asymmetric growth and intensity of seismicity are controlled by the shape of the fluid-filled fracture (e.g. Fischer, Hainzl and Dahm, 2009, Dahm et al., 2010)

# I) Fracture model for asymmetric & unilateral growth

Injection, bilateral growth

Post-injection, unilateral growth

growing style is controlled by stress gradient g!

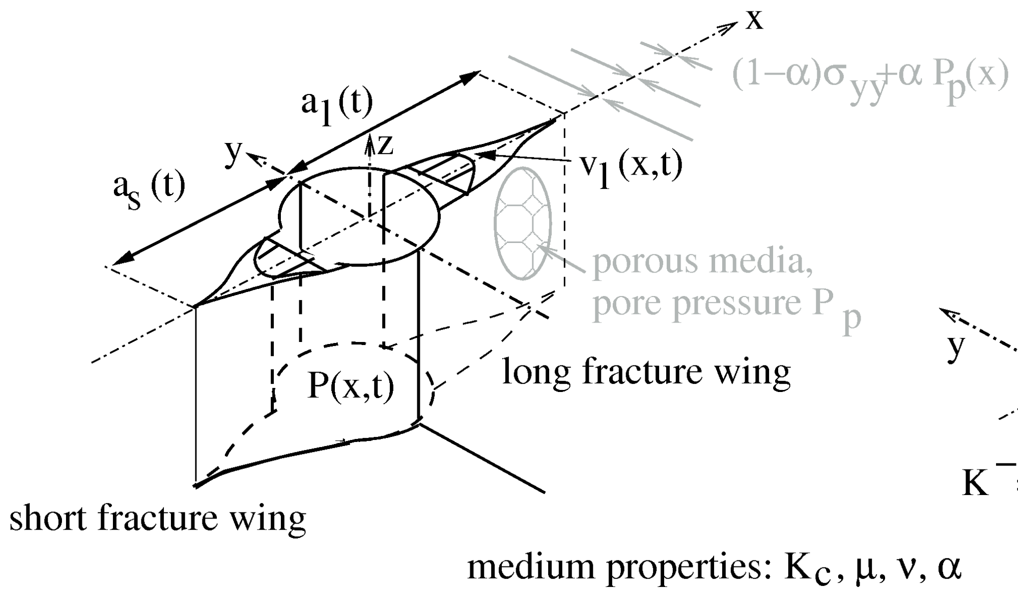


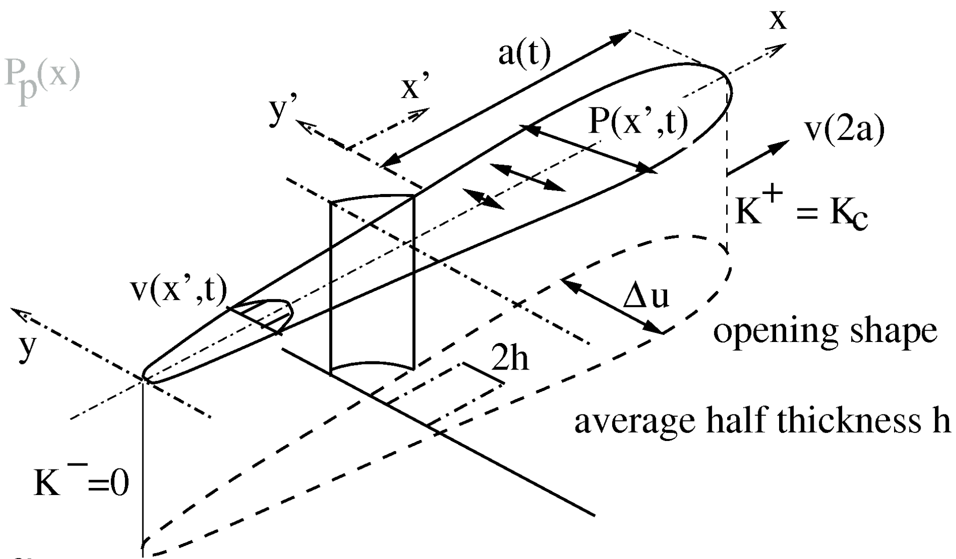


borehole

(Dahm, Hainzl and Fischer, JGR 2010)

# Injection phase: driving pressure and flow

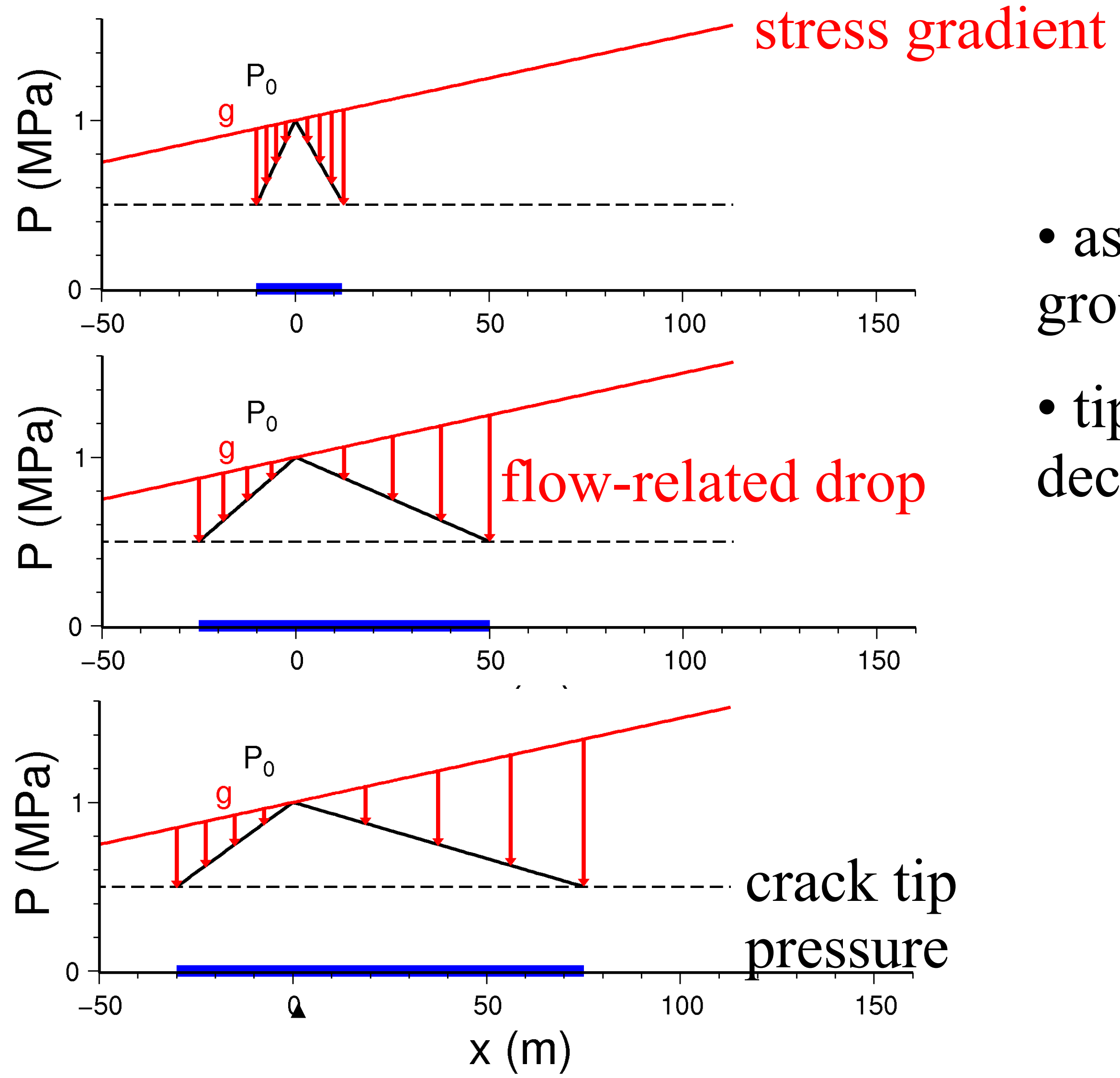


- asymmetric bilateral growth
- tip grow velocity decreasing with length

injection point

fracture length

Dahm et al., 2010

# Asymmetric growth during injection

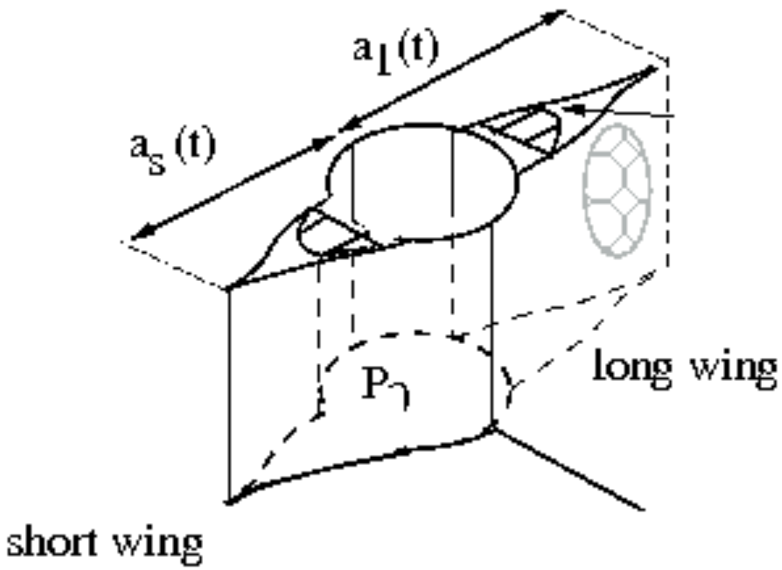


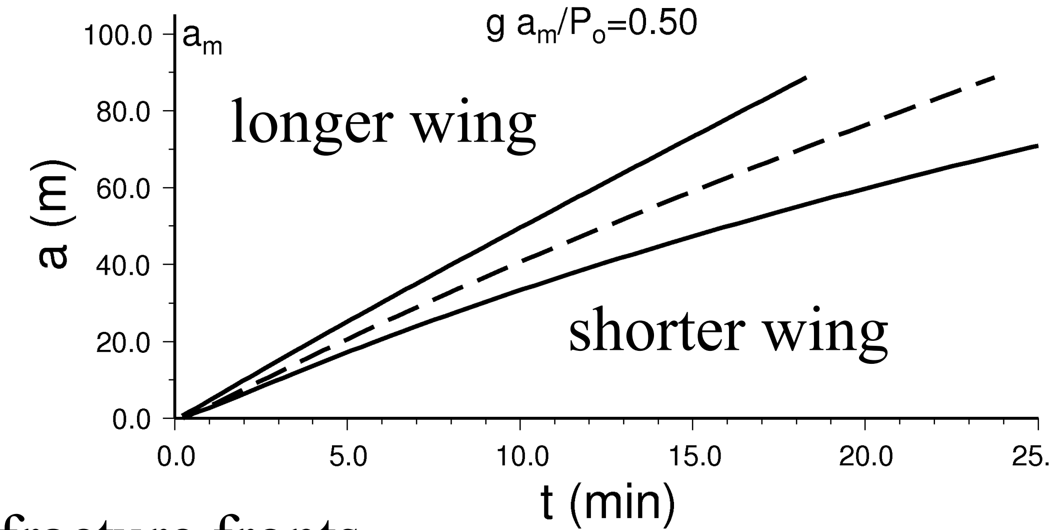


fracture fronts

$$\pi \left( \frac{a_l(t) - a_s(t)}{a_s^2(t) + a_l^2(t)} \right) \approx \frac{g}{P_0}$$

gradient / overpressure

a(t) is the time dependent wing length of the fracture

see Fischer, Hainzl and Dahm (2009)

# self-expanding unilateral growth

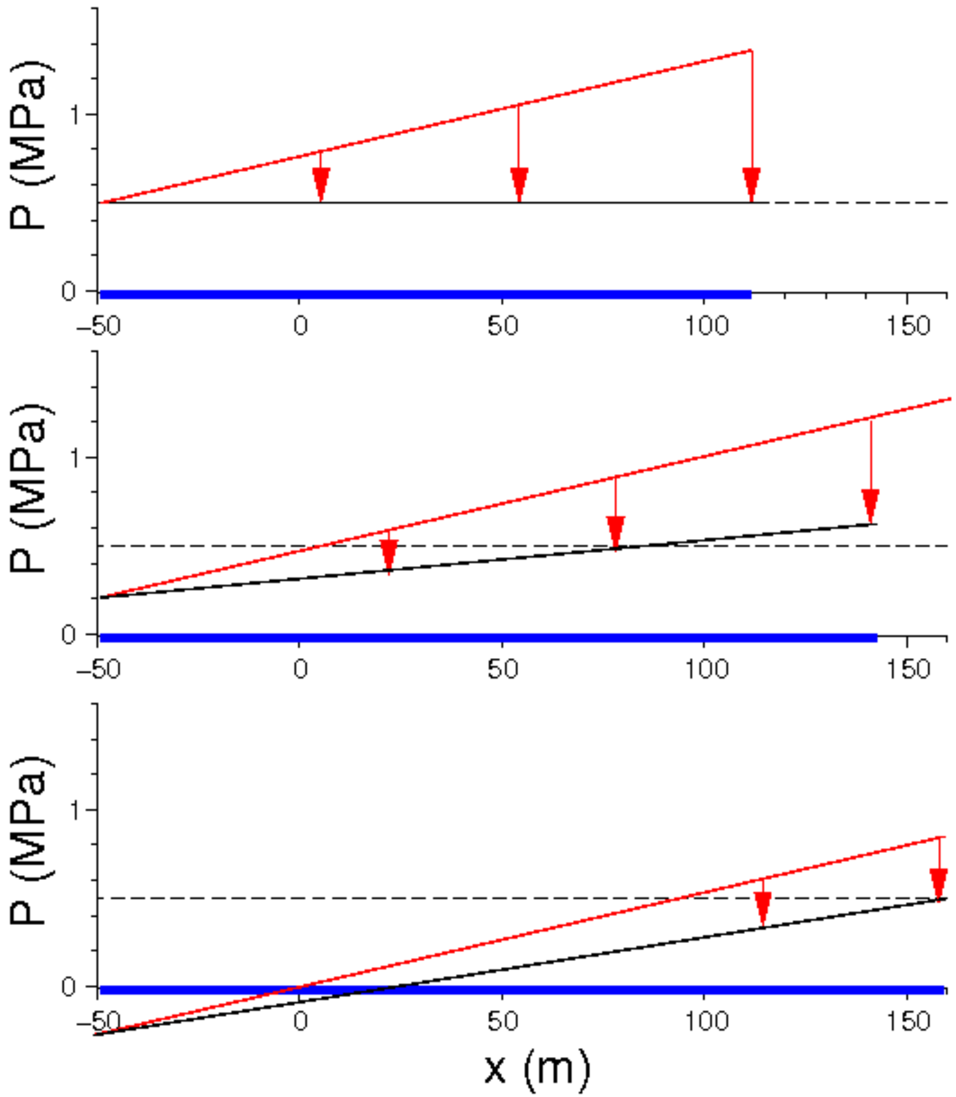


- unilateral growth
- ambient overpressure is further decreasing
- overpressure at taller tip is decreasing below critical value
- at final stage the overpressure at taller tip is below zero (Weertman crack)

Dahm et al., 2010

# Unilateral growth during post-injection

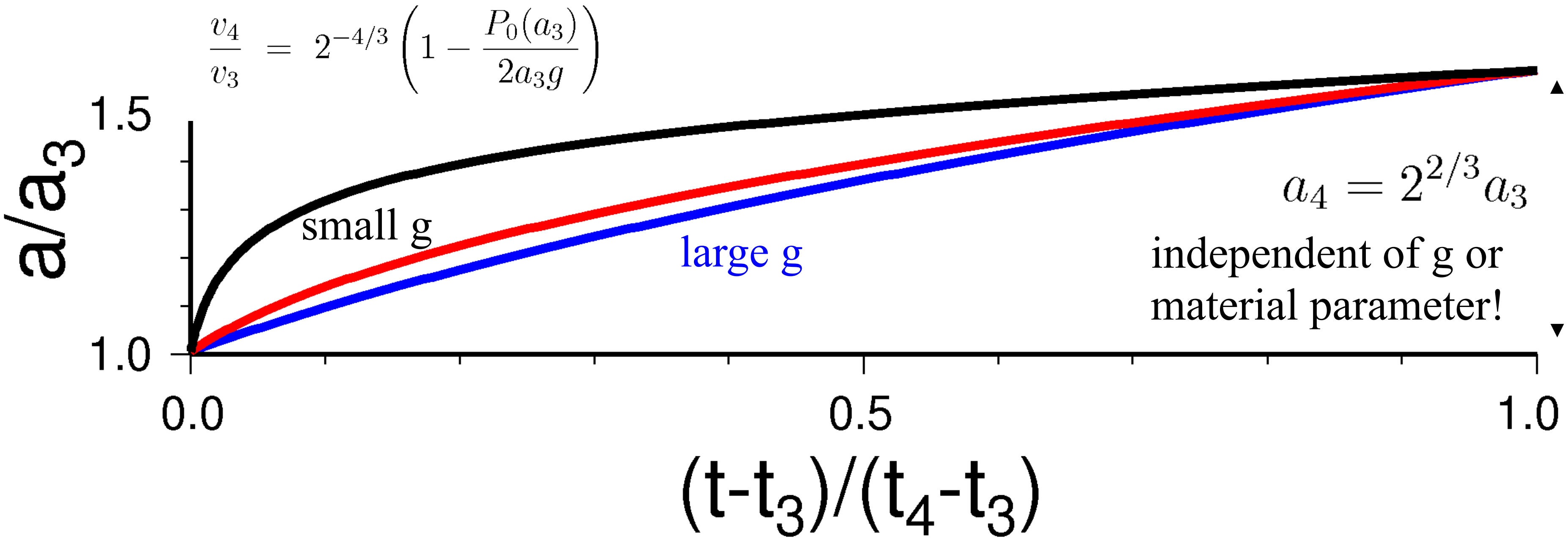


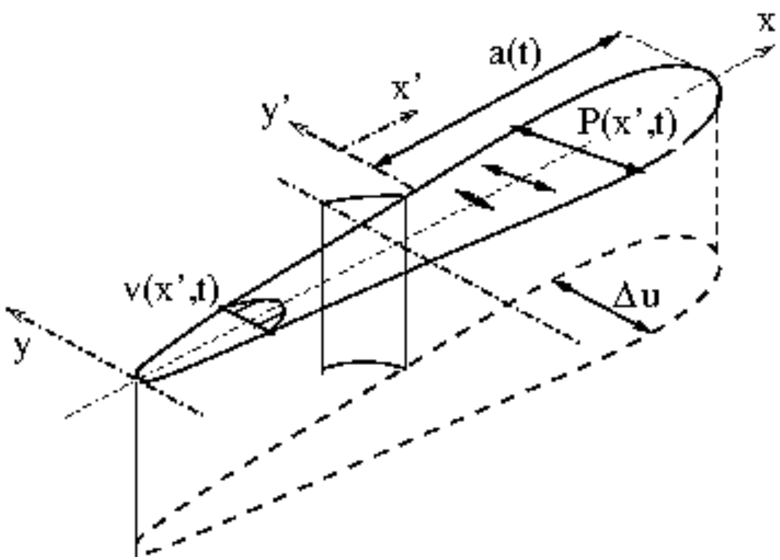

# Fit to seismicity data

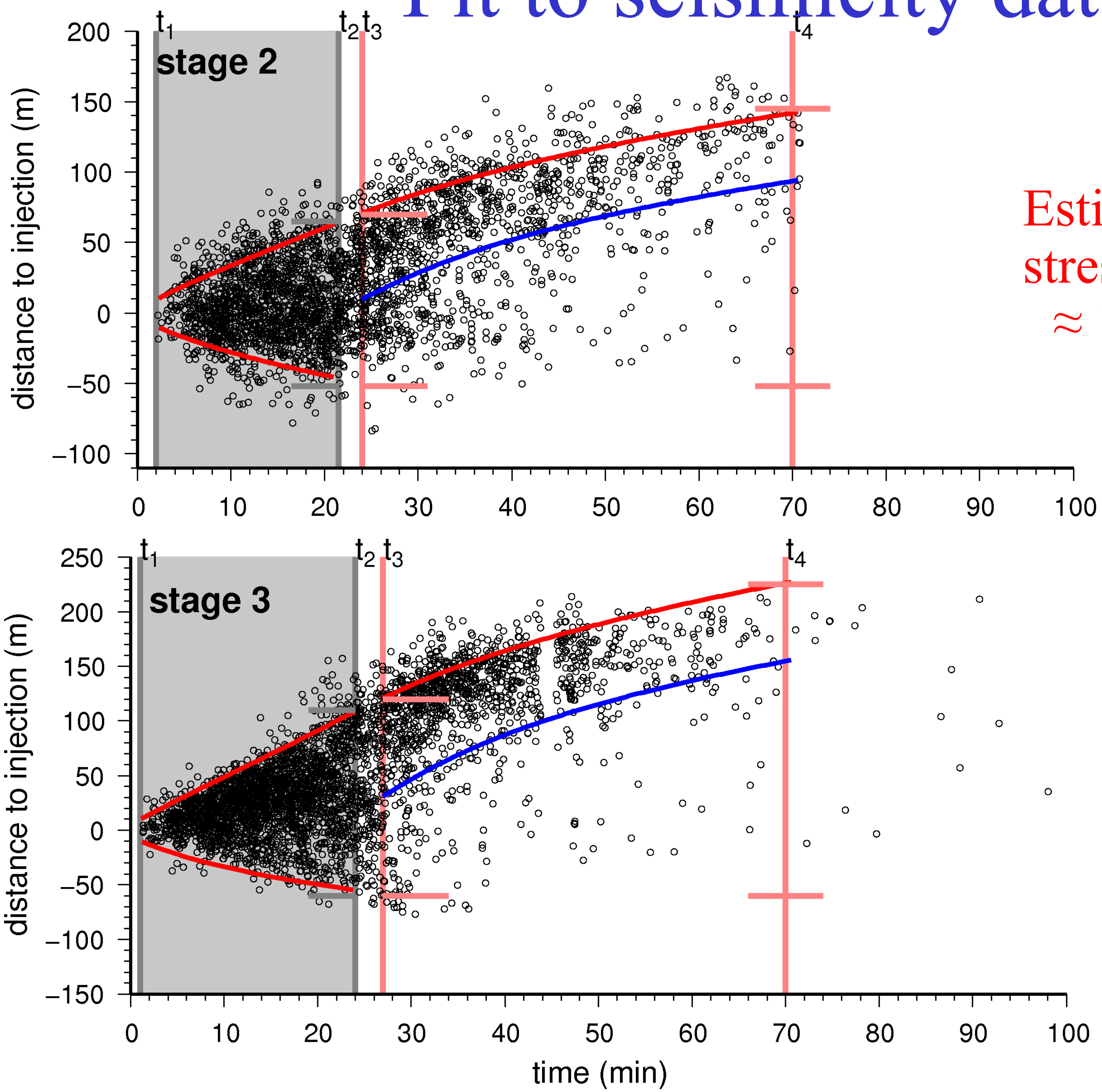


Estimated driving stress gradient: ≈ 10 MPa/km

Dahm et al., 2010

# II) Modeling stress changes: Input to BE Method

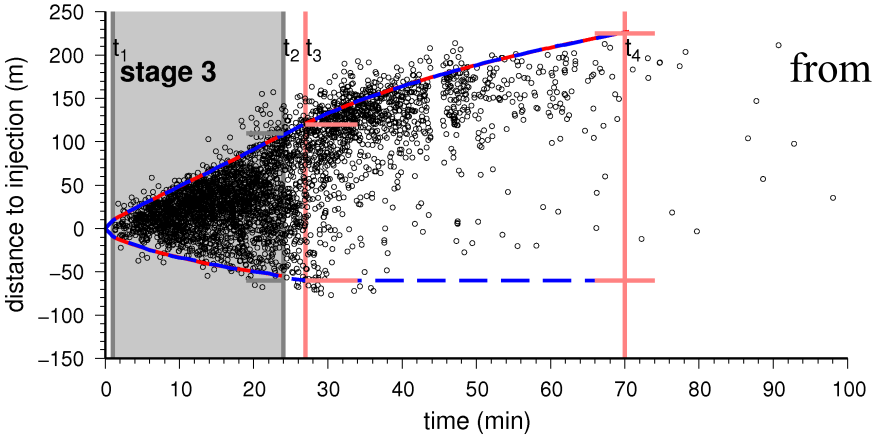


from Dahm, Hainzl and Fischer (JGR, 2010)

hydrofrac length

internal effective pressure

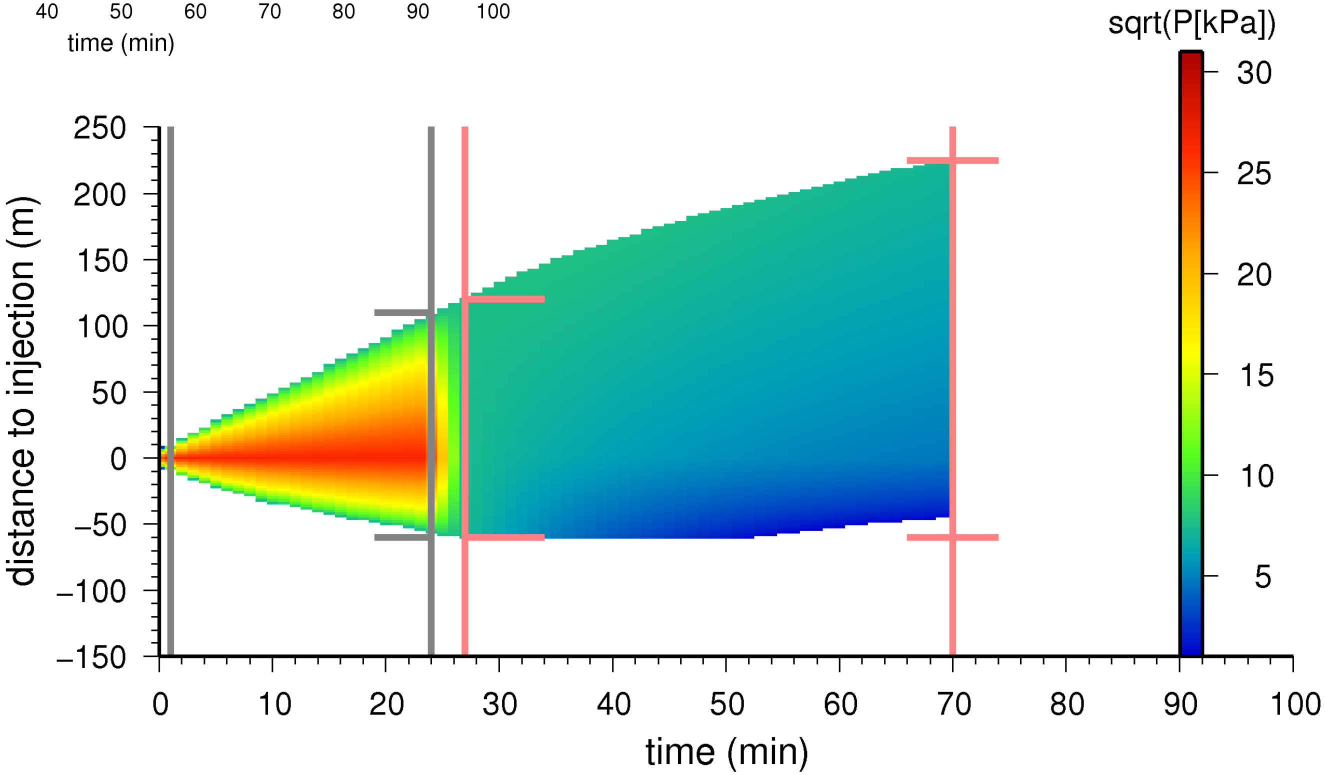

# Associated opening and Coulomb stress change (CFF)

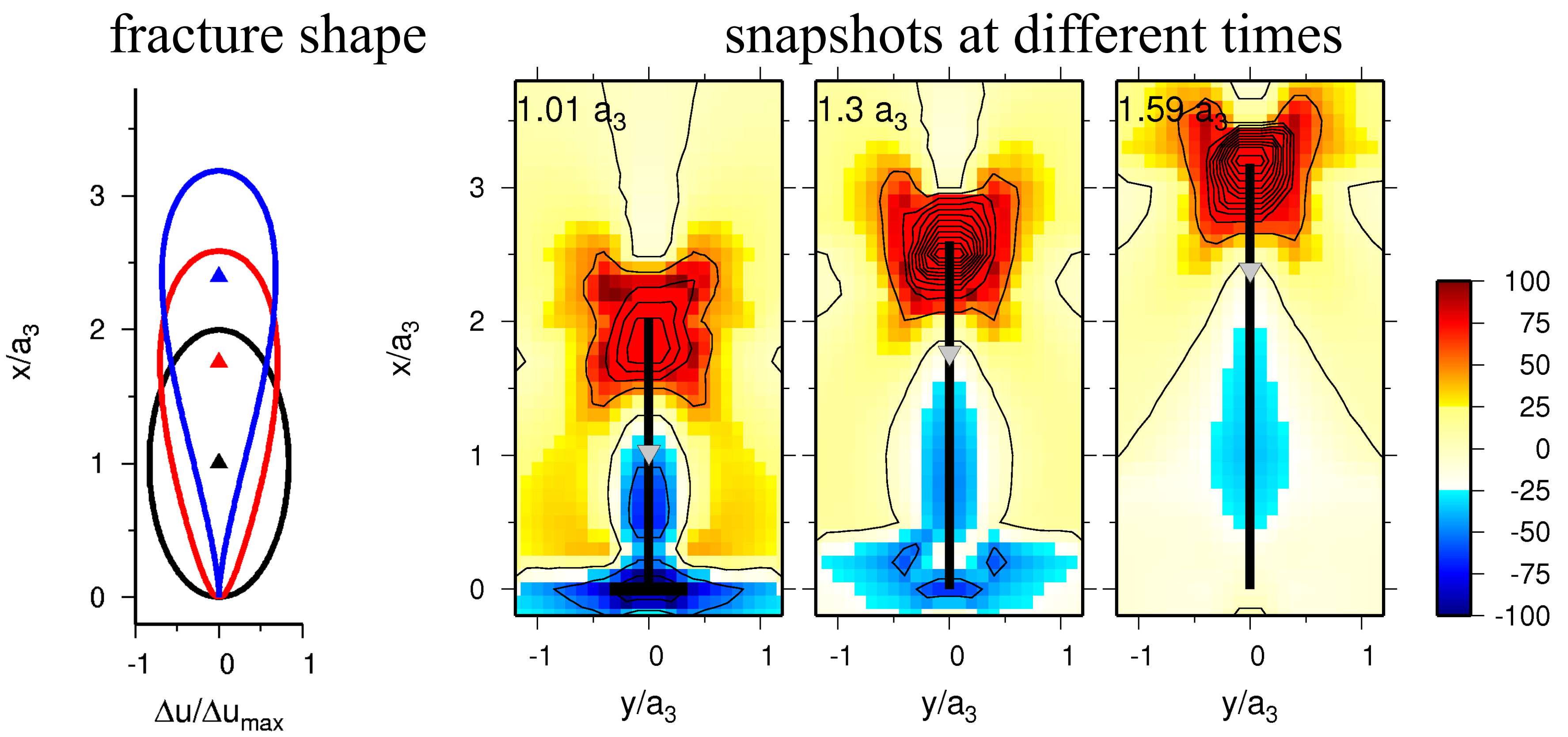


- unilateral migration of front and backfront

# Positive CFF projected on fracture axis

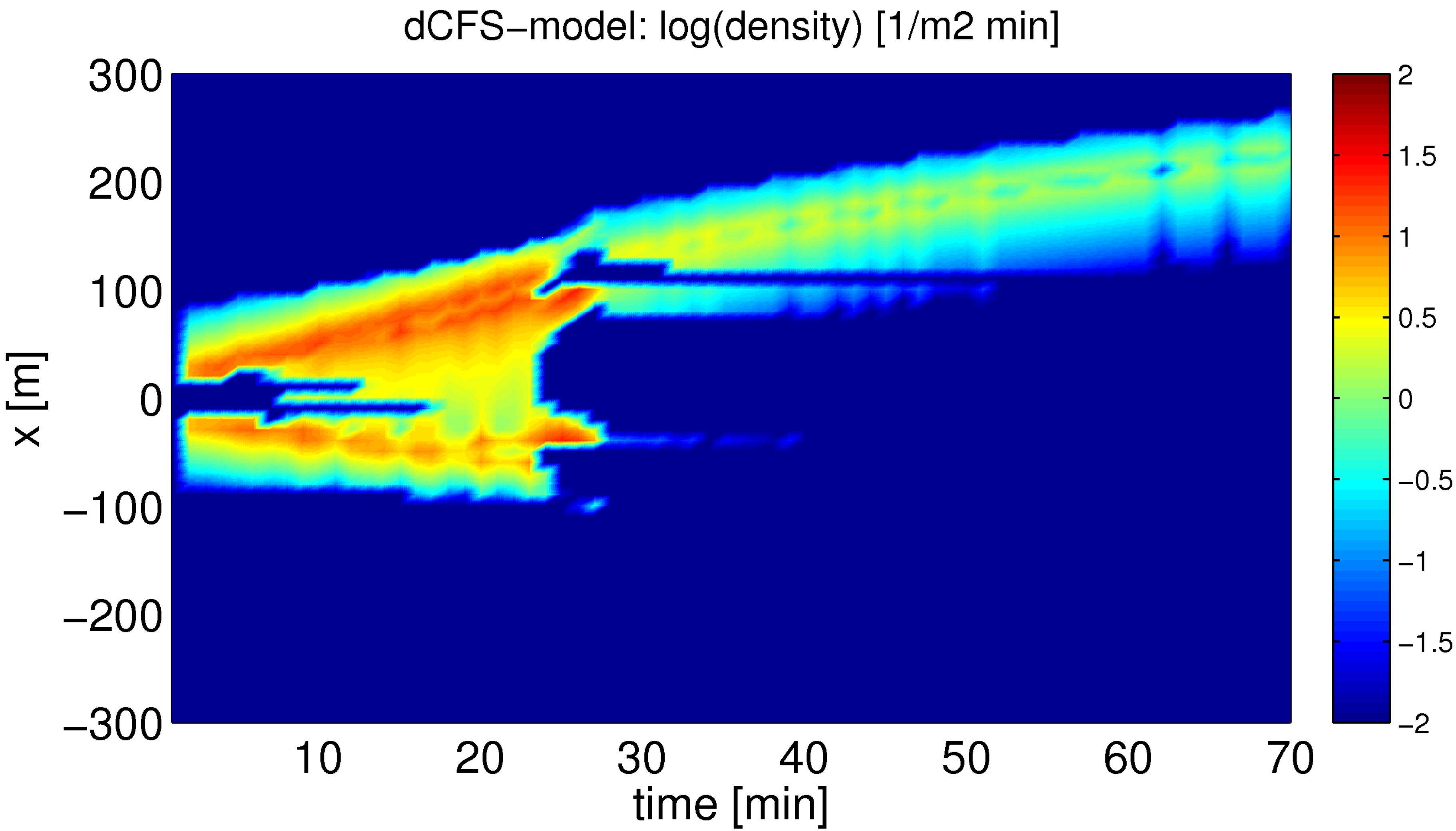

# Positive CFF projected on fracture axis

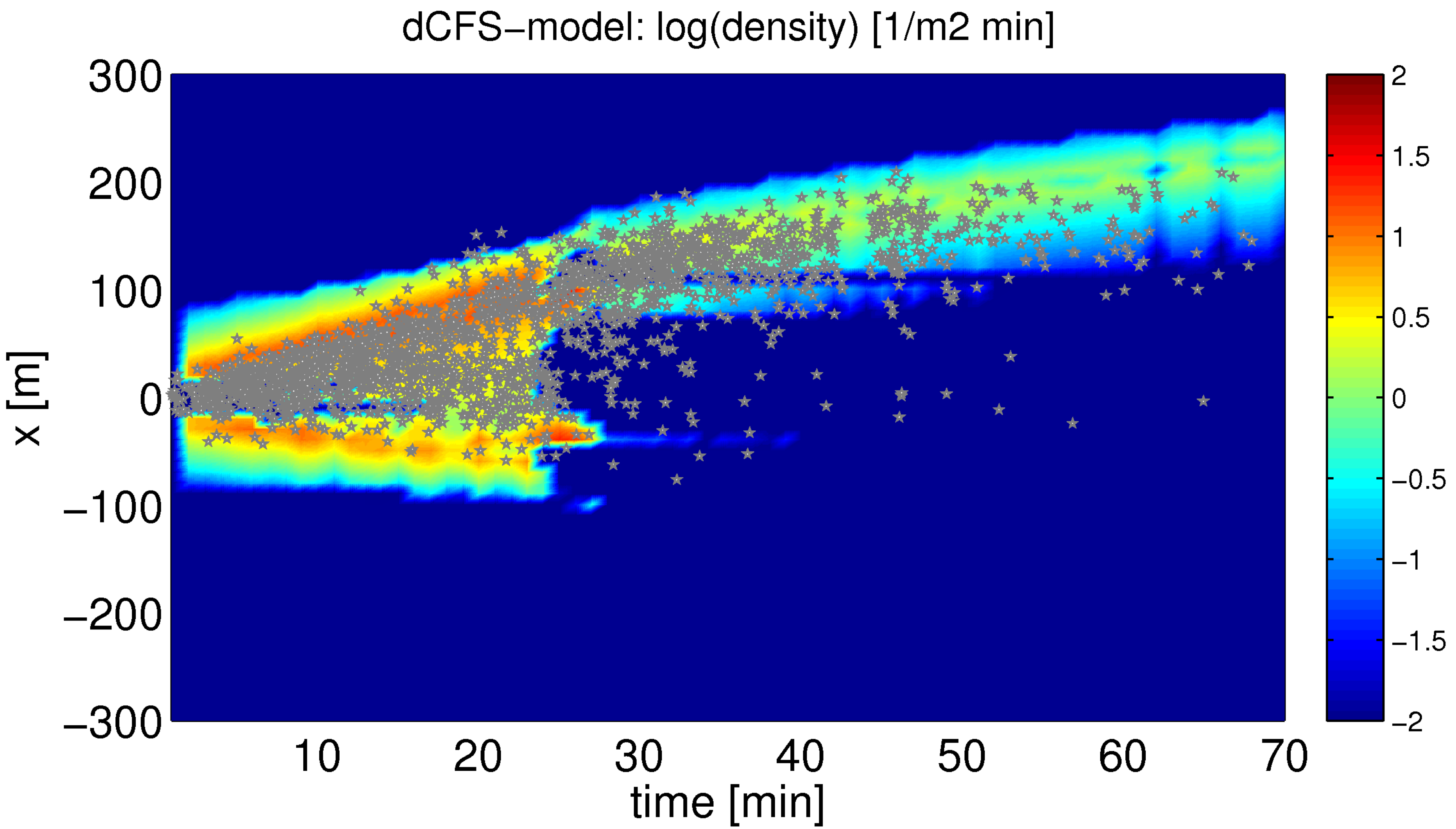

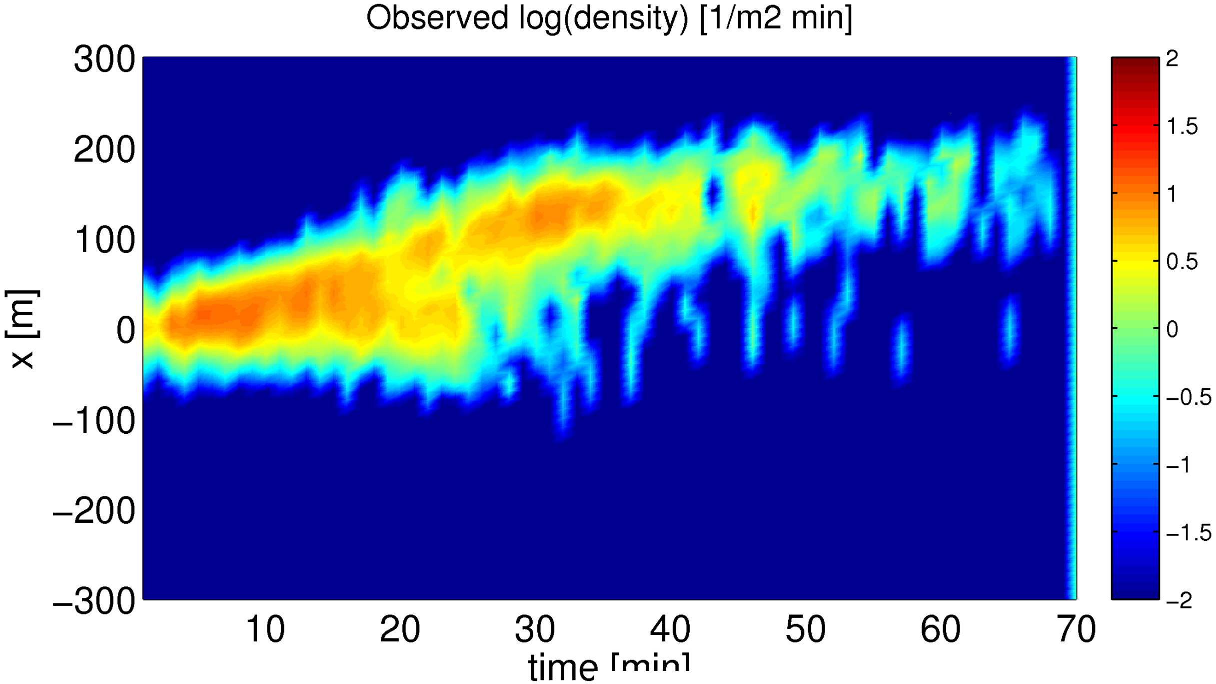


# Observed seismicity

# Simulated seismicity

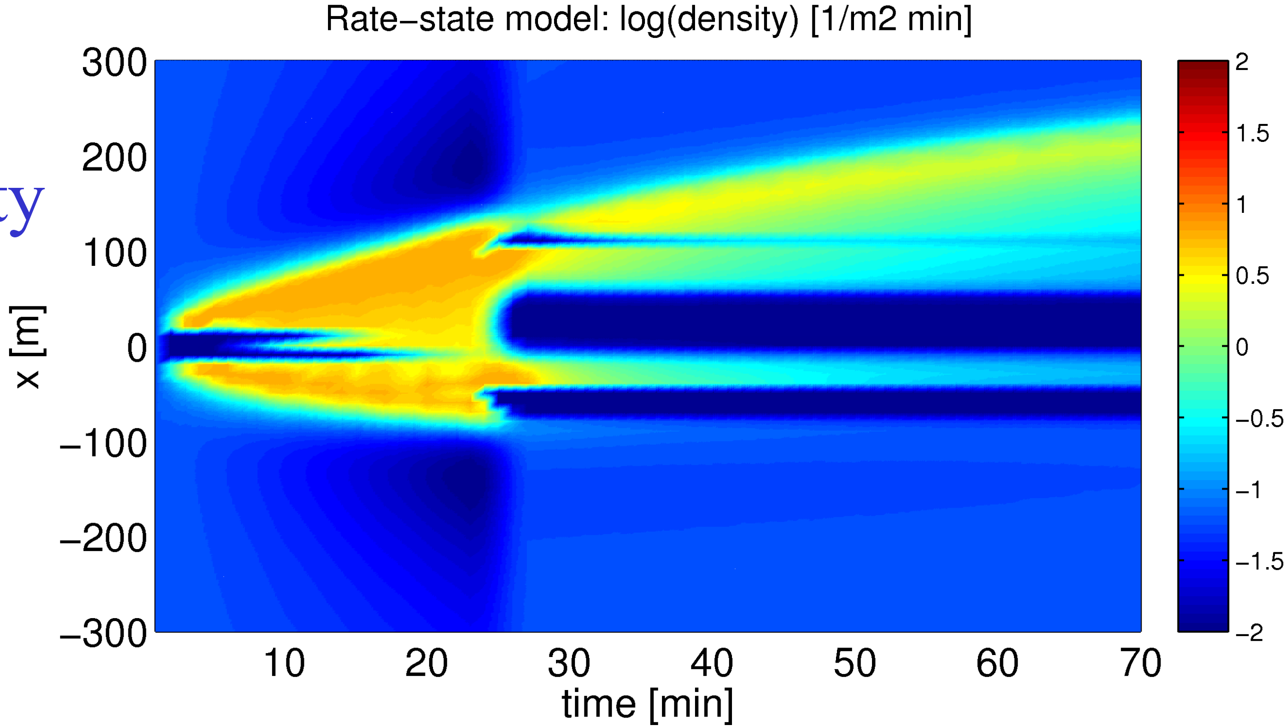

# Conclusion

1. Hydrofracture-flow model predicts time-dependent length, opening shape and effective internal pressure
2. Asymmetric and uni-directional growth can be explained by fracture model with stress or pore pressure gradients
3. Rate and state dependent seismicity model explains main features of observed seismicity

Induced seismicity can be linked to deterministic hydrofrac model

# Seismicity during the Krafla rifting events Dec75 - Jan81

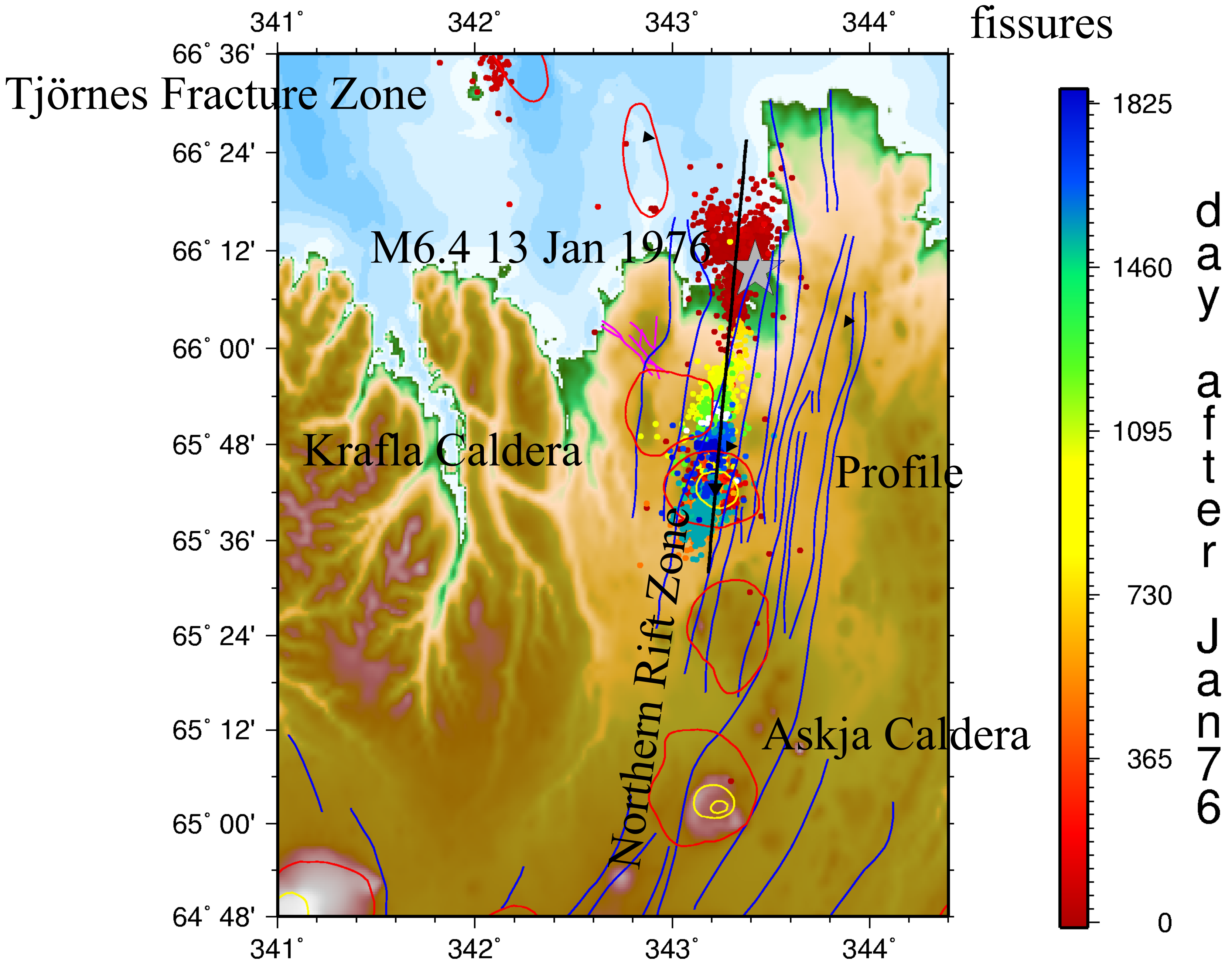

# Along strike seismicity and caldera deflation

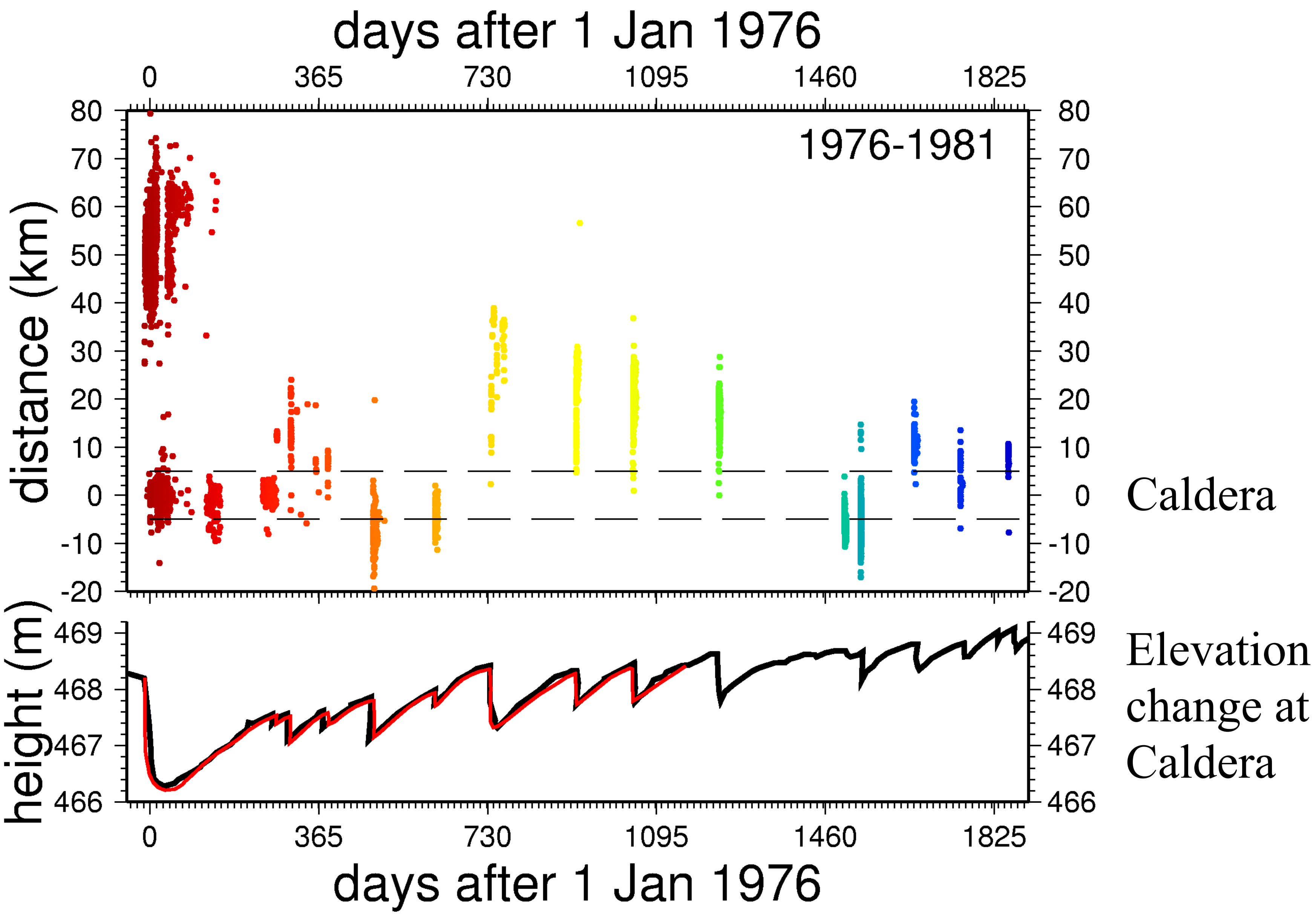


see Einarsson, 1991, Buck et al., 2006 and references therein

# induced seismicity: Sep 77 intrusion

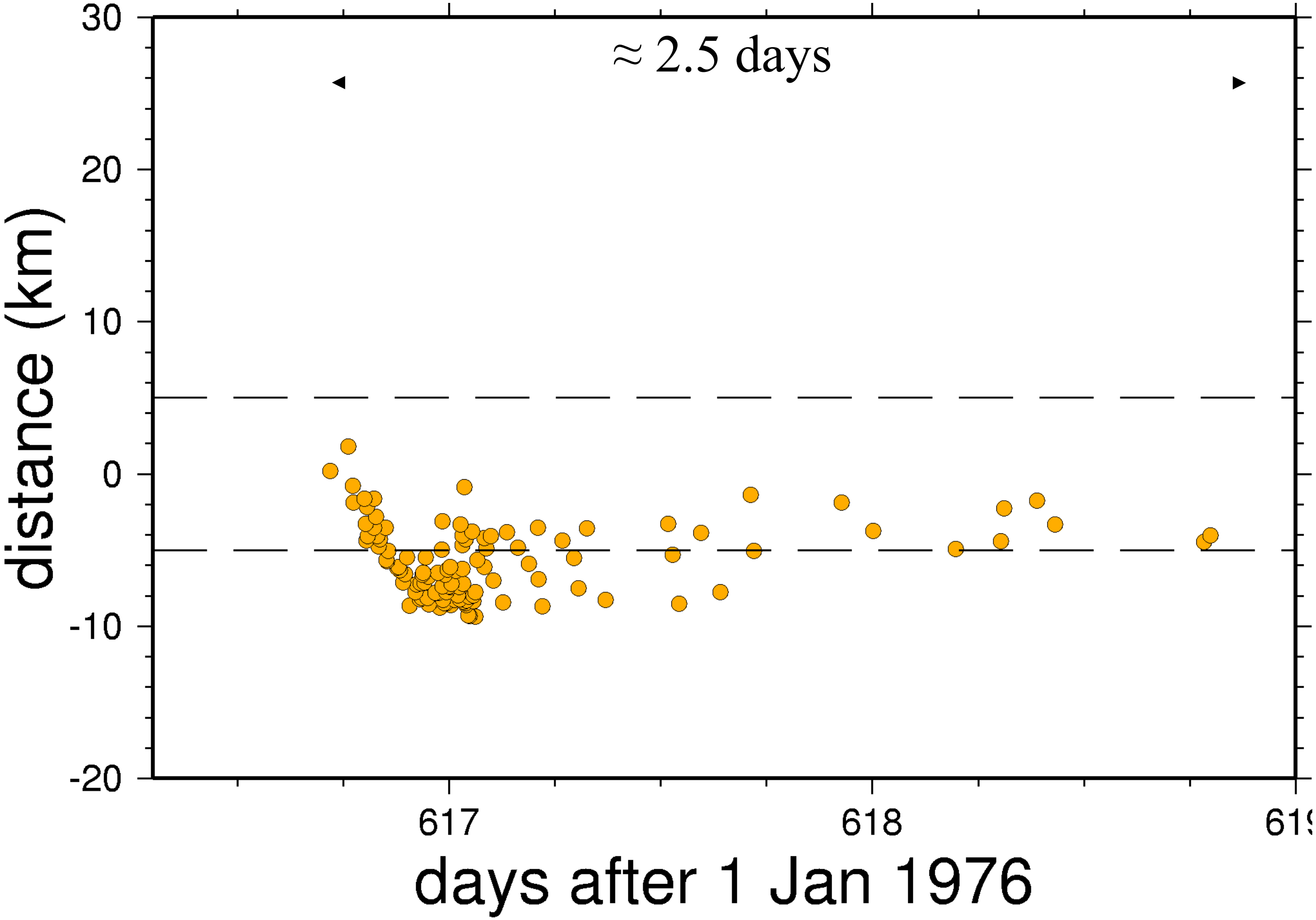

# induced seismicity: Jul 78 intrusion

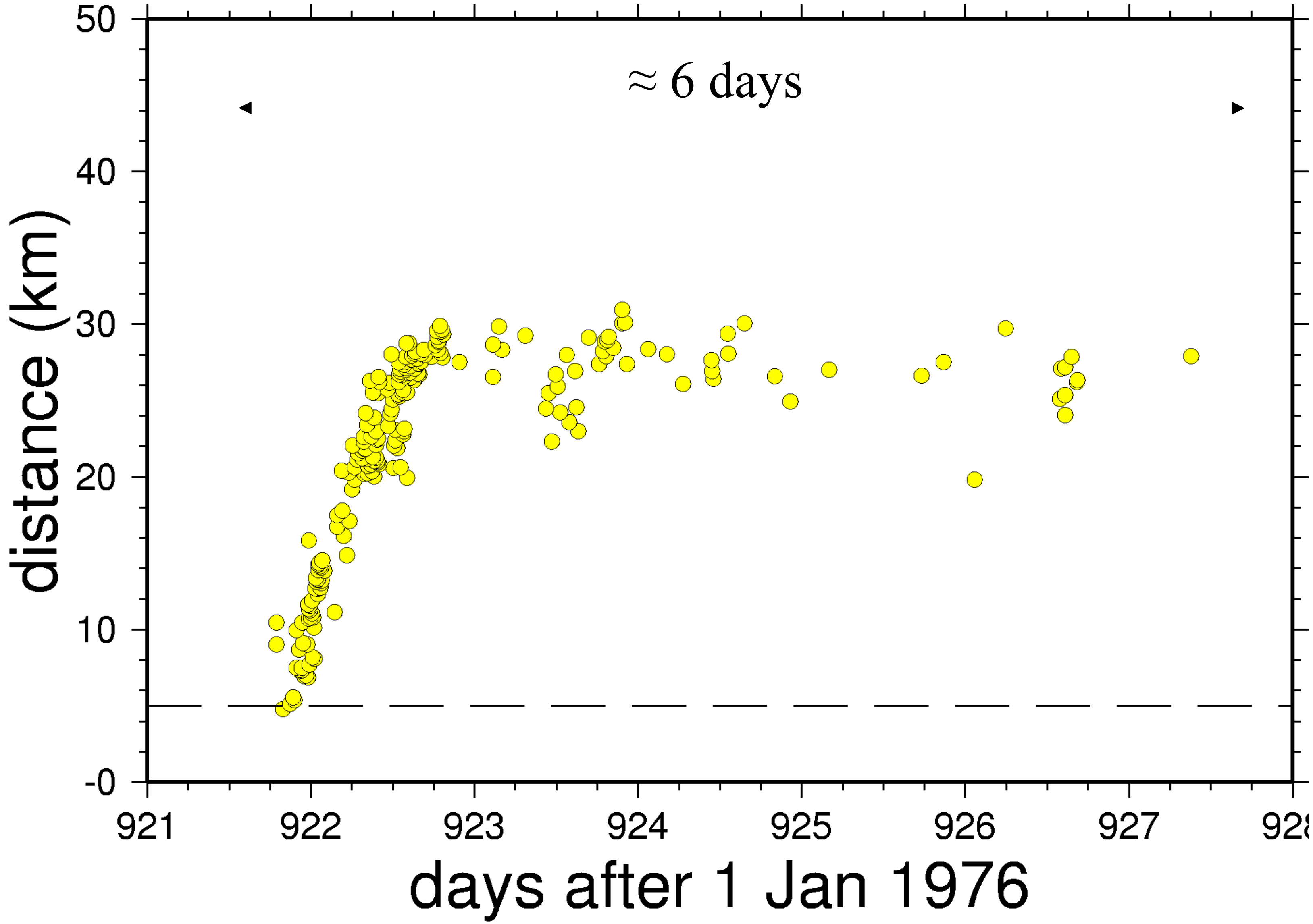

# Questions

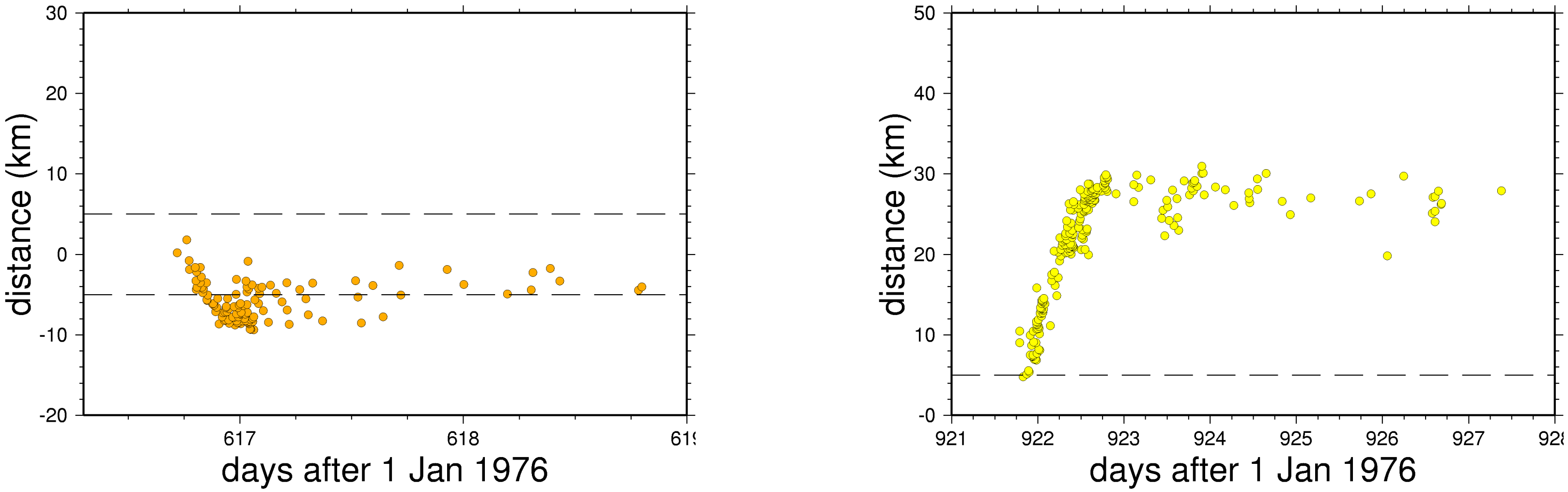


- Why do we observe a one-directional migration of seismicity?
- Why is there a backfront of the seismicity cloud ?
- Can we model the time-dependency of front and backfront?

# Rifting at Krafla: topography may control stress gradients

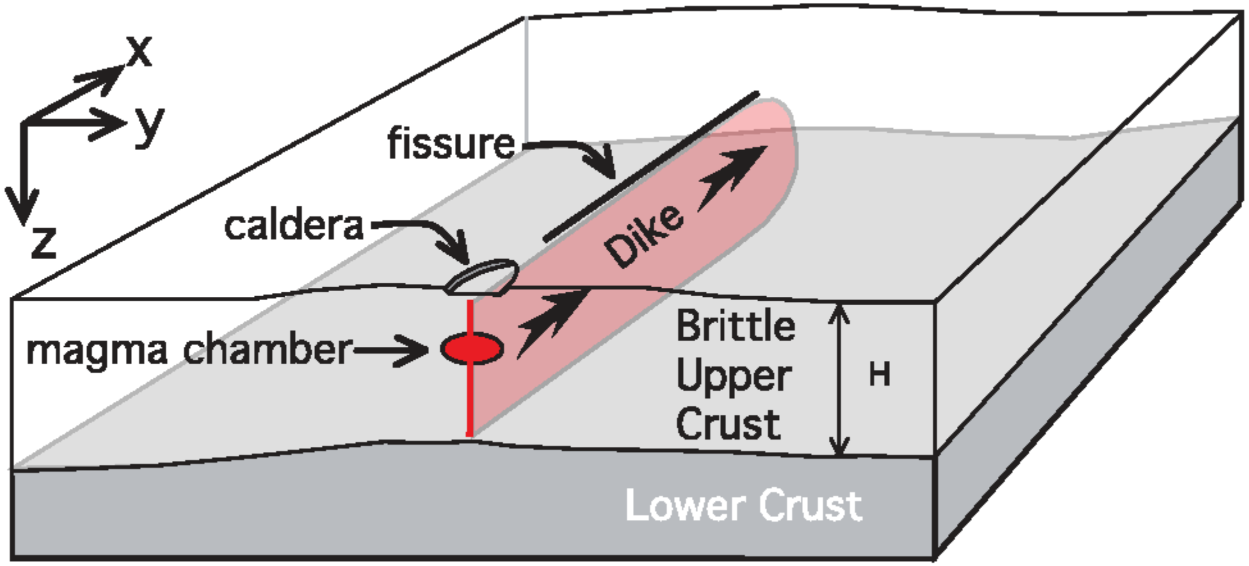


Buck et.al. (2006)

g from infinite slope model with mu=0.25 and rho=2800 kg/m^3

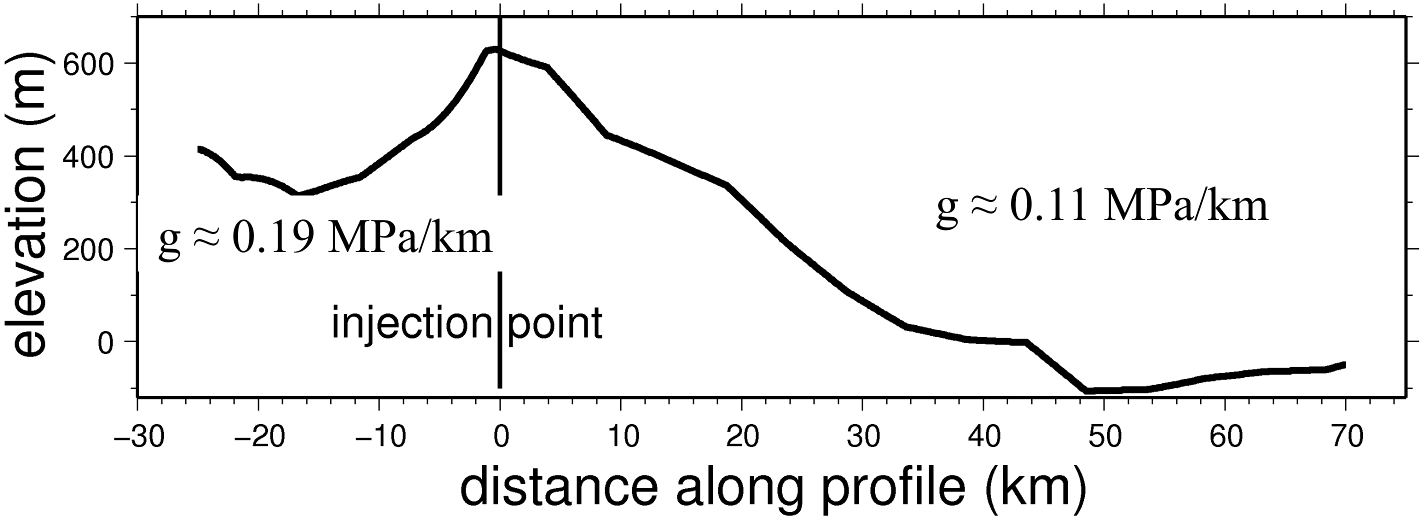

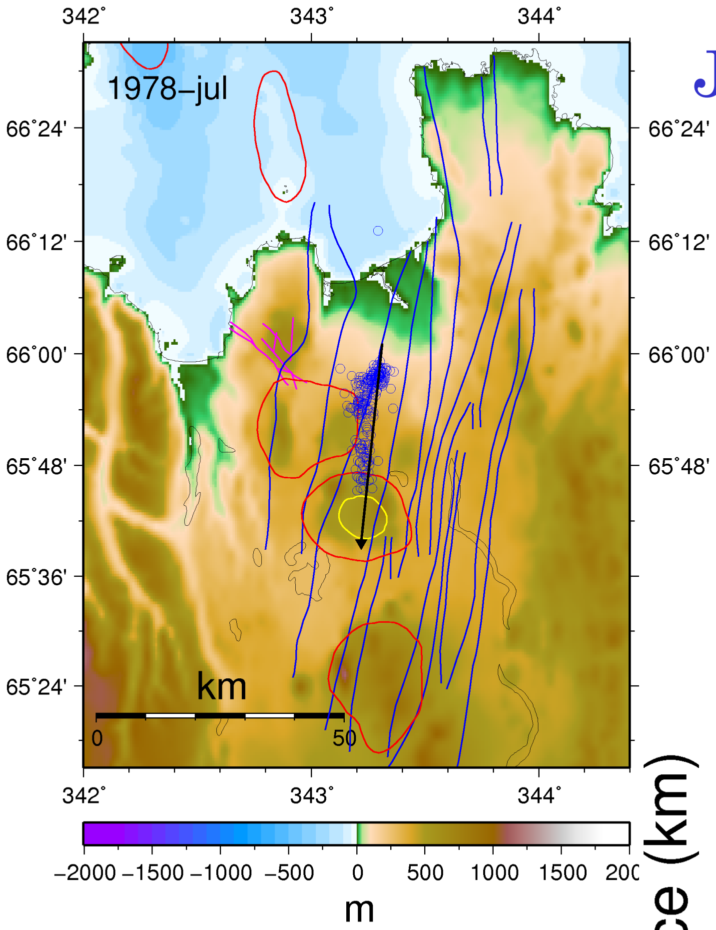


# July 1978 intrusion northward

- self-expansion starts after 9 h
- injection controlled length is 19-22 km
- final length is 34 km
- gap after7 h: re-organisation of flow

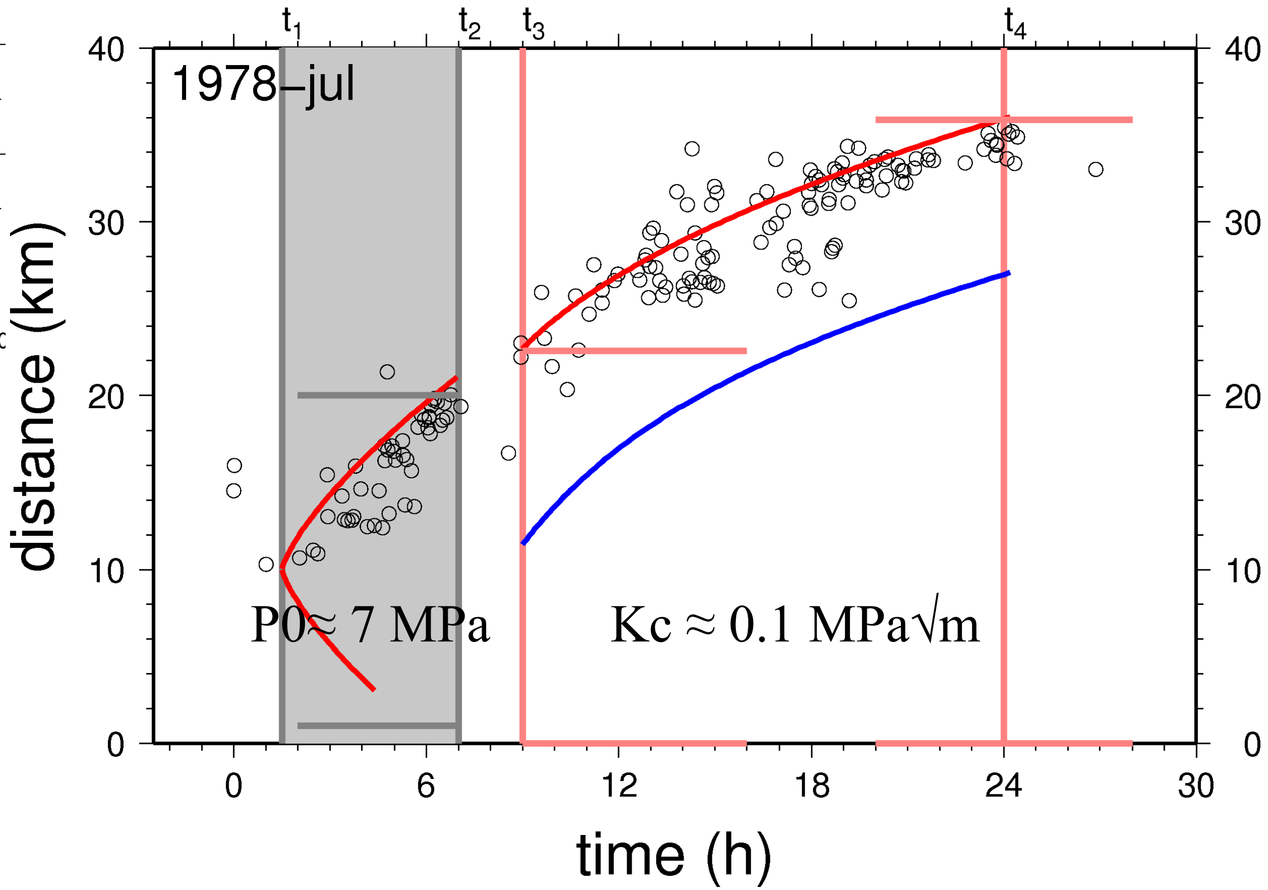


assuming g≈0.11 MPa/km

η ≈ 20 Pa s

# Sep 1977 intrusion southward

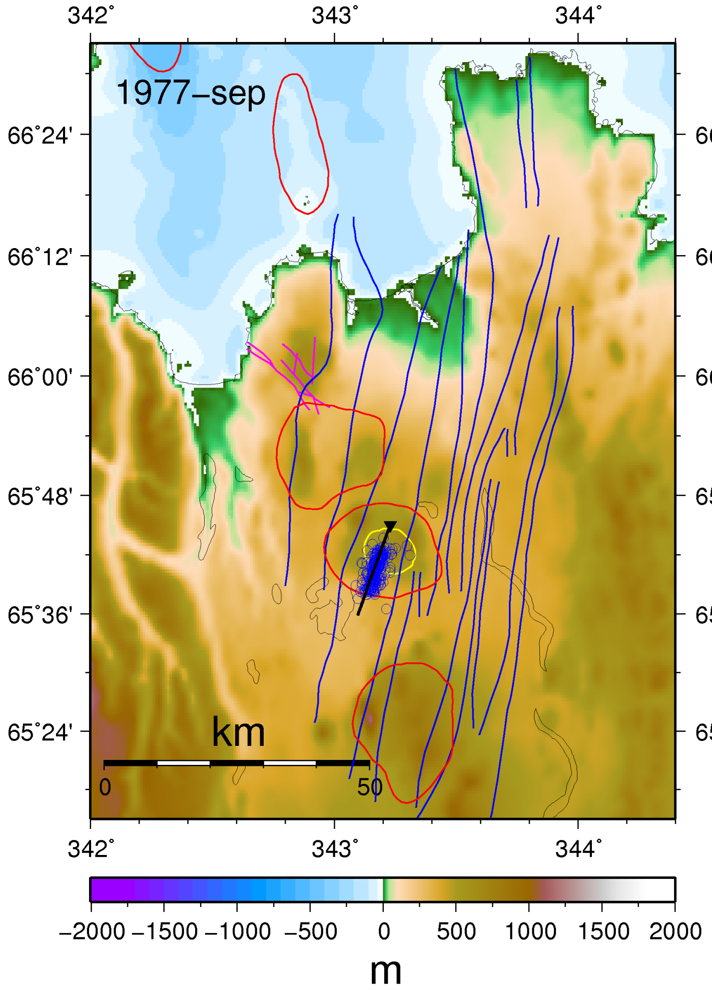


- self-expansion starts after 2.5 h
- injection controlled length ≈ 10 km
- final length is ≈ 15 km

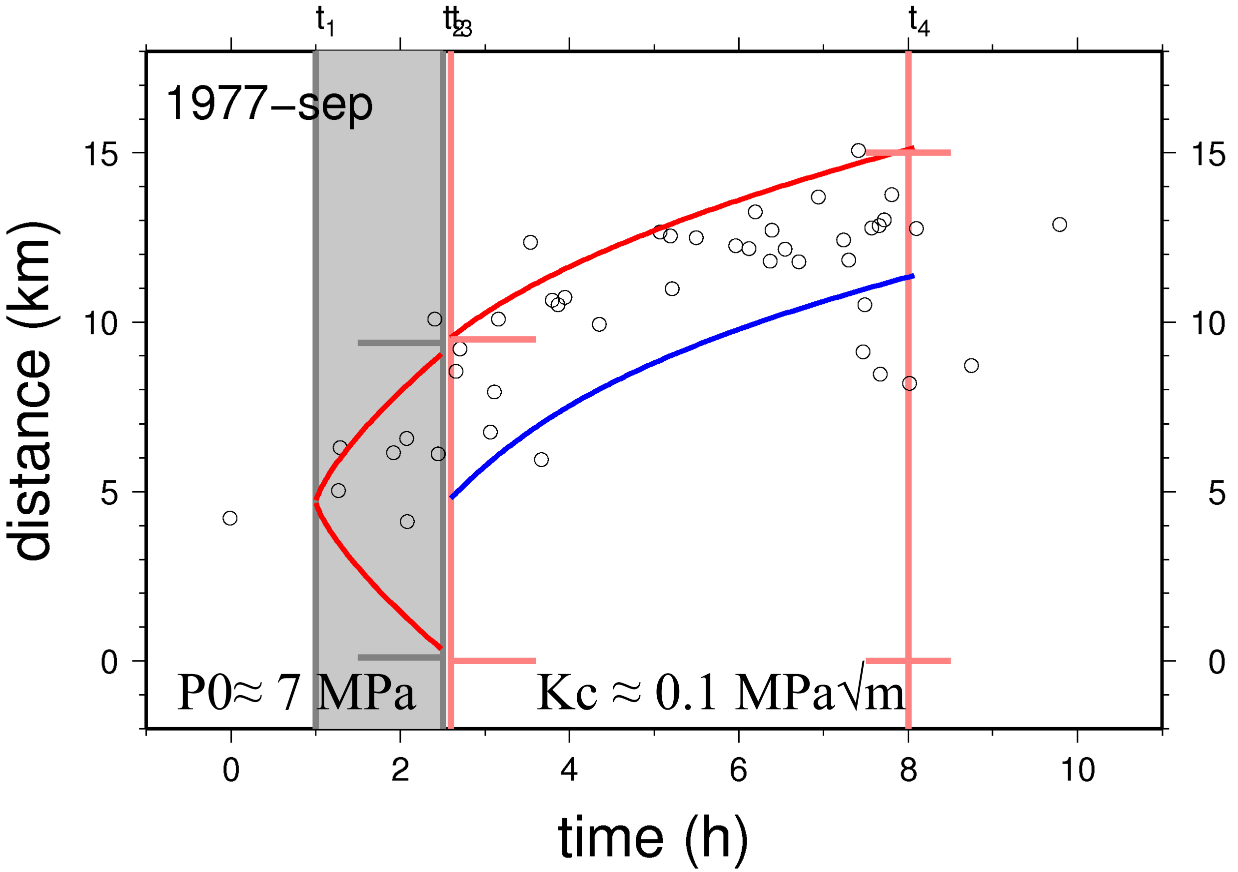


assuming g≈0.19 MPa/km

η ≈ 20 Pa s

# Estimated post-injection driving pressure P3 is only a few kPa

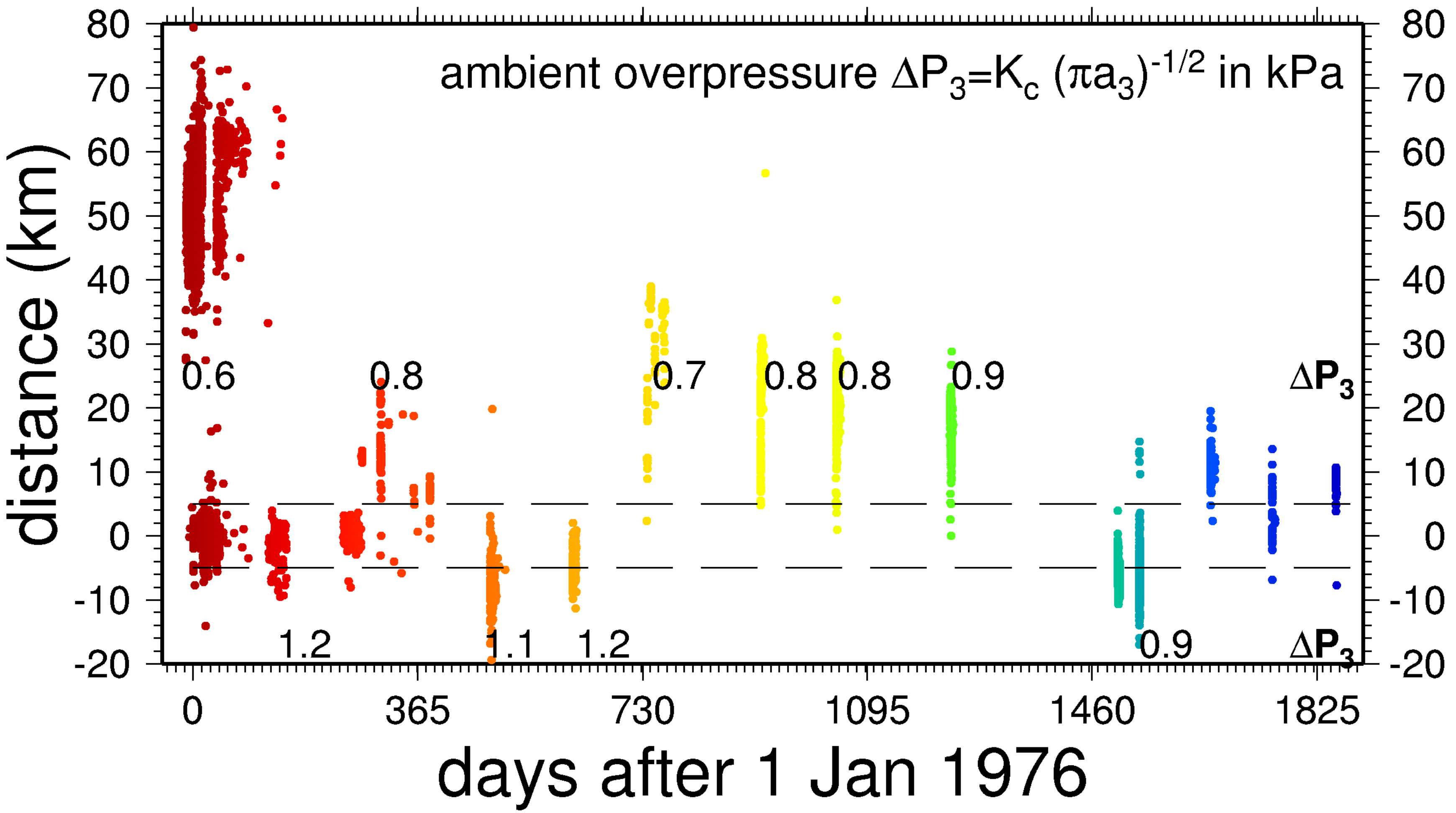

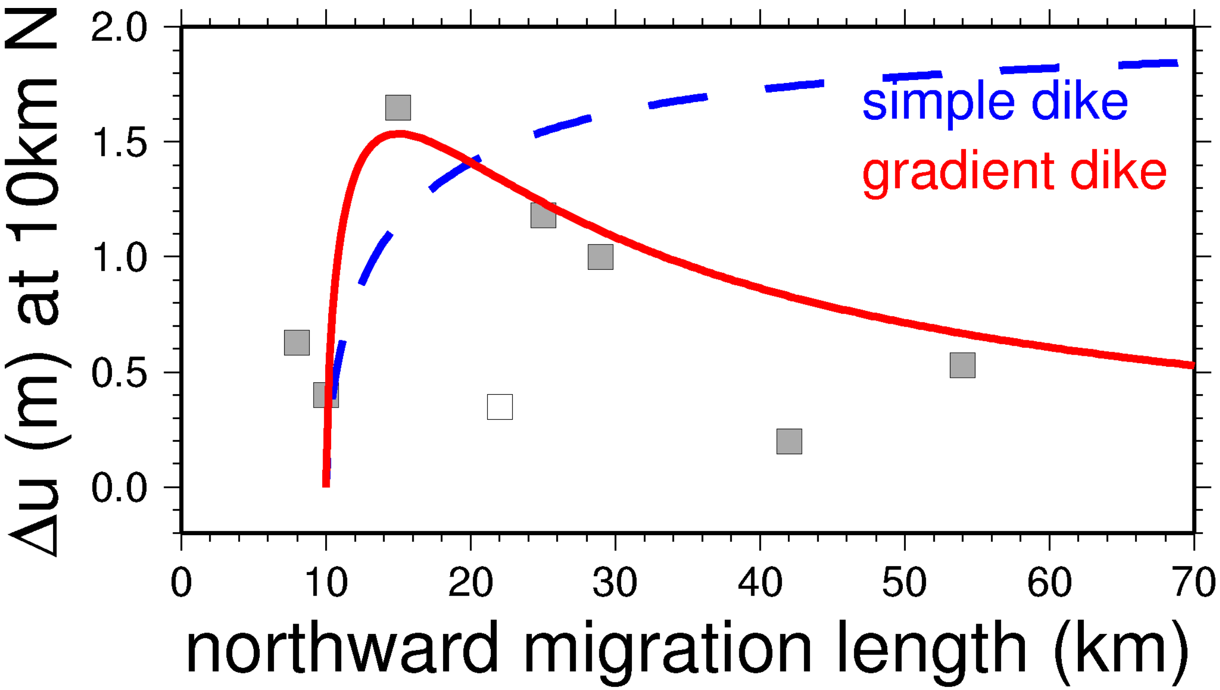


# opening north of caldera: (static model)

data from Tryggvason (1984)

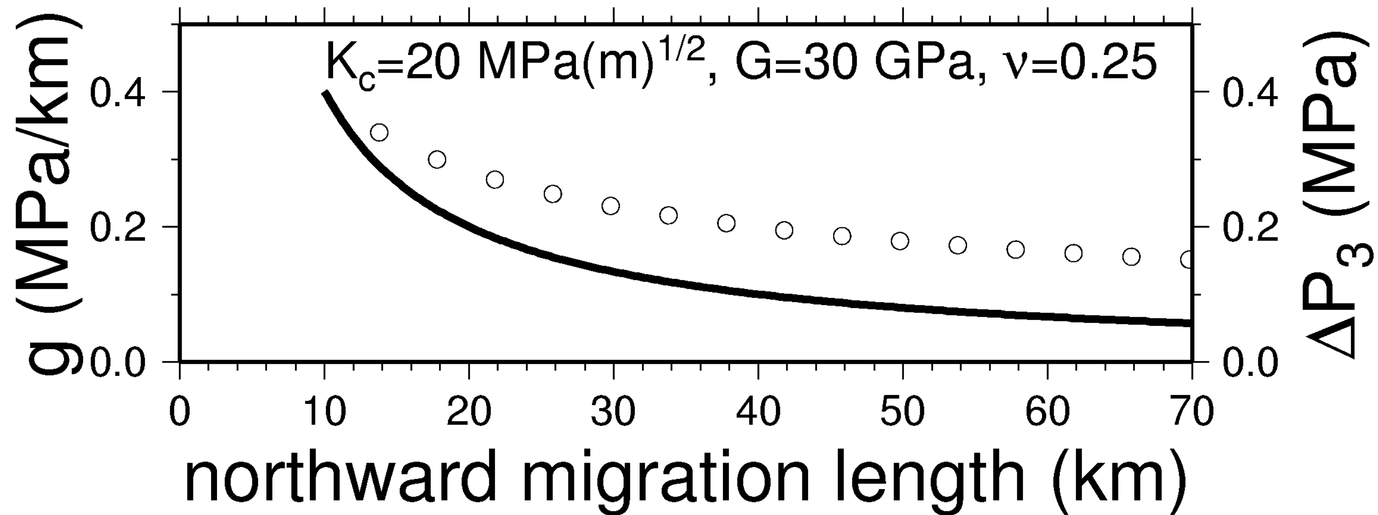

# Results

- Stress-gradient crack-model explains unilateral dike intrusion and seismicity patterns (injection, post-injection phase).
- Overpressure during injection is $\approx$ 7 MPa
- Final ambient overpressure is only $\approx$0.2 MPa
- Largest opening is far from Caldera
- Kc to stop dikes is $\approx$ 50 MPa $\sqrt{m}$
- Kc during re-injection is $\approx$ 0.1 MPa $\sqrt{m}$
- g possibly decreased with distance to Caldera

# Case III

Slow natural intrusions

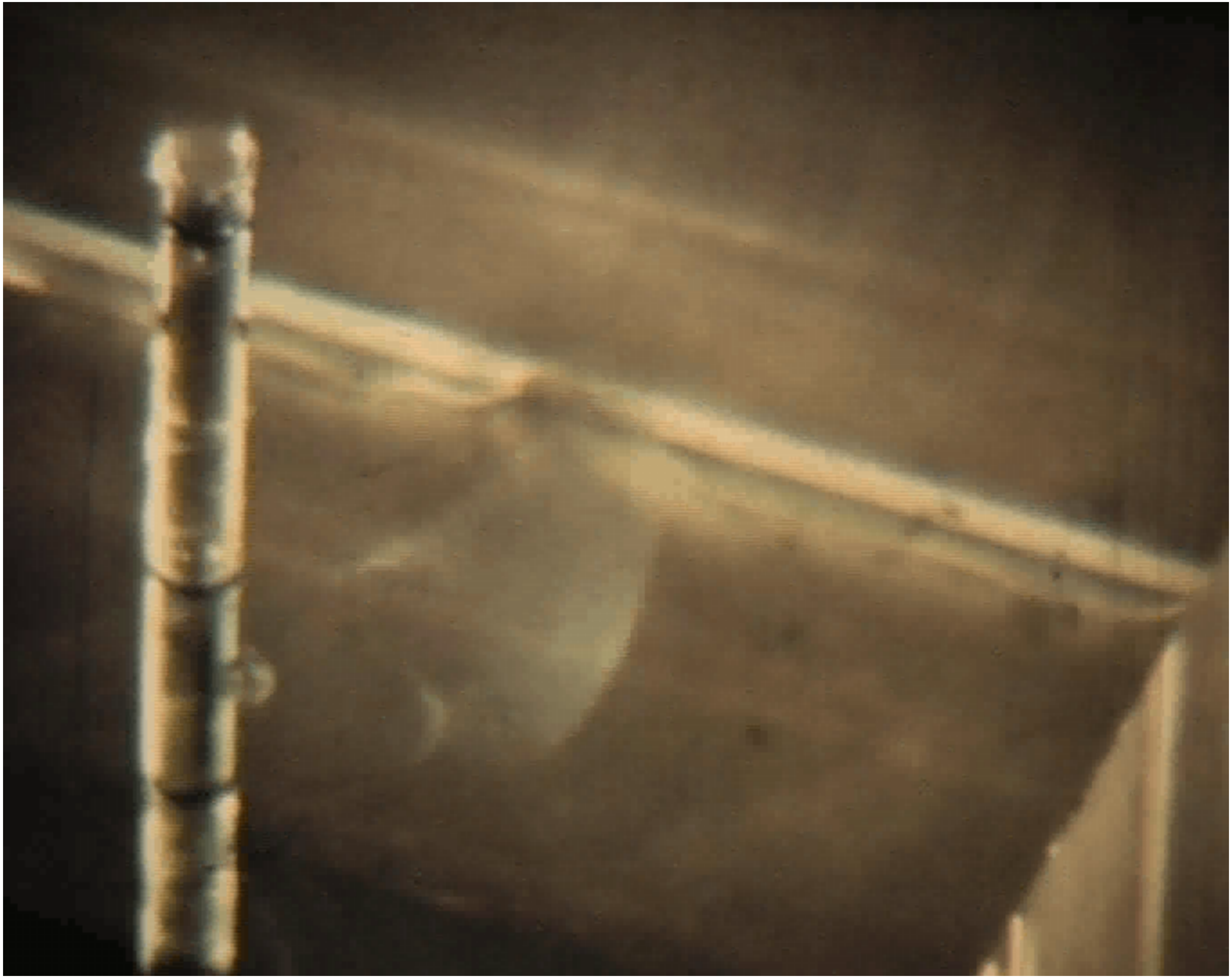

# Hydrofrac in plexiglass

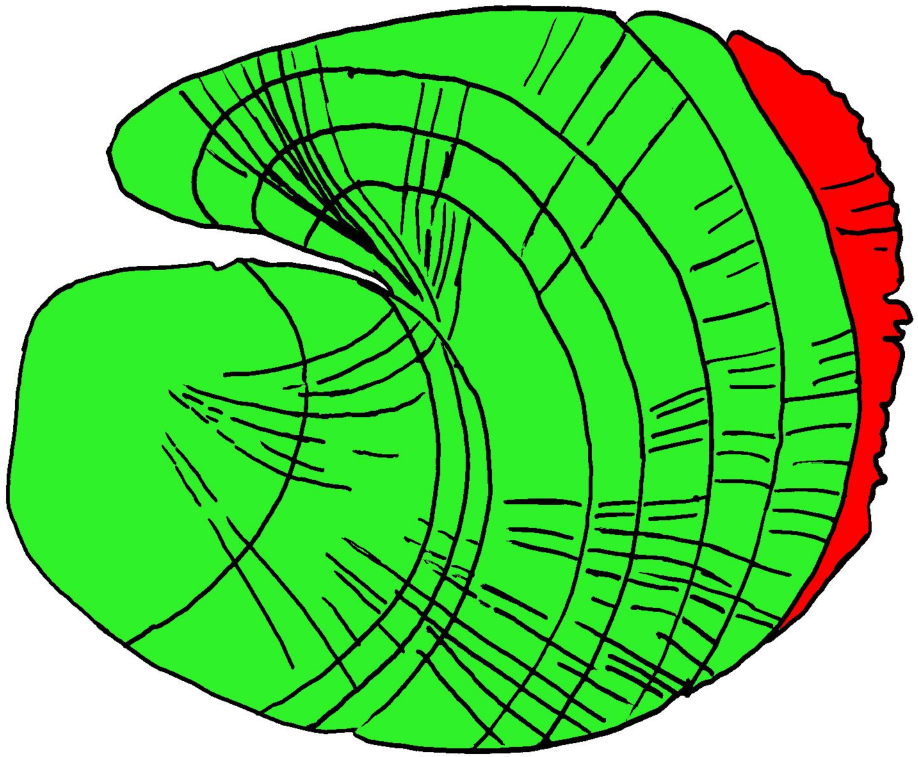

- episodic path-like growth of the fracture
- final shape is circular or ellitpical

# Example A: Izu Bonin Magma Intrusion Apr 2000

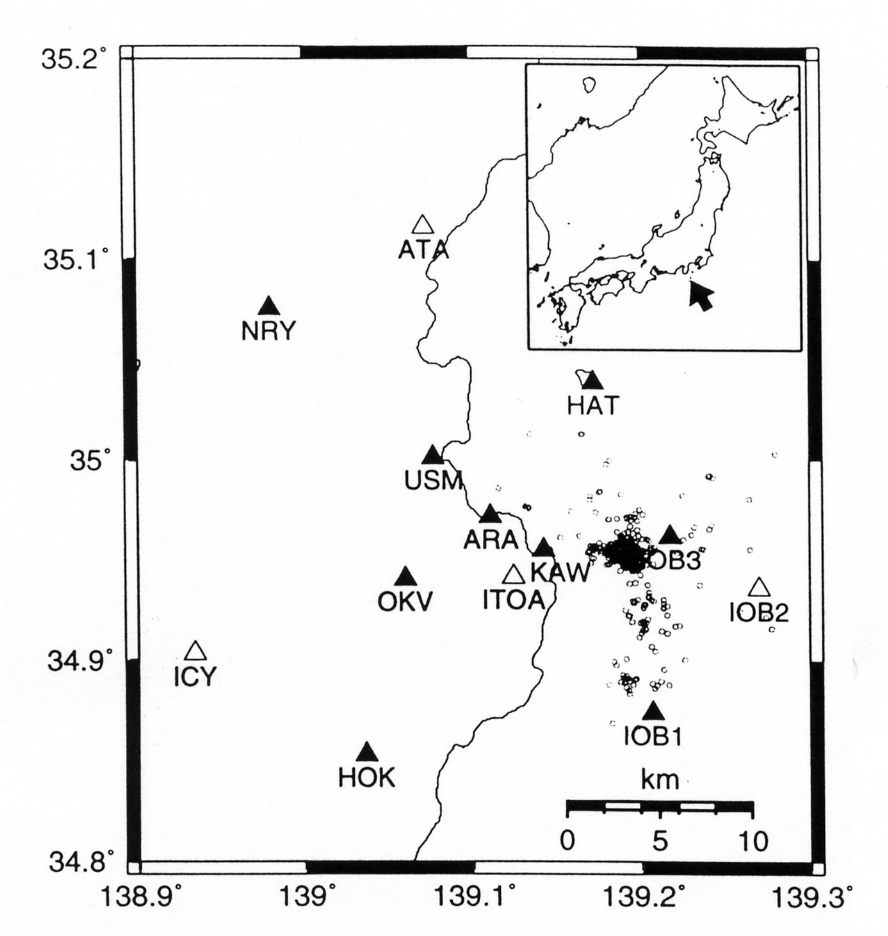


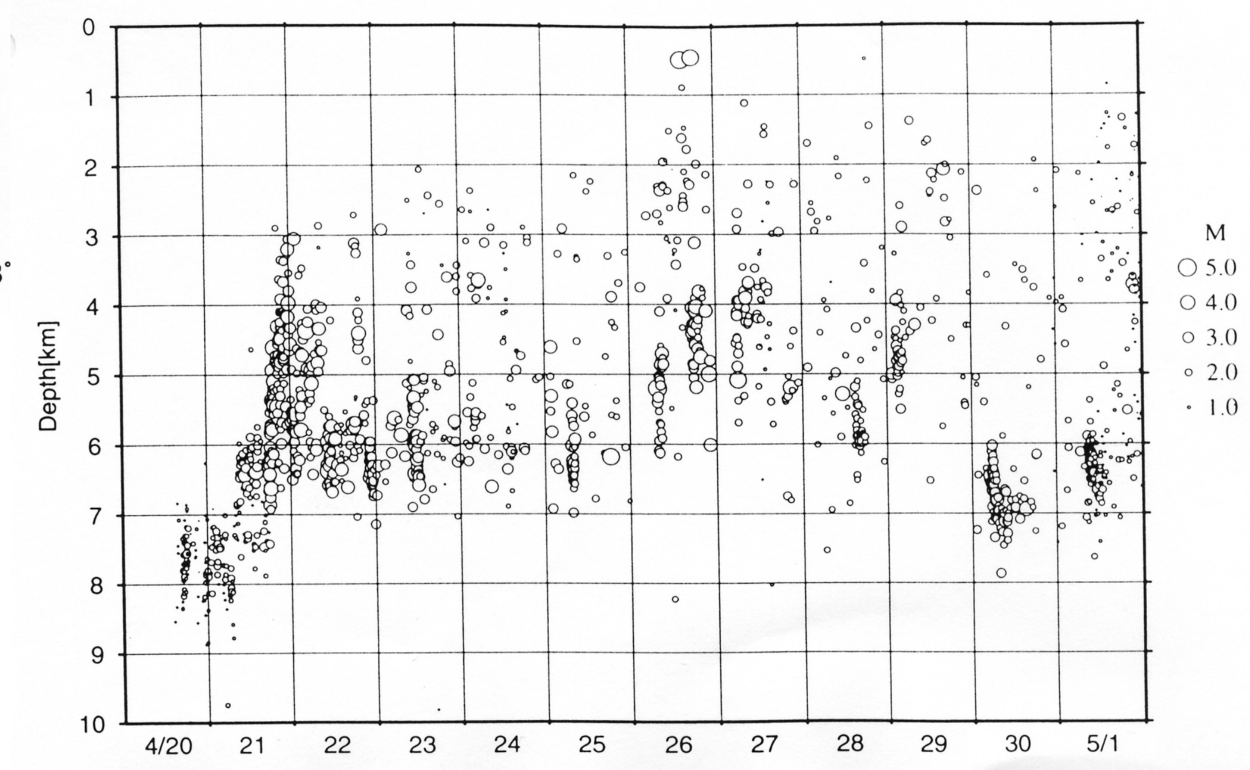


time (days)

Hayashi & Morita (2002): A magma intrusion process inferred from hypocenter migration of earthquake swarms, GJI

# Penny-shaped hypocenter pattern

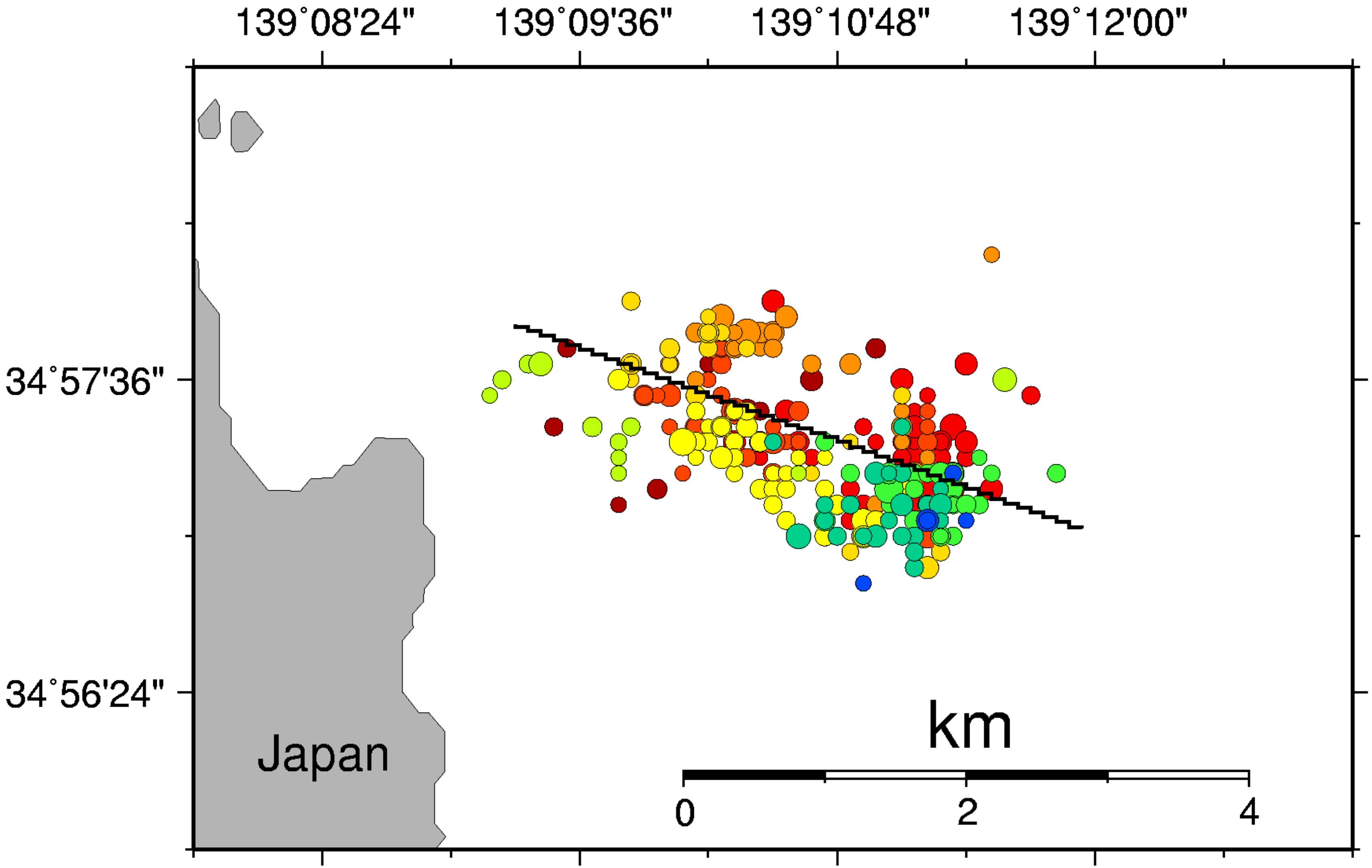

# Penny-shaped hypocenter pattern

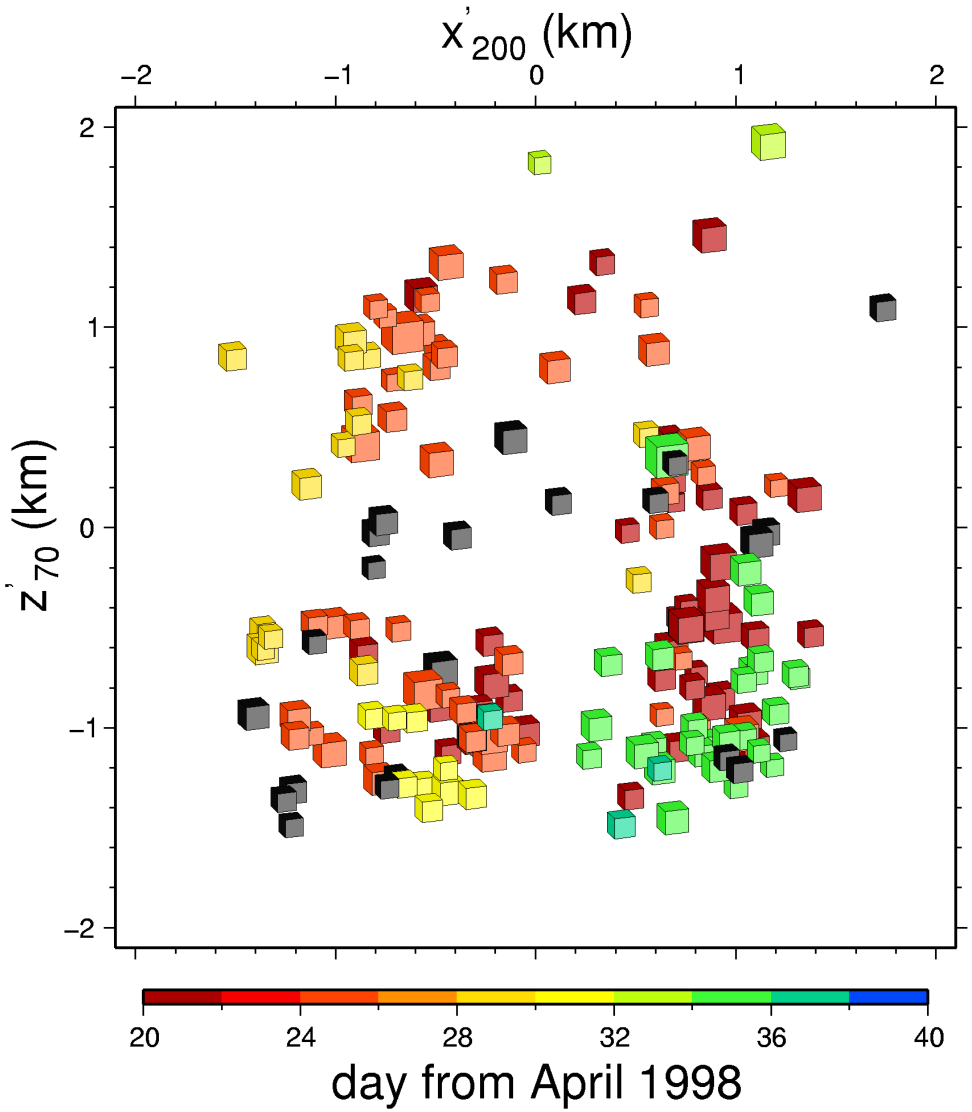

# Penny-shaped hypocenter pattern

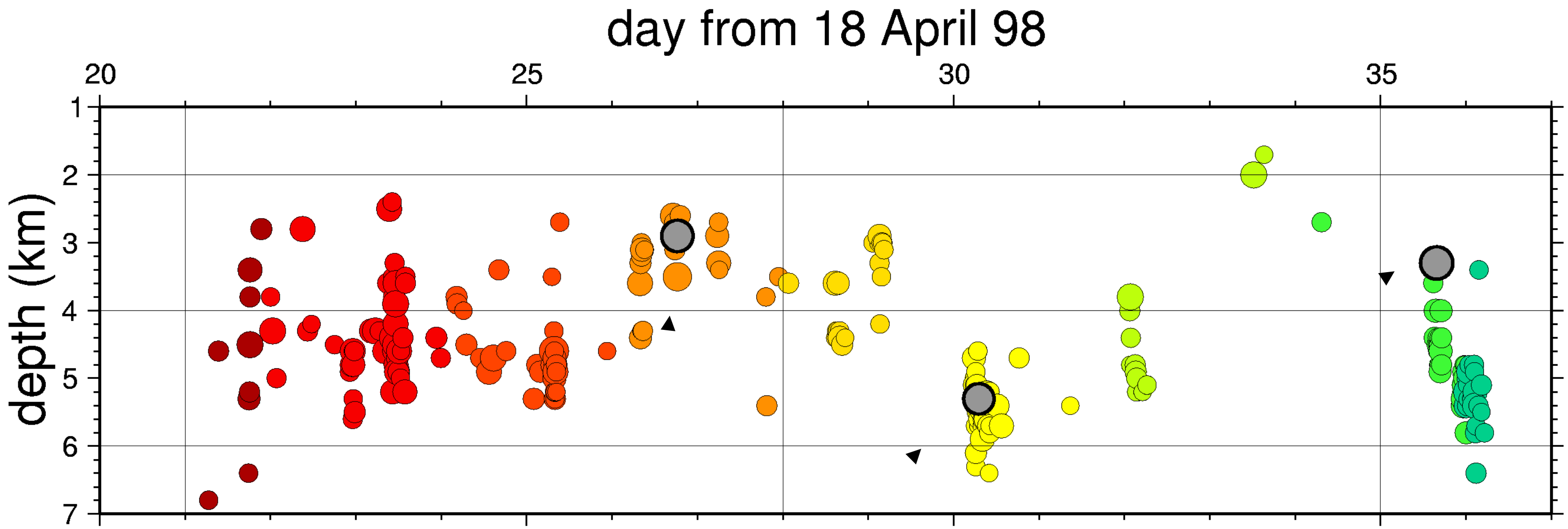


strongest events occur at the end of the sequence

maximal magnitudes ≈ M 4.5

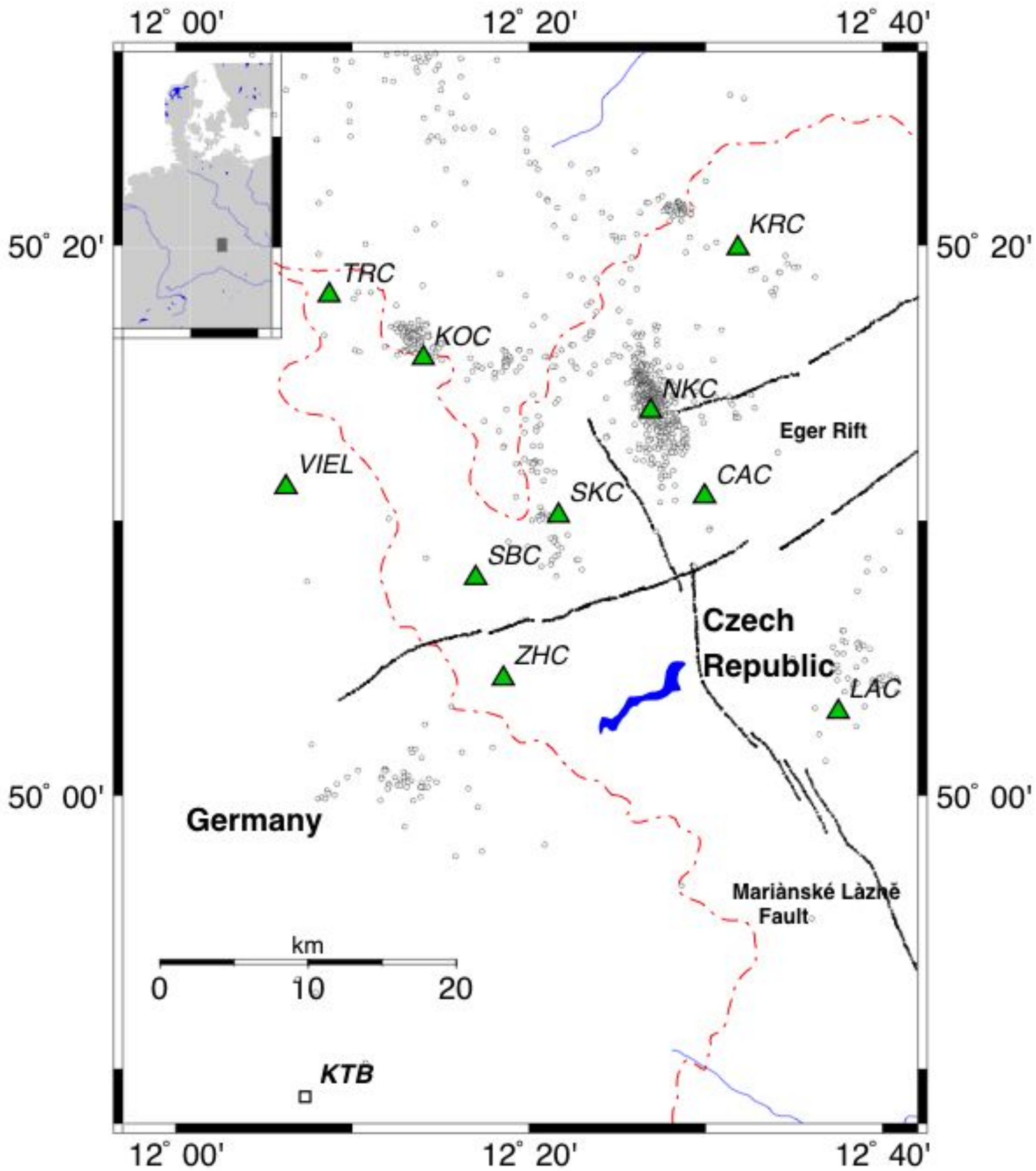


# Example B: Earthquake swarm NW-Bohemia 2000

several 100 events in 2 month

Max Ml ≈ 3

Hypo depth ≈ 8 km

# “Weekly” migration of hypocenters

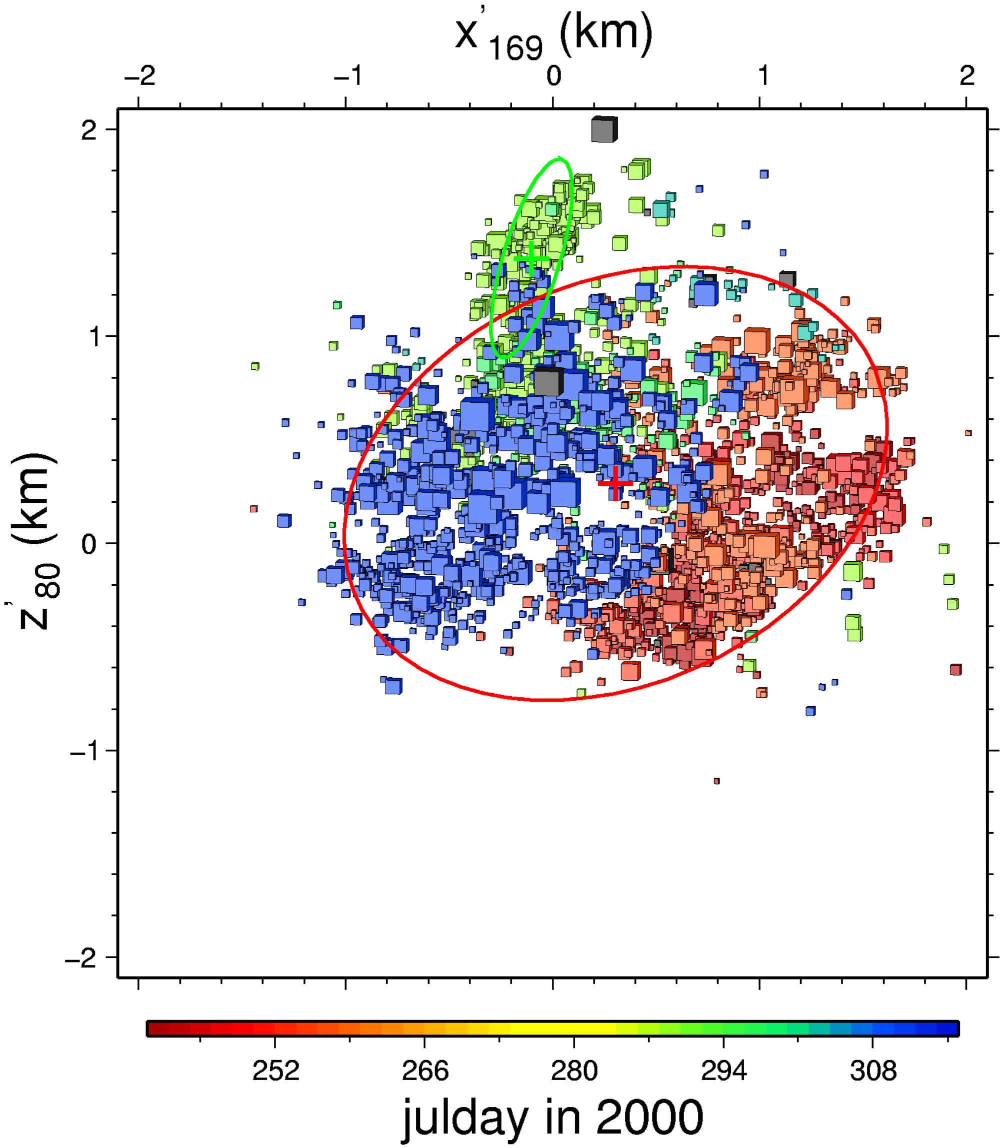

# Elliptical crack develops under mixed loading

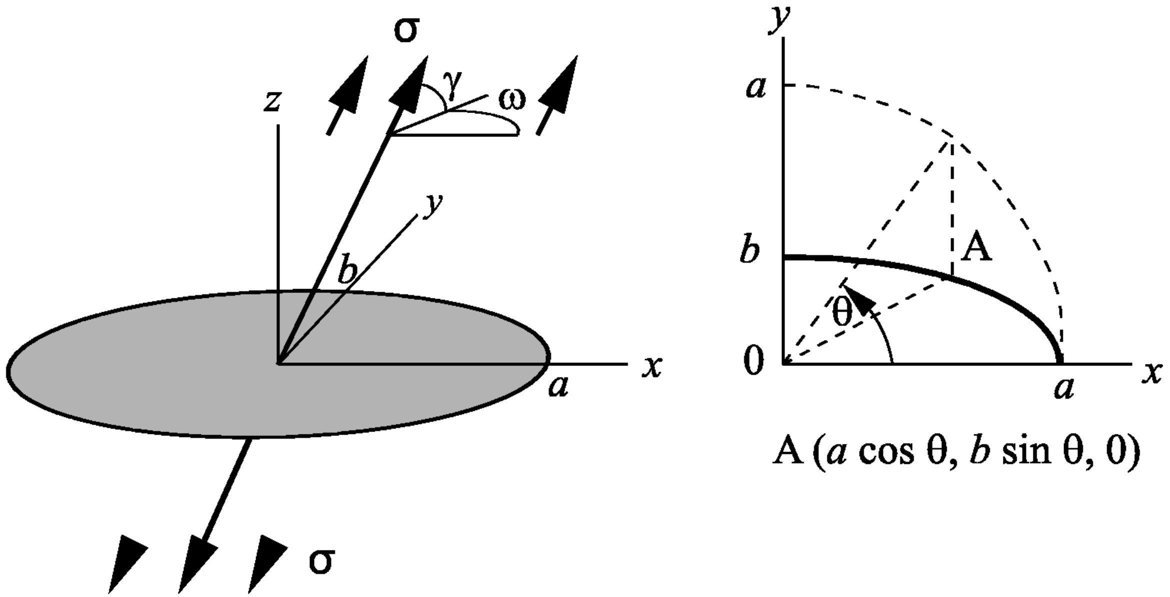


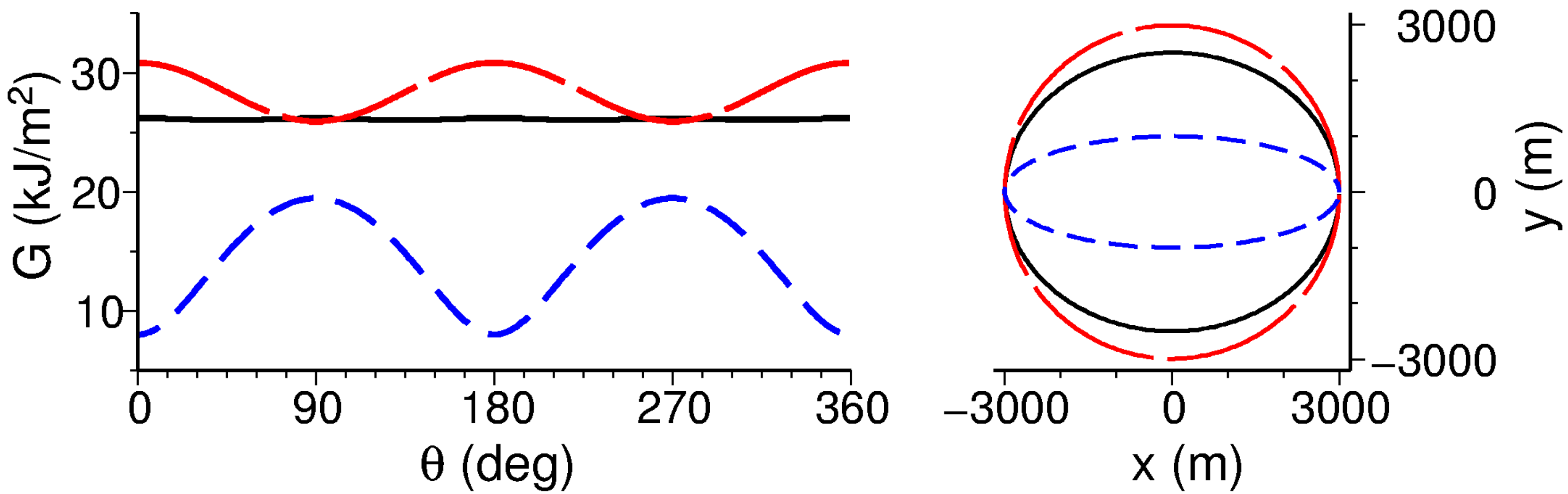


Dahm, Fischer and Hainzl (2008), Studia Geofisica

# strongest events at the end of the sequence

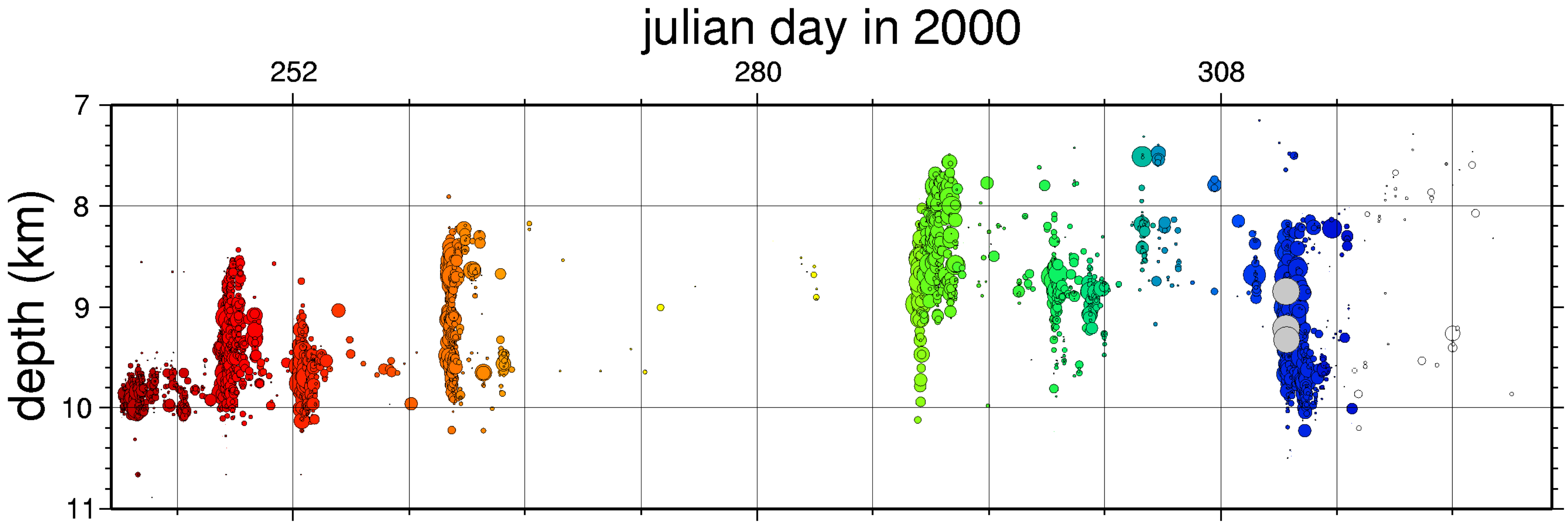

# “scaling relations” of intrusion-induced seismicity ?

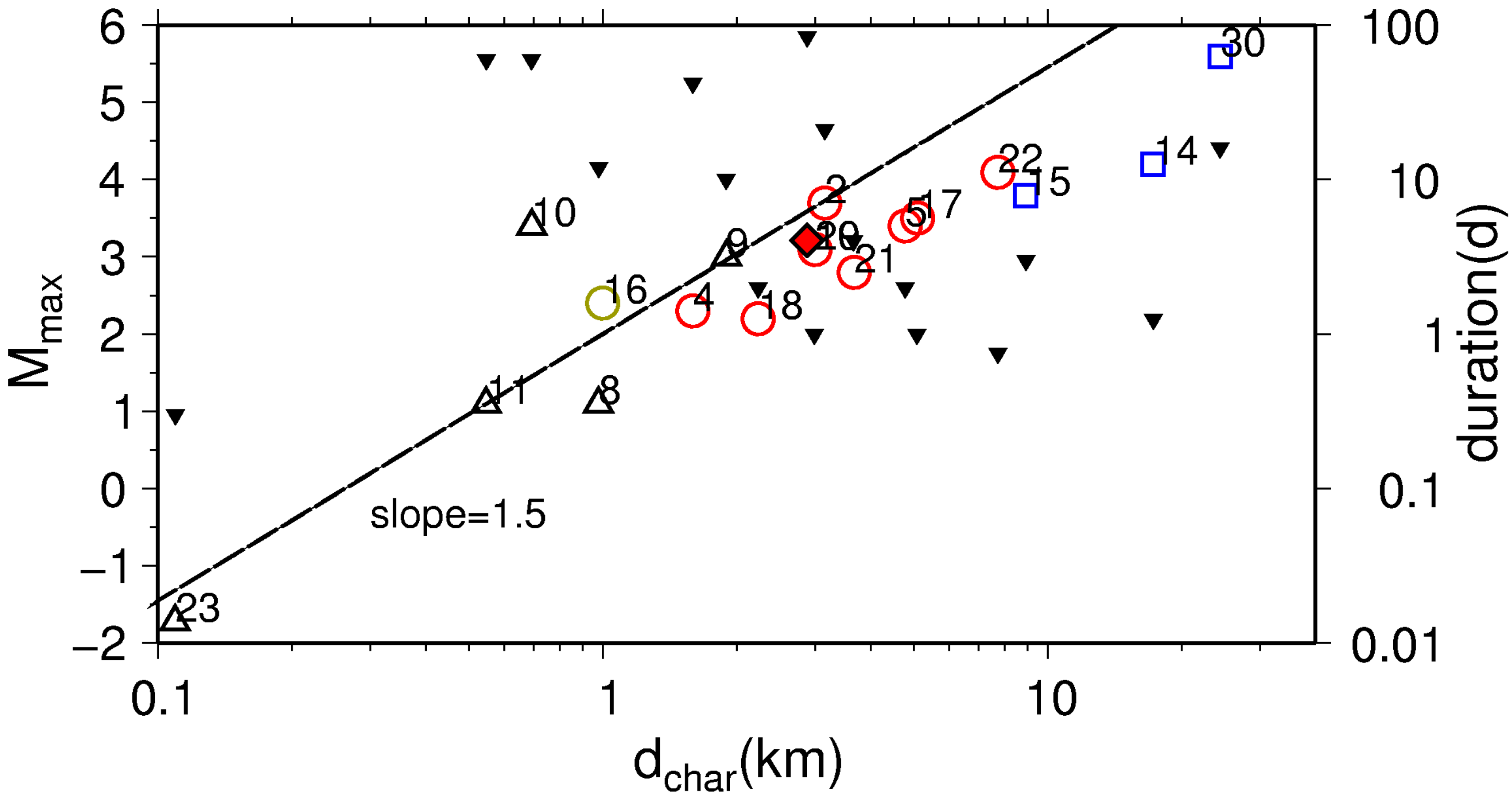


Dahm, Fischer and Hainzl (2008), Studia Geofisica

# Summary of fluid-fracture growth

1. Fluid-filled fractures (non-buoyant) grow towards circular or elliptical final shape
2. The growth is episodic and discontinuous when the overpressure is small
3. Tendency that strongest induced earthquakes occur at the end of fracture growth

# Case IV

## Gas field depletion

# Trigger potential outside the reservoir

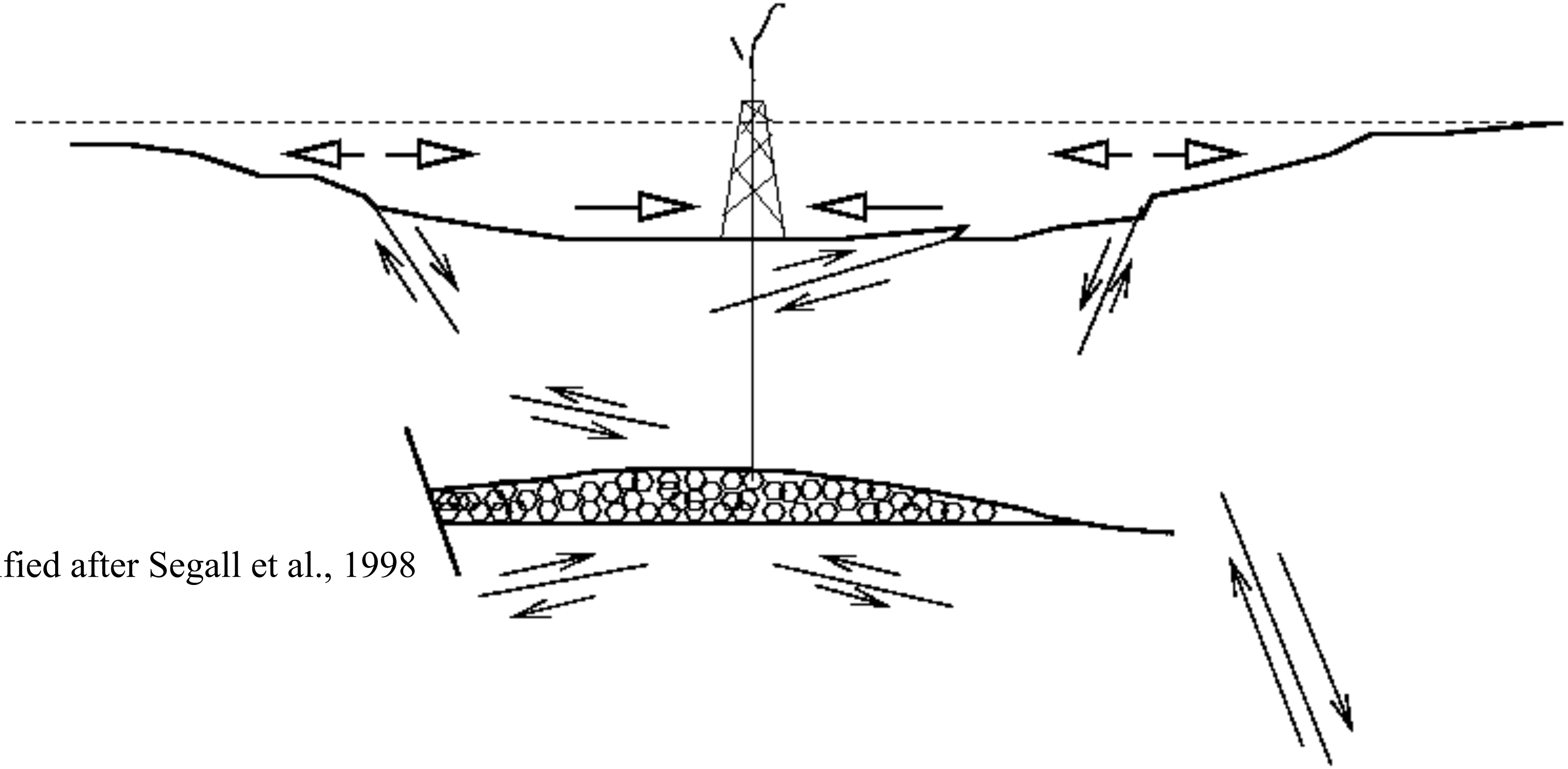

modified after Segall et al., 1998

- Can distant earthquakes be triggered and what is mechanical evidence?
- Can seismic trigger potential be estimated ?

# Outline

1. numerical method to calculate subsidence and stress
2. kinematic rupture of induced earthquakes
3. comparison of rupture and stress field

# 3D boundary element method (in-house)

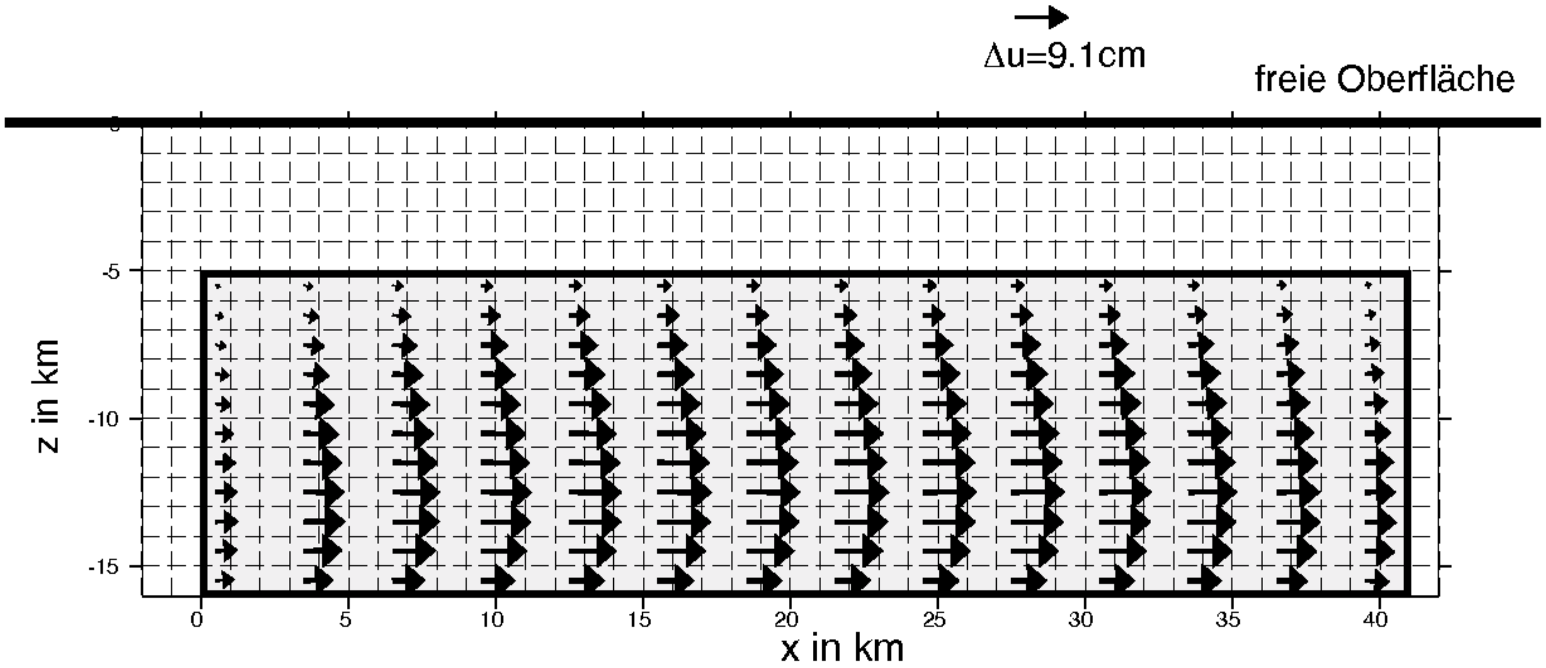


shear stress linearly growing with depth

# Simulation of deflating penny shaped cracks

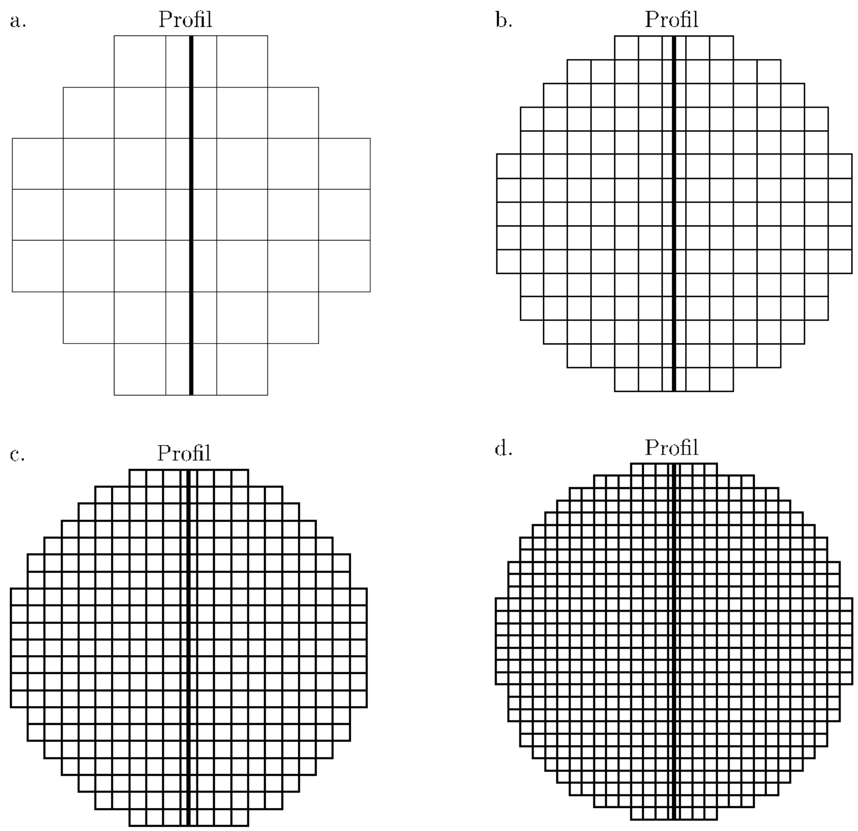

# Accounting for internal porous field effect

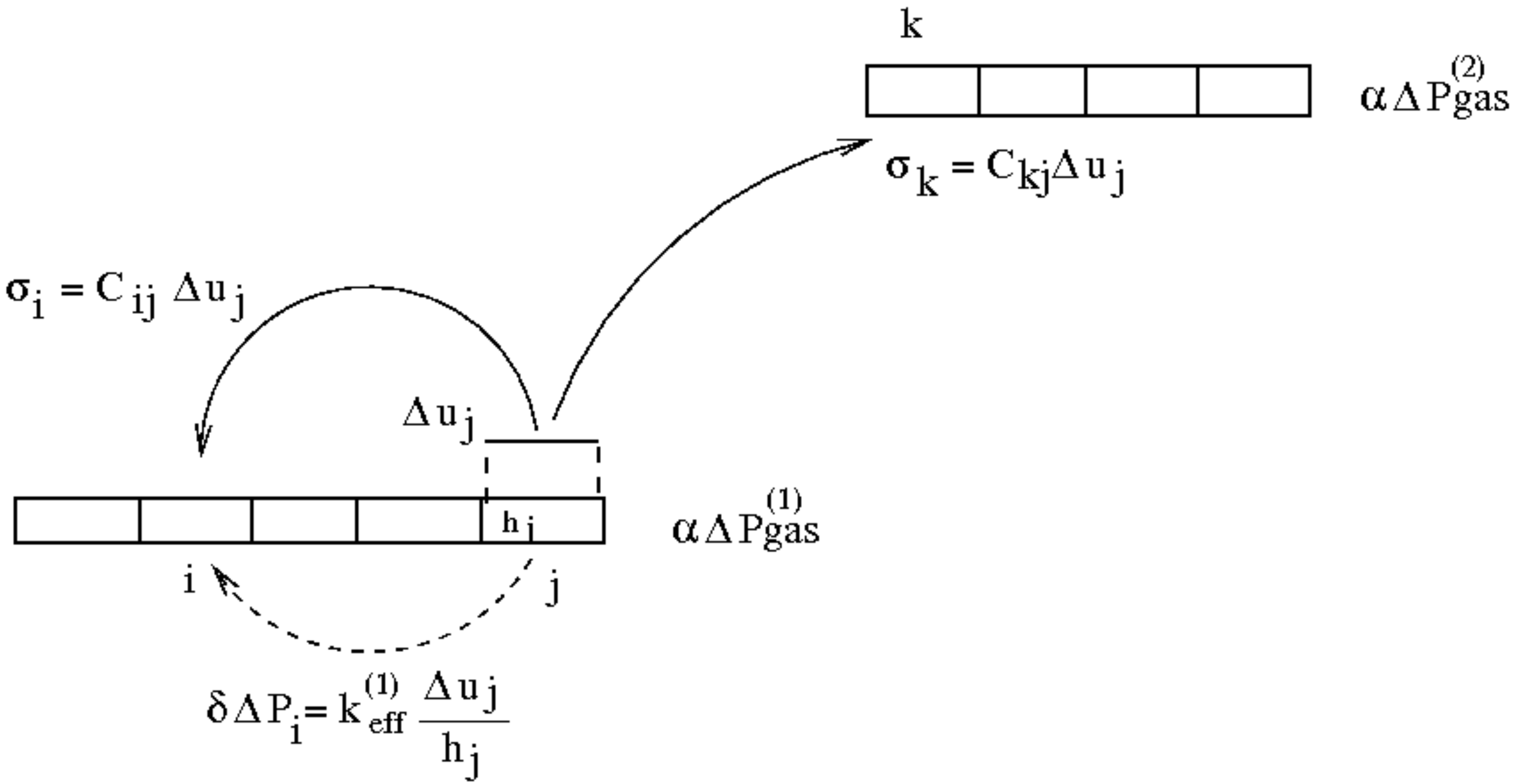

# Comparison to Geertma's disk reservoir

## z=4km, h=200m, ΔP=30MPa, k=16GPa, alpha=1

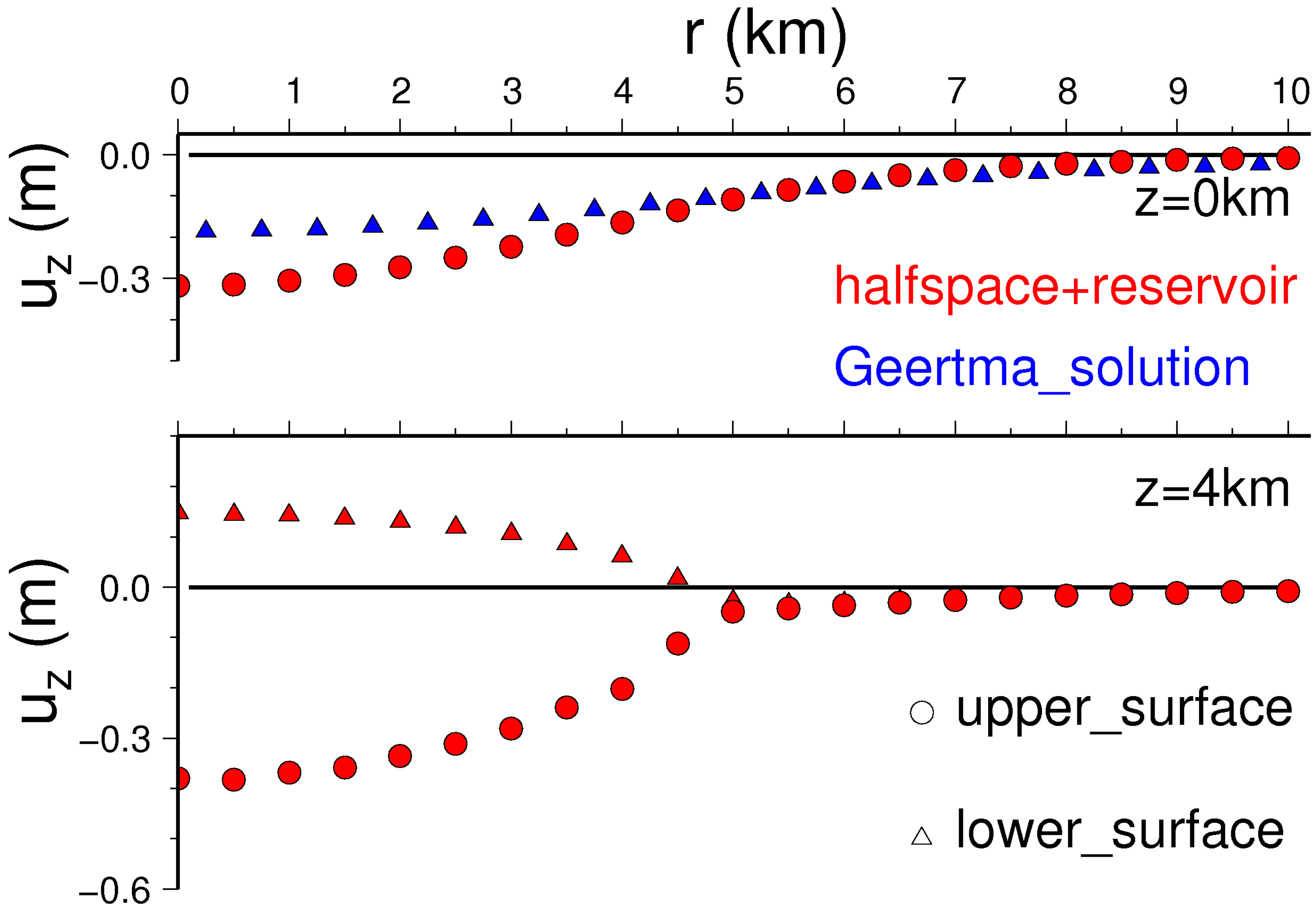

# The Ekofisk oil field subsidence bowl

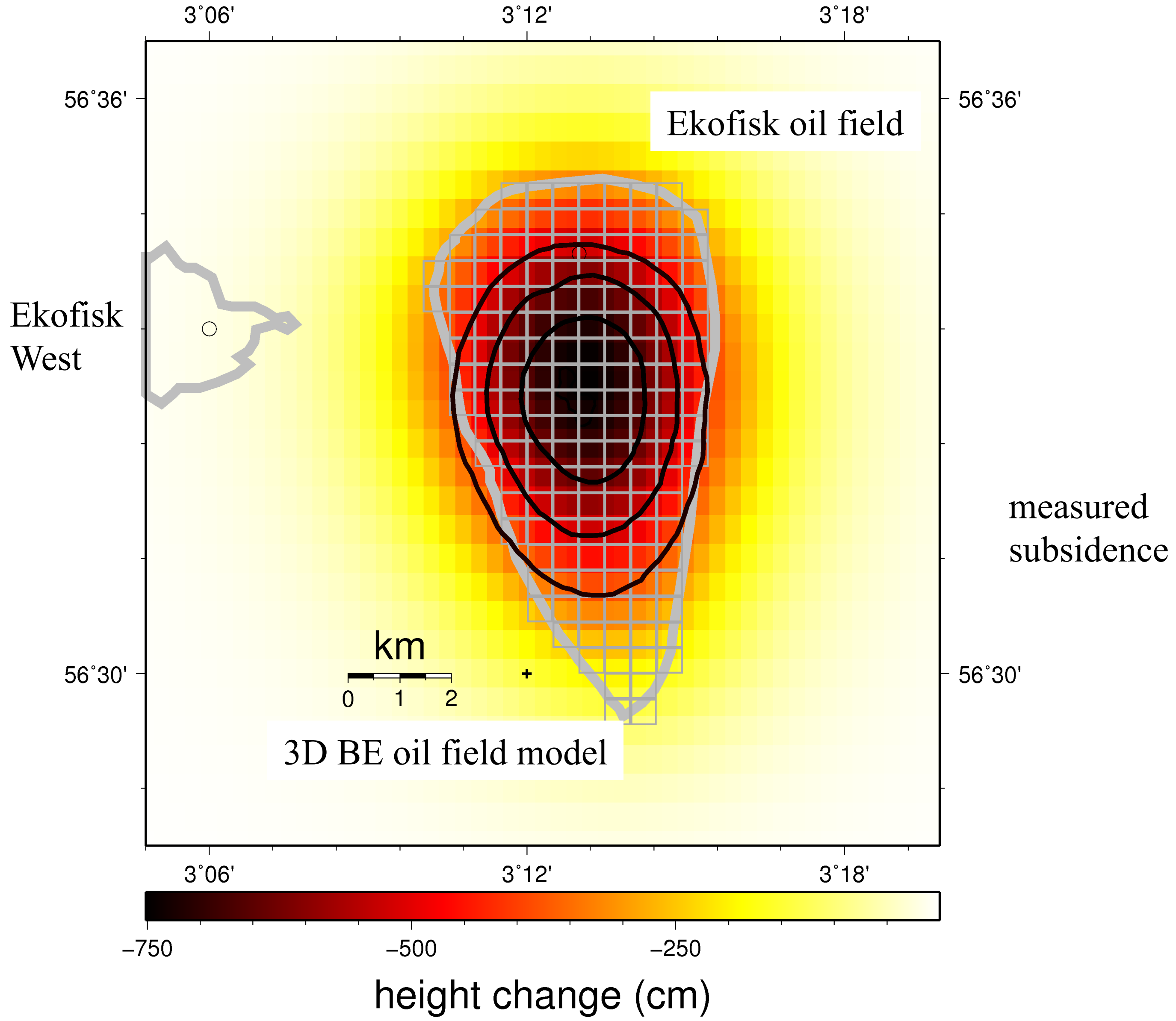

# Ekofisk: Depletion induced stress

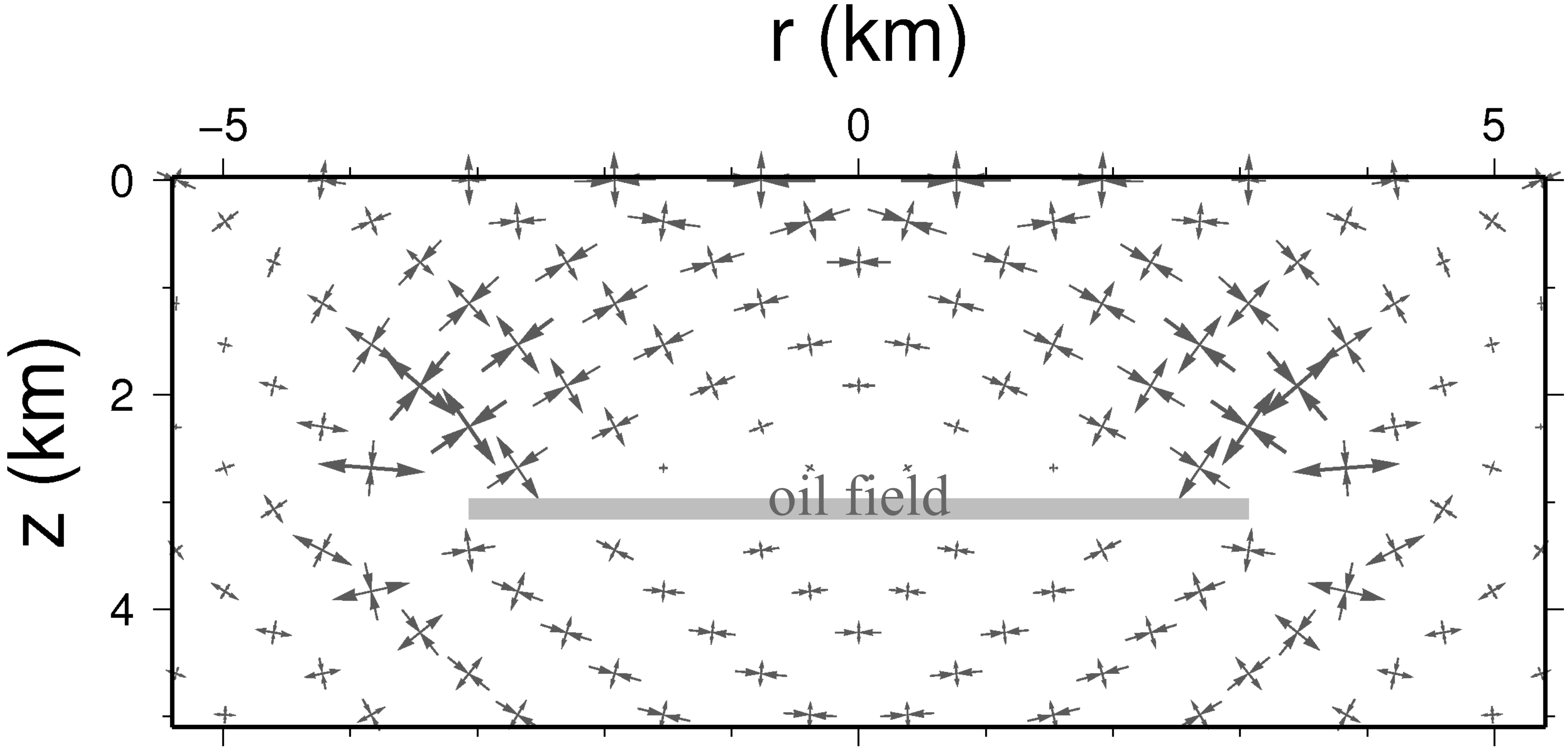


depletion-induced stress

# The Ekofisk 2001 M 4.2 induced earthquake

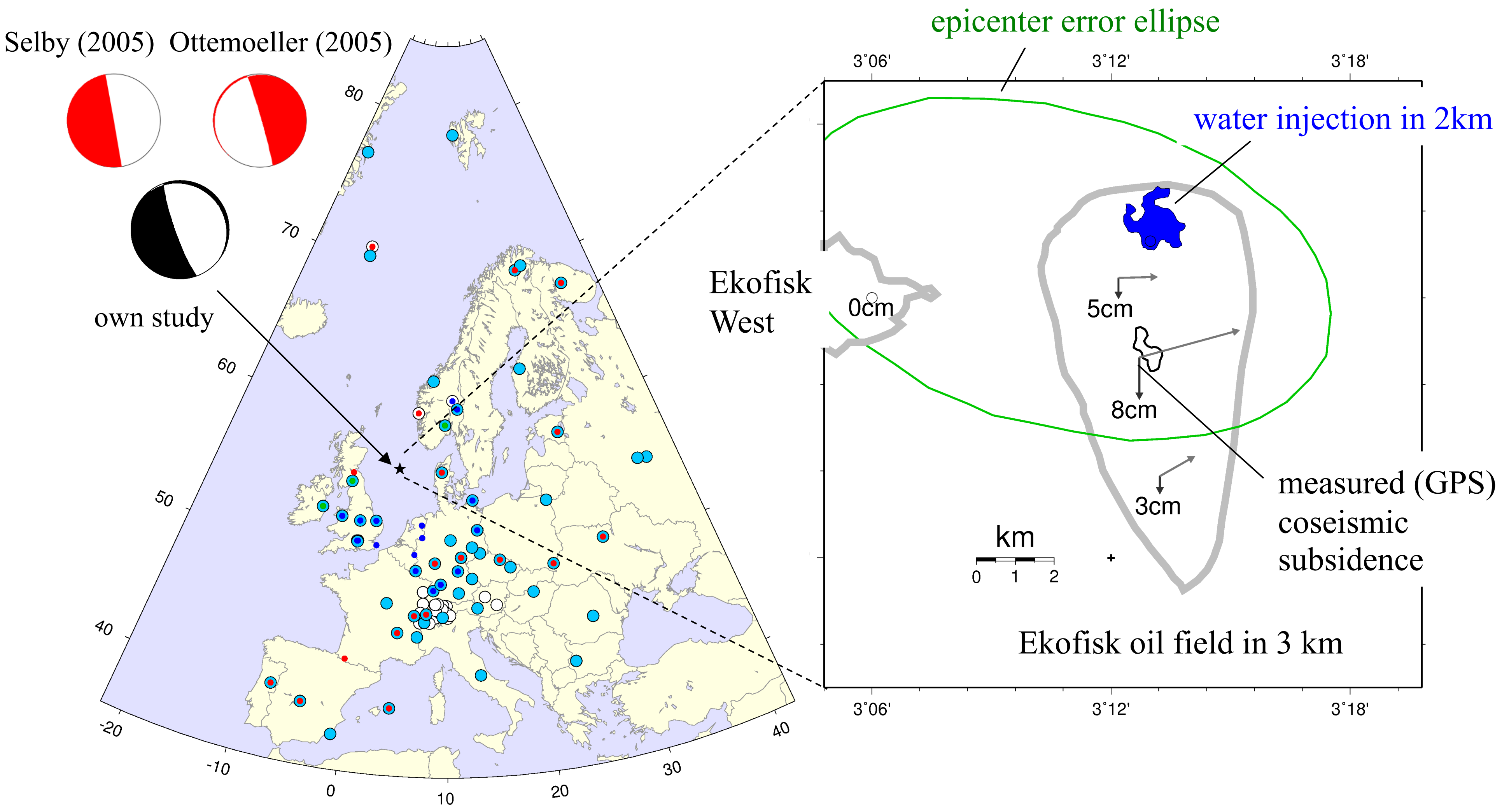

# Multi-step amplitude spectra / full waveform inversion

**Step 1** Focal mechanism, Depth, $M_0$ (from amplitude spectra)

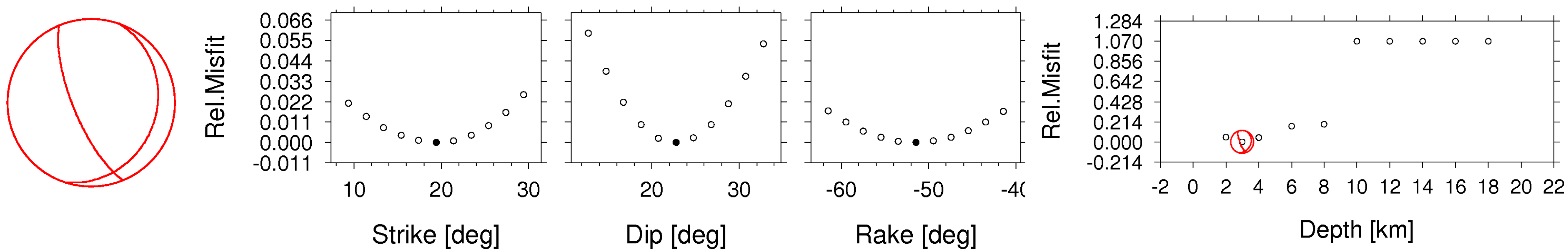


**Step 2** sense of slip, centroid location, apparent duration (from waveforms)

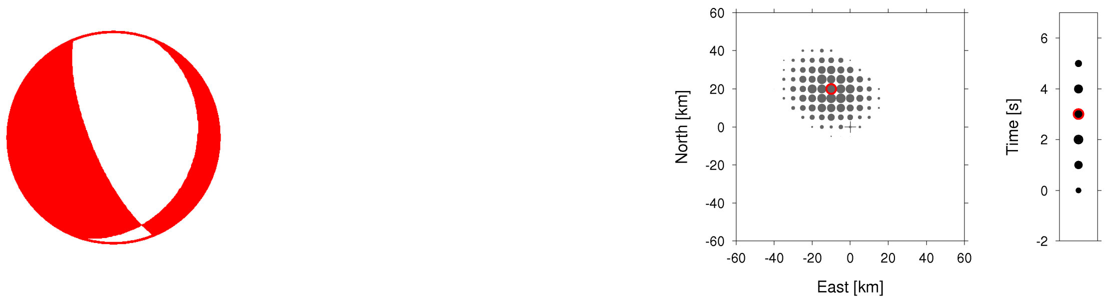


*CMT inversion, KINHERD-KIWI project (Uni Hamburg, Uni Potsdam, GFZ, BGR)*

# Unidirectional rupture in 140°

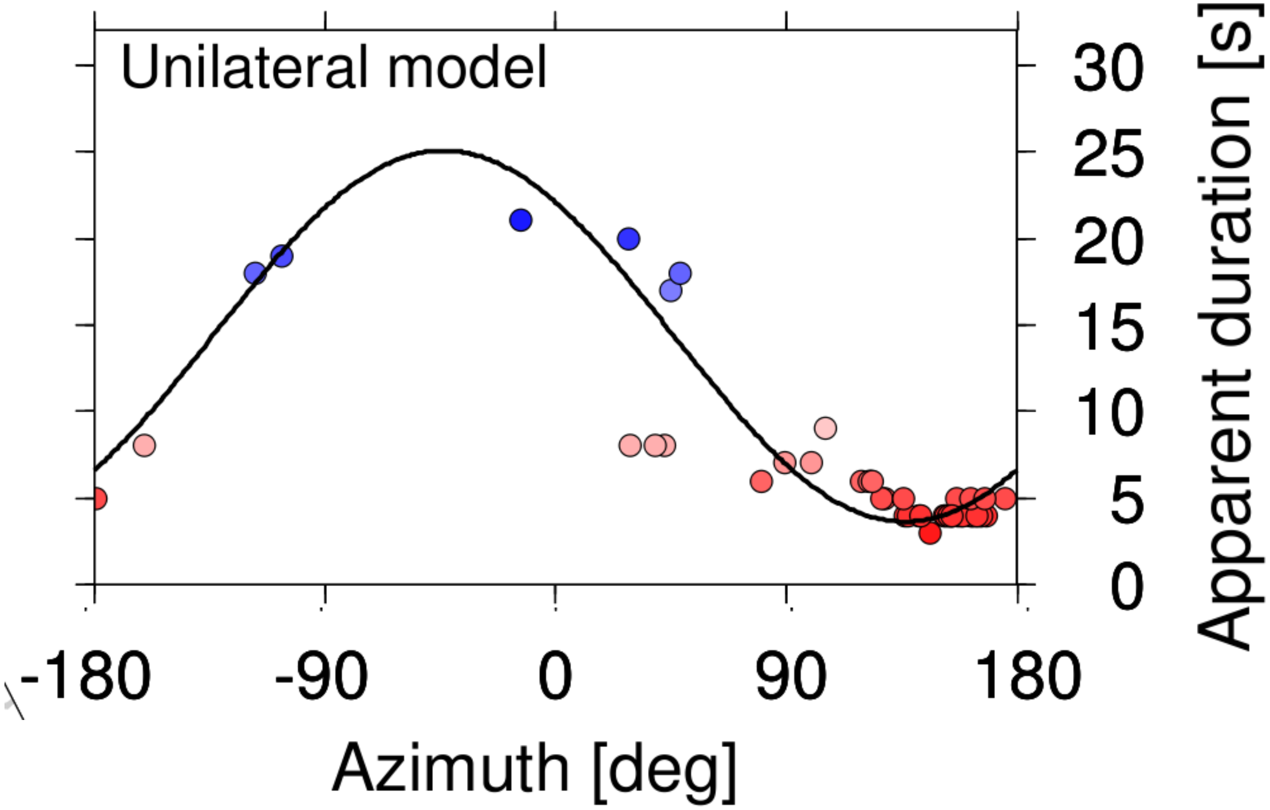


Cesca et al., in preparation

# Was the earthquake triggered by the pre-seismic hydrofrac in 2 km depth

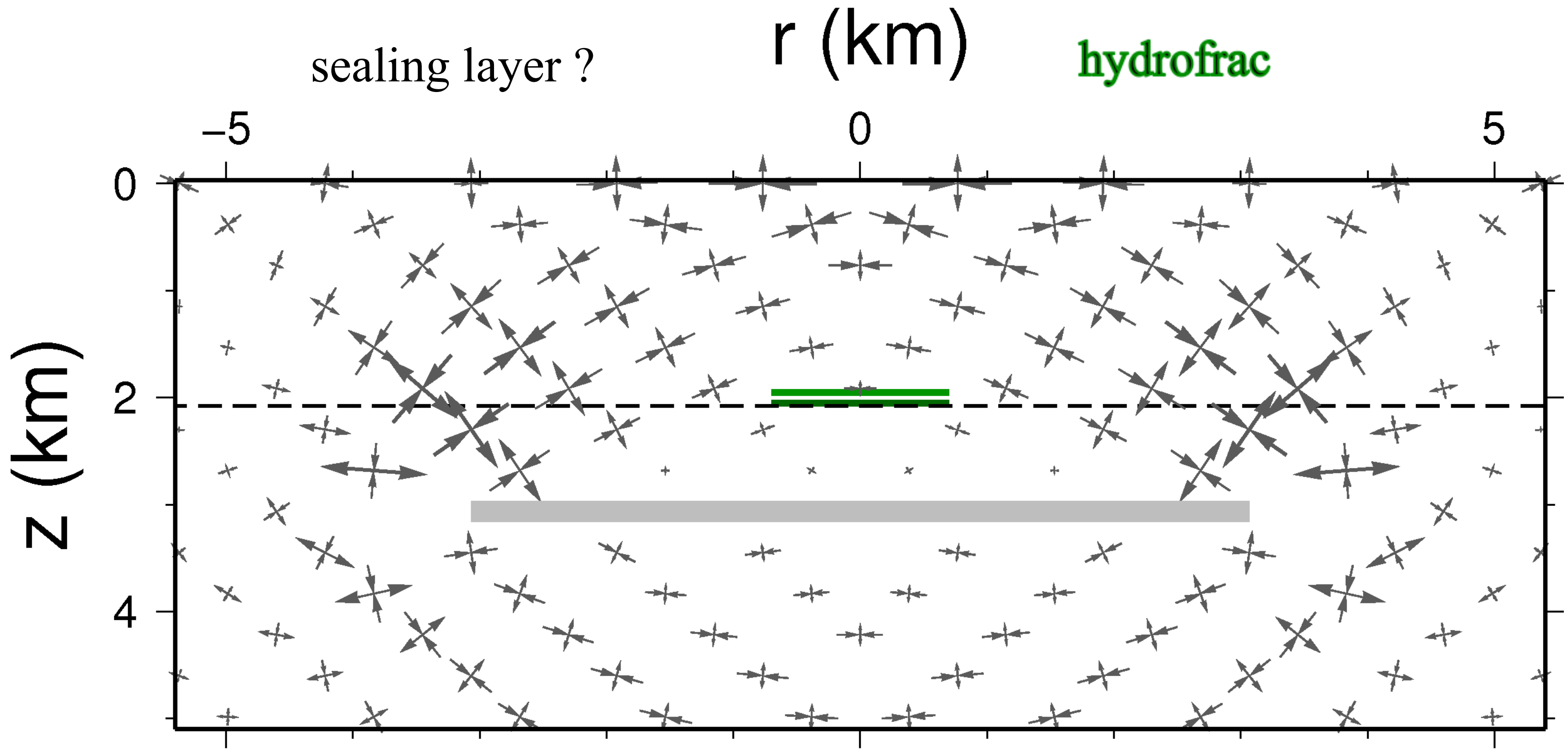

# Ekofisk: Depletion induced shear stress in 2 km depth

Selby (2005) Ottemoeller (2005)

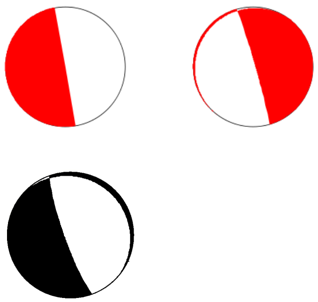

own study

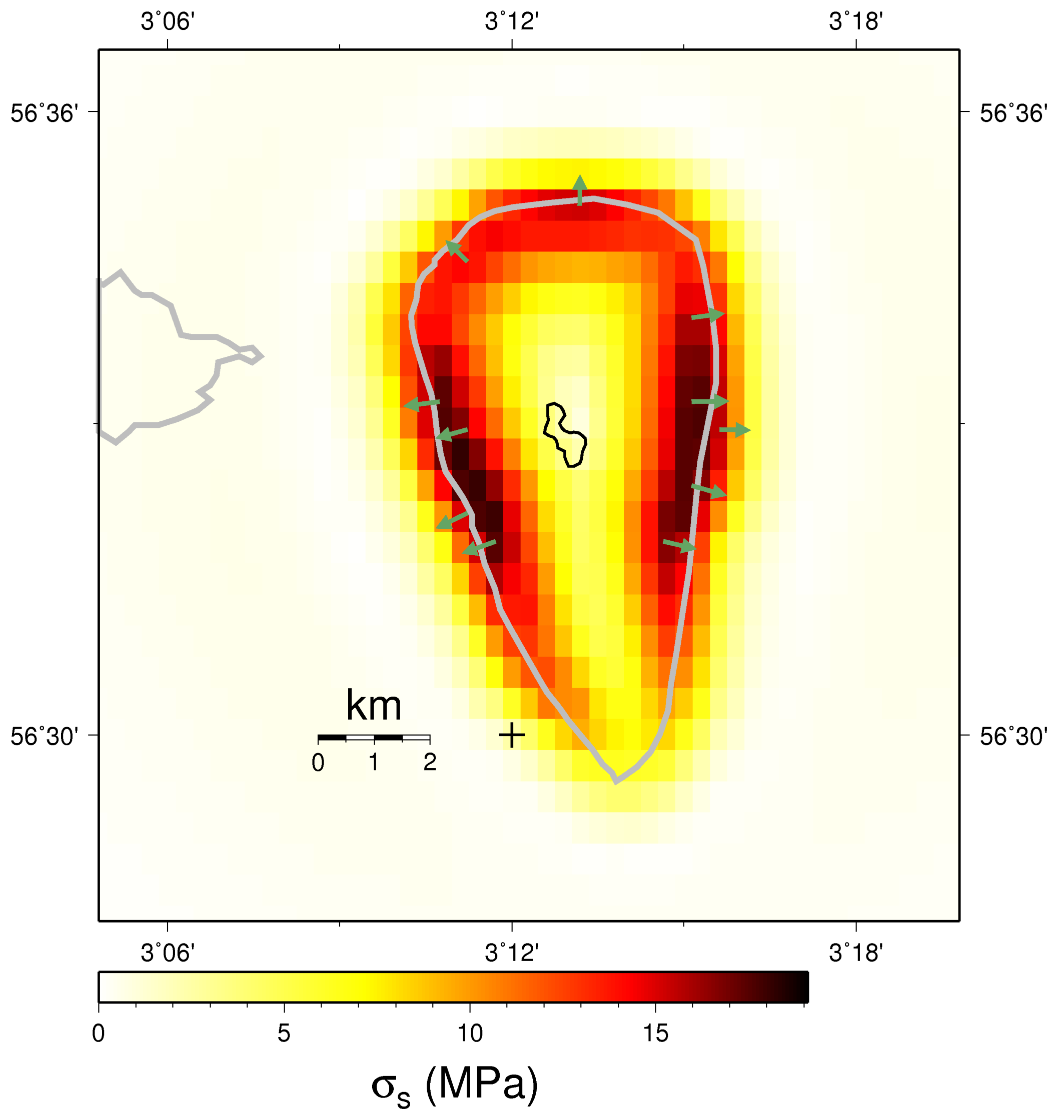

# Possible location of the earthquake

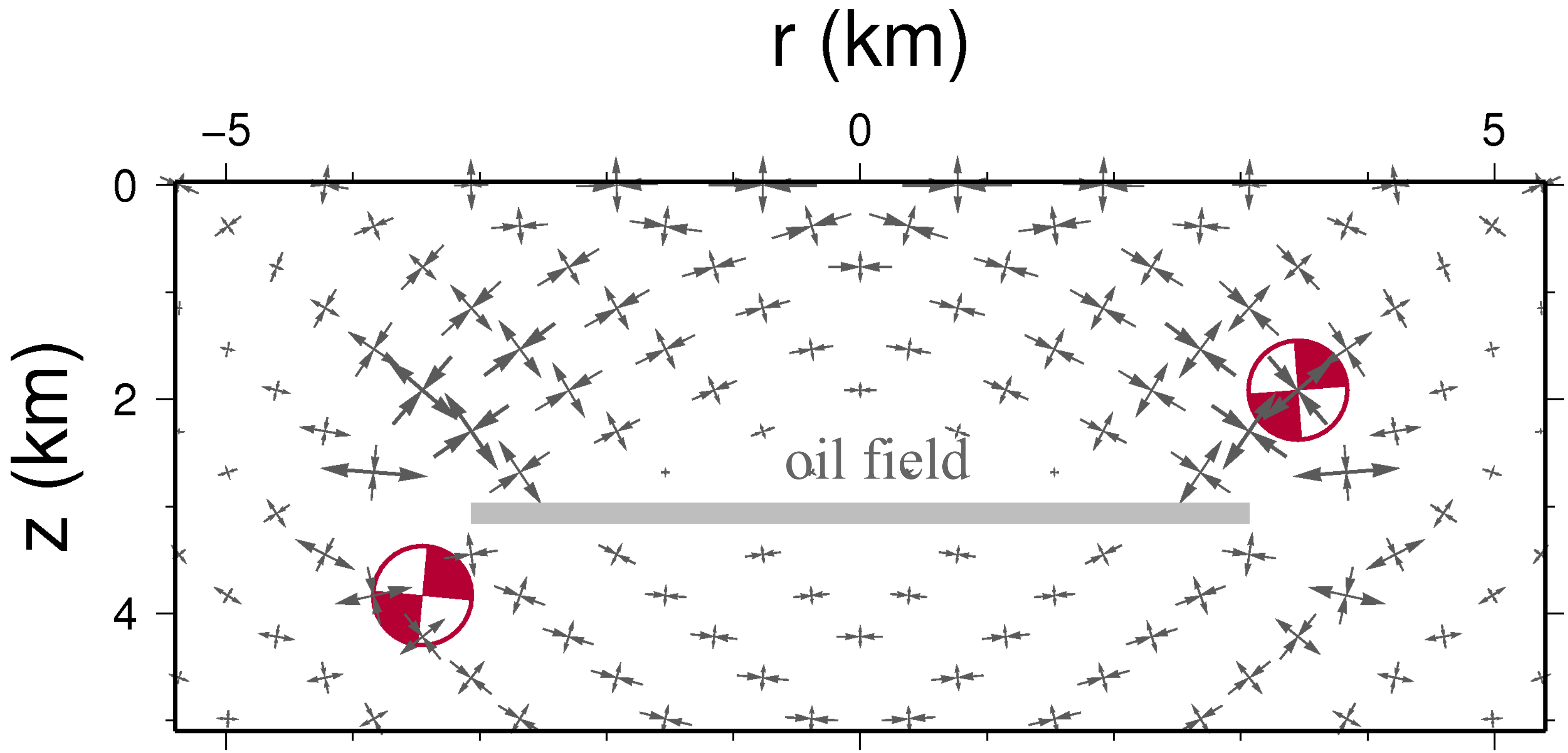


own study and Selby et al. (2004)

# Possible location of the earthquake

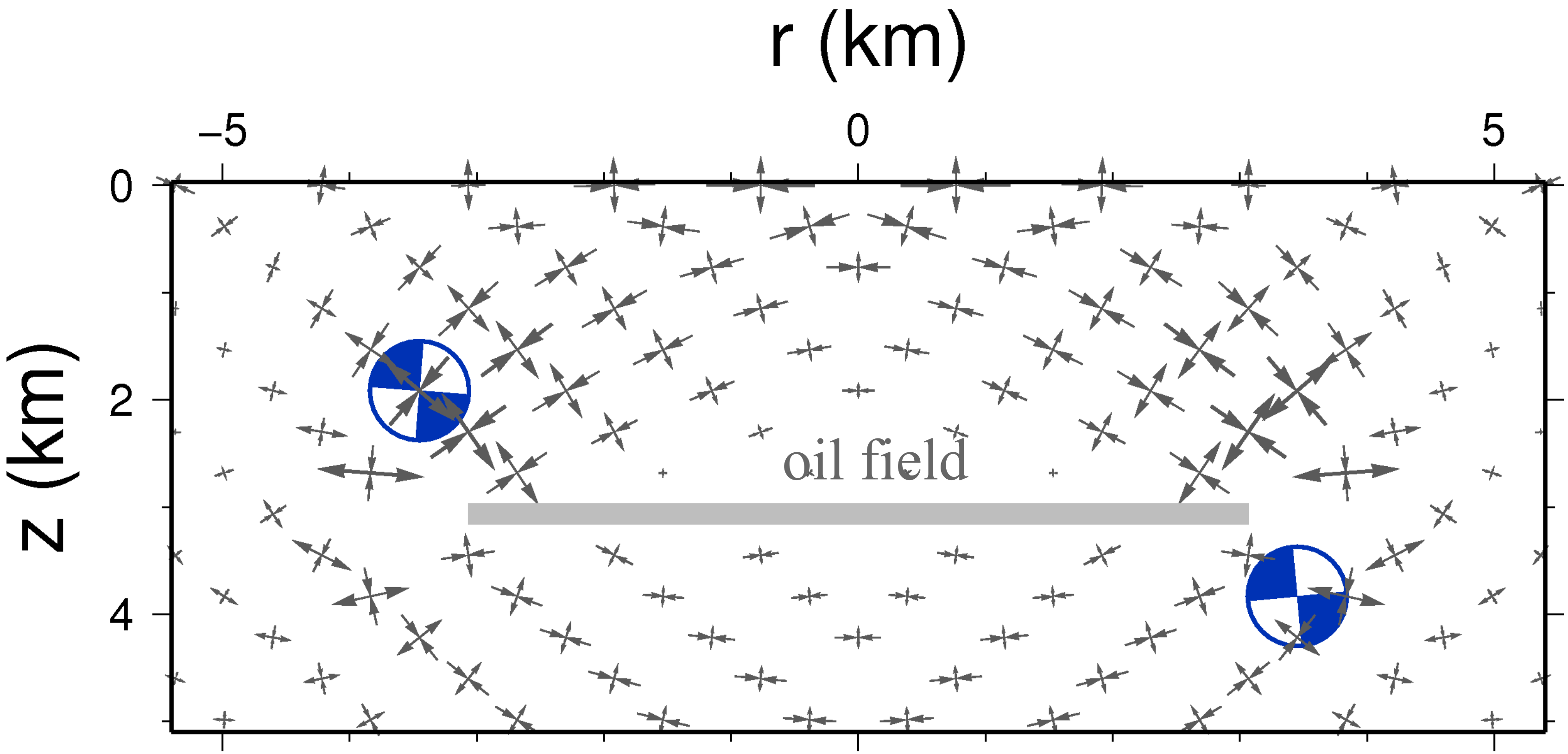


Ottemöller et al. (2004)

# Co-seismic displacement (GPS) verifies eastern border solution in 2 km depth

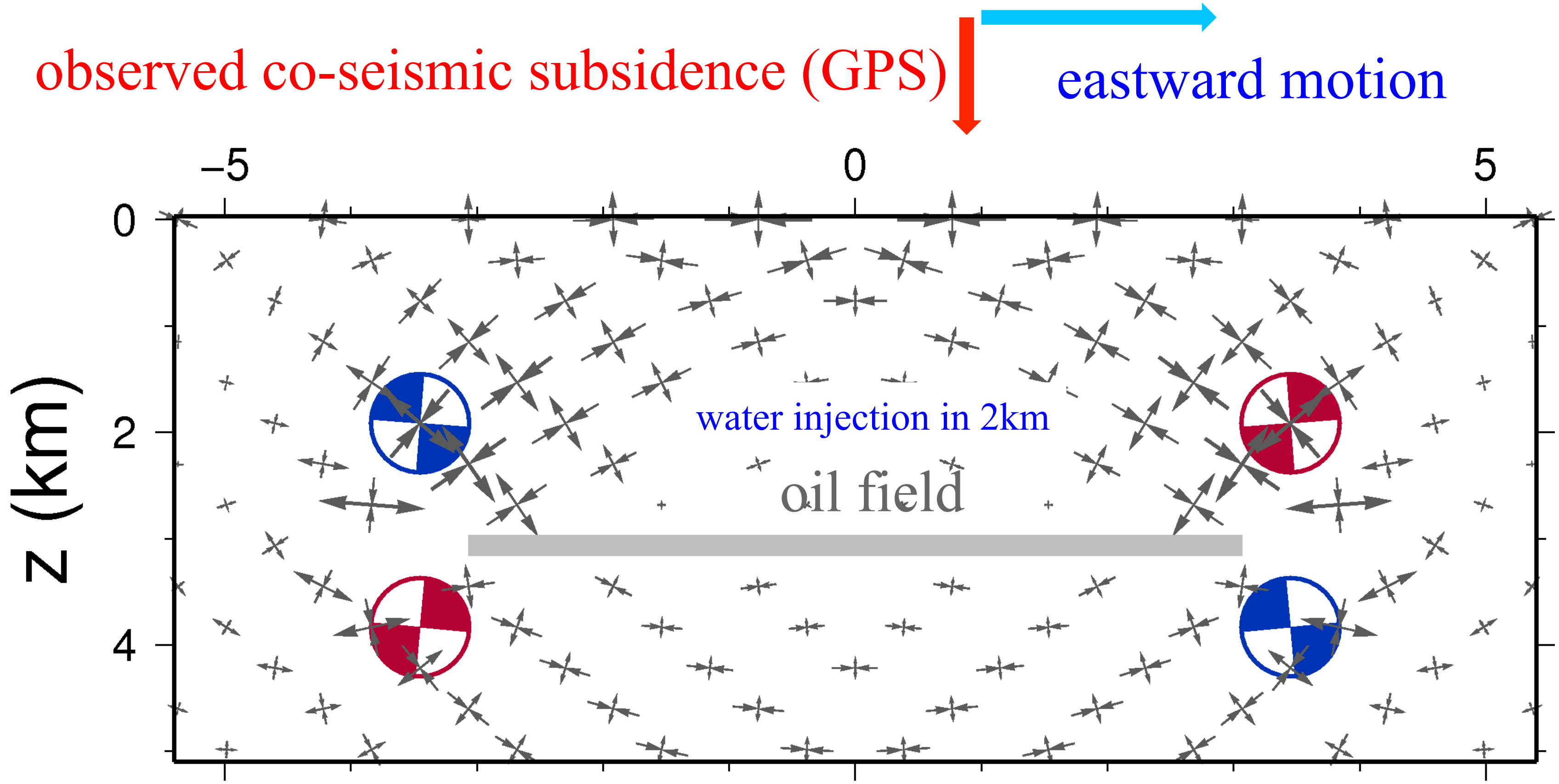

# Shear stress resolved in slip direction

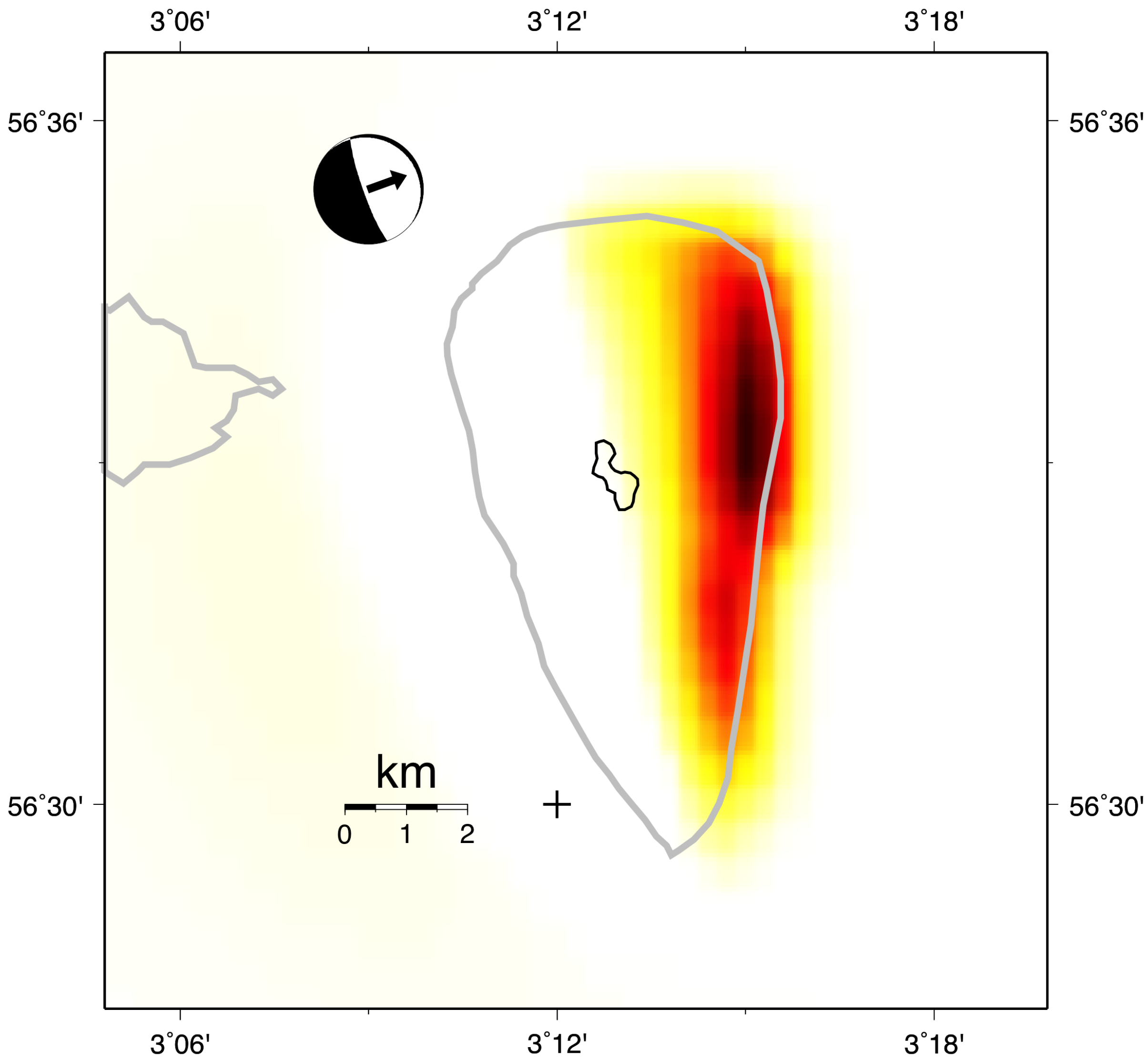

# BE modeling of fault slip on patch of high shear stress

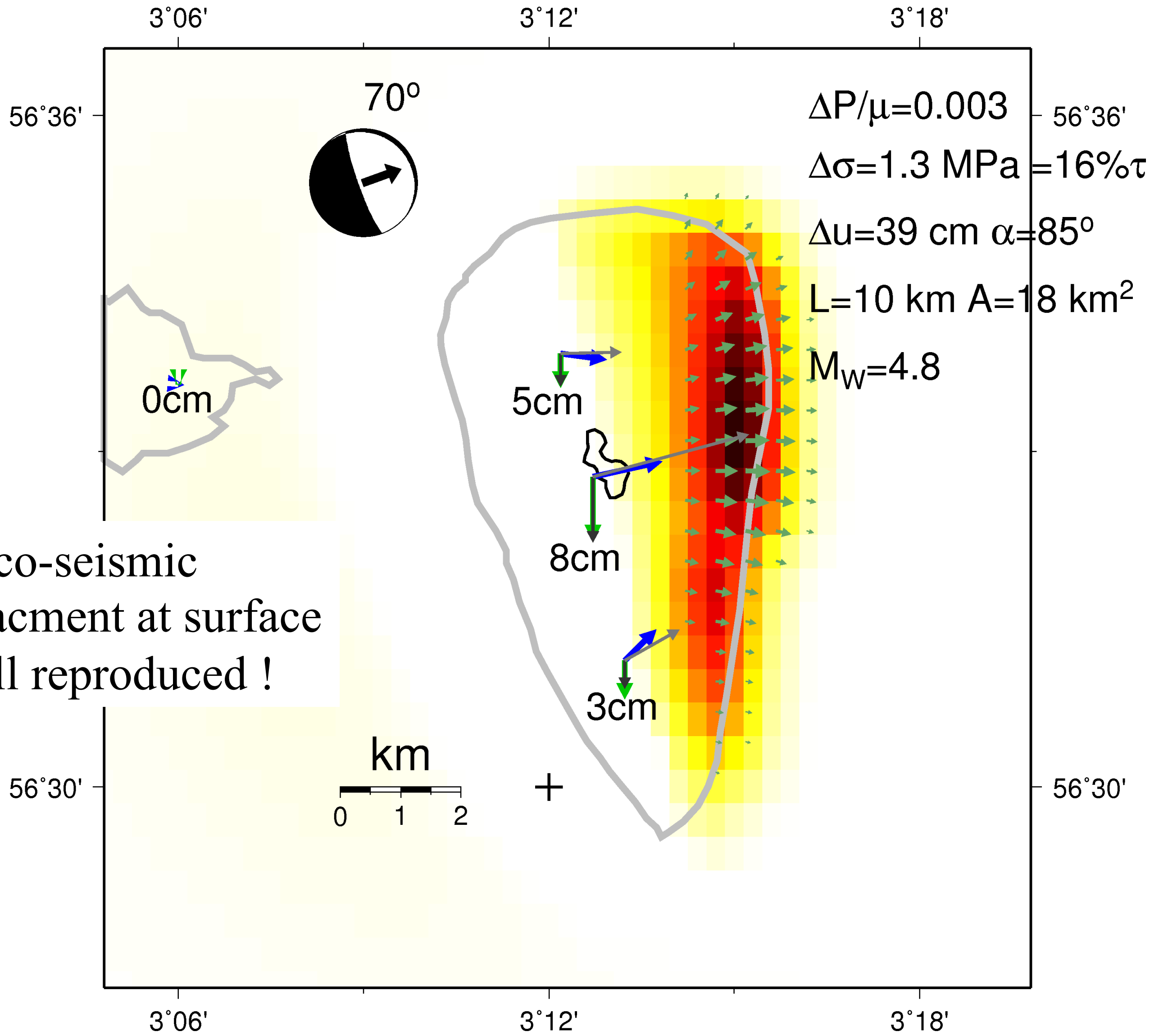


GPS co-seismic displacment at surface is well reproduced !

# Rupture propagated “downhill” towards patch of high stress

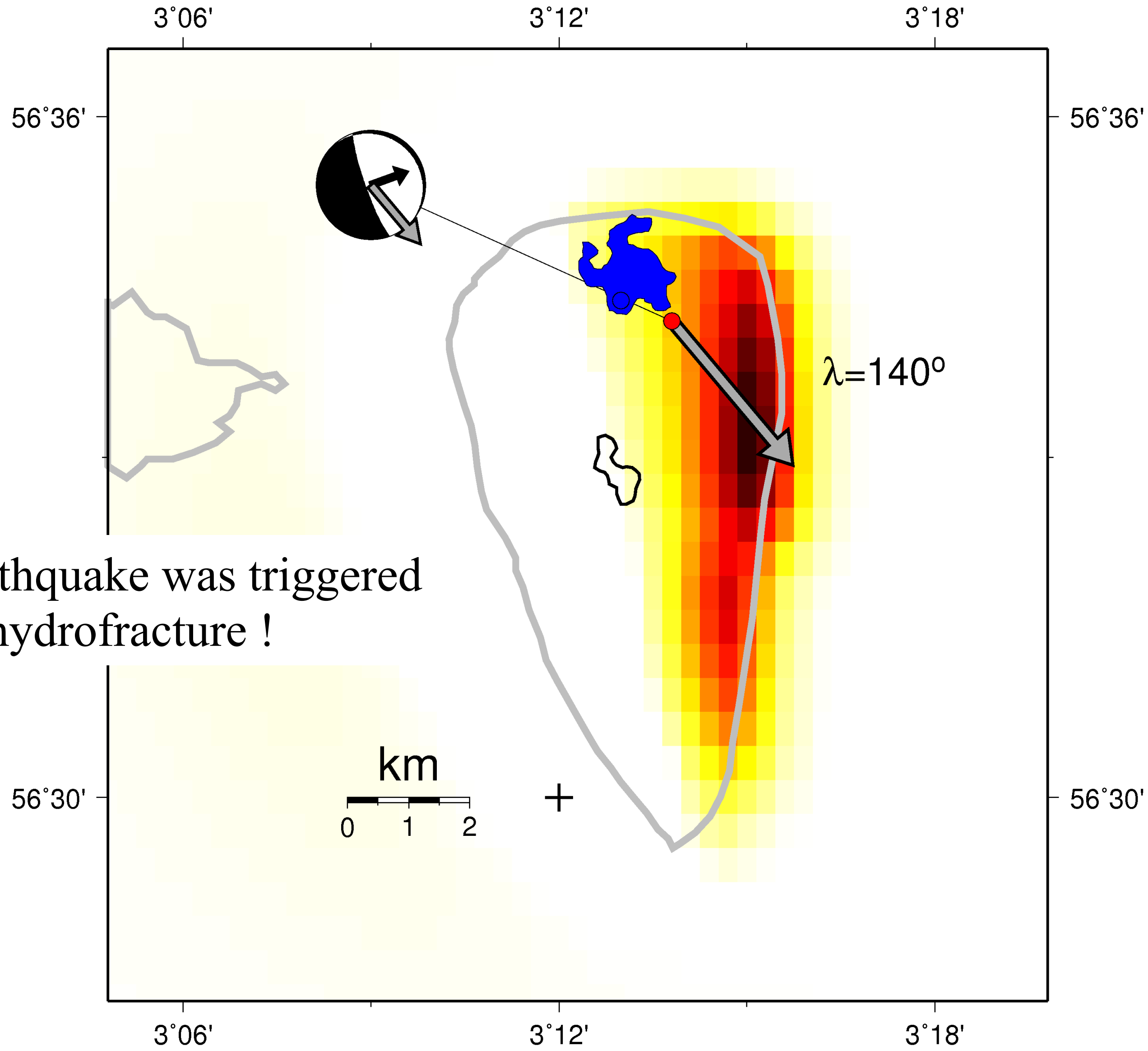


earthquake was triggered
at hydrofracture !

# Conclusion Ekofisk study

• Source mechanism, rupture plane, epicenter, centroid and rupture direction is resolved

•The Ekofisk earthquake was possibly fluid-triggered

• The rupture in 2 km was driven by field-induced shear stress

• Rupture propagation towards high stress regions

• The modeling of “resolved Coulomb stress” is a valid approach to discriminate induced, triggered and natural earthquakes

# Overall summary

- Induced and triggered seismicity has many causes and is often difficult to distinguish from natural seismicity
- It is not sufficient to correlate a loading cycle with earthquake statistical parameter. A time dependent stress model is needed to strengthen the trigger hypothesis
- Natural fluid-induced seismicity can be used to study the intrusion parameter
- Many tools are needed to study triggered and induced seismicity (relative location and depth studies, source mechanism, modeling of fluid diffusion, intrusion, depletion related stress changes)

# supplement material

- lecture III: techniques (relative location and relative moment tensor inverison)
- plotting moment tensors: New Package MOPAD by Krieger & Heimann (2010)

# references


Becker, D., Cailleau, B., Dahm, T., Shapiro, S., and Kaiser, D., 2010. Stress triggering and stress memory observed from acoustic emissions records in a salt mine. Geophys. J. Int., pp. 10.1111/j.1365–246X.2010.0464.x.

Cocco, M. and Rice, J., 2002. Pore pressure and poroelasticity effects in Coulomb stress analysis of earthquake triggering. J. Geophys. Res., 107:10.1029/20000JB000138.

Dahm, T. and Brandsdóttir, B., 1997. Moment tensors of micro-earthquakes from the Eyjafjallajökull volcano in South Iceland. Geophys. J. Int., 130:183–192.

Dahm, T., Fischer, T., and Hainzl, S., 2008. Mechanical intrusion models and their constraints on the density of fluids injected in the nw bohemia swarm region at 10 km depth. Studia Geofisica, 52:529–548.

Dahm, T., Fischer, T., and Hainzl, S., 2010. Linear fracture growth during hydrofracturing: the role of driving stress gradients. in press, pp.

Dahm, T., Krüger, F., Stammler, K., Klinge, K., Kind, R., Wylegalla, K., and Grasso, J., 2007. The $m_w = 4.4$ Rotenburg, Northern Germany, earthquake and its possible relationship with gas recovery. Bull. Seism. Soc. Am., 97(10.1785/0120050149):691–704.

Dieterich, J., 1994. A constitutive law for rate of earthquake production and its application to earthquake clustering. J. Geophys. Res., 99:2601–618.

Dieterich, J., Cayol, V., and Okubo, P., 2000. The use of earthquake rate changes as a stress meter at Kilauea volcano. Nature, 408:457–460.

Einarsson, P. and Brandsdóttir, B., 1980. Seismological evidence for lateral magma intrusion during the July 1978 deflation of the Krafla volcano in NE-Iceland. J. Geophys., pp. 160–165.

Fischer, T., Eisner, L., Shapiro, S., and LeCalvez, J., 2008a. Microseismic signatures of hydraulic fracture growth in sediment formations: observations and modelling. 113, B02307:doi:10.1029/2007JB005070.

Fischer, T., Michalek, J., and Bouskova, A., 2008b. Microearthquake activity near Novy Kostel in the period 2001-2007: fault plane after a swarm. Studia Geophysica et Geodetica, 0:submitted.

Hainzl, S., Kraft, T., Wassermann, J., Igel, H., and Schmedes, E., 2006. Evidence of rainfall-triggered earthquake activity. Geophys. Res. Lett., 33:10.1029/2006GL027642.

Hayashi, A. and Morita, Y., 2003. An image of a magma intrusion process inferred from precise hypocentral migrations of the earthquake swarm east of the Izu Peninsula. Geophys. J. Int., 153:159–174.

Jonsson, S., Segall, P., Pedersen, R., and Björnsson, G., 2003. Post-earthquake ground movements correlated to pore-pressure transients. Nature, 424:179–183.

# references


Köhler, N., Spies, T., and Dahm, T., 2009. Seismicity patterns and variatoin of the frequency-magntiude distribution of microcracks in salt. Geophys. J. Int., x:10.1111/j.1365–246X.2009.04303.x.

Kuempel, H.-J., 1991. Poroelasticity: parameters reviewed. Geophys. J. Int., 105:783–799.

Ogata, Y. and Zhuang, J., 2006. Space-time ETAS models and an improved extension. Tectonophysics, 413:13–23, 10.1016/j.tecto.2005.10.1016.

Ottenmöller, L., Nielsen, H., Atakan, K., Braunmiller, J., and Havskov, J., 2005. The 7 May 2001 induced seismic event in the Ekofisk oil field, North Sea. J. Geophys. Res., B10301:i10.1029/2004JB003374.

Pandey, A. and Chadha, R., 2003. Surface loading and triggered earthquakes in the Koyna-Warna region, western India. Phys. Earth and Planet. Inter., 139:207–233.

Pollard, D. and Fletcher, R., 2005. Fundamentals of structural geology. 497, pp.

Rice, J. and Cleary, M., 1976. Some basic stress diffusion solutions for fluid-saturated elastic porous media with compressible constituents. Reviews of Geophysics and Space Physics, 14:227–241.

Rohzko, A., Podladchikov, Y., and Renard, F., 2007. Failure patterns caused by localized rise in pore-fluid overpressure and effective strength of rock. Geophys. Res. Lett., 34:10.1029/2007GL031696.

Scholz, H. C., 1990. The mechanics of earthquakes and faulting. 439, pp.

Seeber, L. and Armbruster, J., 2000. Earthquakes as bacons of stress change. Nature, 407:69–72.

Seeber, L., Armbruster, J., and Kim, W.-Y., 2004. A fluid-injection-triggered earthquake sequance in Ashtabalu, Ohio: Implications for seismogenesis in stable continental regions. Bull. Seism. Soc. Am., 94:76–87.

Segall, P., 2010. Earthquake and volcano deformation. Princeton University Press, pp. 1–423.

Segall, P. and Fitzgerald, S., 1998. A note on induced stress changes in hydrocarbon and geothermal reservoirs. Tectonophysics, 289:117–128.

Selby, N., Eshun, E., Patton, H., and Douglas, A., 2005. Unusual long-period Rayleigh wave radiation from a vertical dip-slip source: The 7 May 2001, North Sea earthquake. J. Geophys. Res., B10301:10.1029/2005JB003721.

Turcotte, D. and Schubert, G., 2002. Geodynamics, 2nd edition. 450, pp.

Wang, H., 2000. Theory of linear poroelasticity. Princeton University Press.